# Methods to Develop Composite Action in Non-Composite Bridge

# Floor Systems: Part II

by

**Brent Ericson Hungerford, B.S.C.E.**

**Thesis**

Presented to the Faculty of the Graduate School of

The University of Texas at Austin

in Partial Fulfillment

of the Requirements

for the Degree of

**Master of Science in Engineering**

**The University of Texas at Austin**

**May 2004**

# Methods to Develop Composite Action in Non-Composite Bridge

# Floor Systems: Part II

**APPROVED BY**
**SUPERVISING COMMITTEE:**

**Richard E. Klingner, Supervisor**

**Michael D. Engelhardt, Reader**

## Dedication


To my family, for their constant support of my dream since I was very young, and

to Lyn, for her love and support.

# Acknowledgements

**Methods to Develop Composite Action in Non-Composite Bridge Floor Systems: Part II**

Brent Ericson Hungerford, M.S.E.

The University of Texas at Austin, 2004

SUPERVISOR: Richard E. Klingner

This thesis describes part of the work associated with TxDOT Study 0-4124 ("Methods to Develop Composite Action in Non-Composite Bridge Floor Systems"). The purpose of Study 0-4124 is to develop and verify at least one structurally adequate, constructible, and cost-effective method of achieving composite action using post-installed shear connectors. The primary objective of this thesis is to determine if using post-installed shear connectors to create composite action is a viable way of strengthening an existing bridge. A literature review was conducted to review and summarize composite action design and behavior, and a survey of existing TxDOT bridges that are non-composite steel

girder and concrete bridge decks was performed.  Methods of shear transfer were identified based on the background research and bridge survey, and 50 single connector, direct shear tests were performed on 22 primary methods and variations, of which 28 tests and 12 methods and variations will be discussed in this thesis.  The results of the direct shear tests were compared to the cast-in-place welded stud based on expected load-slip demand.  It was determined that three post-installed connection methods would meet the criteria of structural performance, constructability, and cost-effectiveness.   Those methods are recommended for further testing in fatigue and in complete bridges.

# Table of Contents

# List of Tables

# List of Figures

# CHAPTER 1

## Introduction

### 1.1 INFORMATION ON TxDOT STUDY 0-4124

Numerous bridges in central Texas were constructed in the 1960s as non-composite steel girders with concrete decks, and many of these have been reconstructed within the last 20 years. For various reasons, these bridges are now required to carry heavier loads than those for which they were originally designed. Because the reconstructed bridges are usually still in good condition, it is preferable to retrofit them rather than rebuild them to increase their capacities. A possible means of retrofitting to achieve increased load-carrying capacity is to post-install shear connectors to transfer shear between the two steel girder and concrete deck, and thereby obtain composite action between the two components.

Composite action in new construction typically connects the steel girder and concrete slab using welded shear studs, installed with a standard stud-welding gun on the top flange of the steel girder, and then surrounded by the cast-in-place concrete deck.

Post-installed shear connectors are installed with the concrete bridge deck already in place, and may require coring or drilling holes in the concrete or steel. While specific installation requirements vary with the type of connection, in general the installation of such a shear connector is more expensive and time-consuming than that of a cast-in-place welded stud. Because of the higher installation cost, it is desirable that each single post-installed connector perform better structurally than a single cast-in-place welded stud, so that fewer post-installed connectors would be required compared to new welded studs that might otherwise have been required in new construction.

1

By using the compressive and tensile strength of the reinforced concrete deck in addition to that of the underlying steel girder, composite flexural capacities as much as 1.5 times that of the otherwise identical but non-composite system can be obtained. If this increase can be achieved in a cost-effective manner, retrofitting for composite action may be an effective response to the need for increased capacity.

## 1.2   SCOPE AND OBJECTIVES OF STUDY 0-4124

The purpose of Study 0-4124 is to develop and verify at least one post-installed shear connector method that is structurally adequate, constructible, and cost-effective for use in retrofitting bridges for increased capacity due to composite action. Structural adequacy is judged on initial stiffness, ultimate capacity, ductility, and failure mode. A wide variety of methods is investigated, and the most promising methods are tested under static loading and cyclic loading, using a test setup involving single connectors. Relatively well-performing methods will then be tested in multiple-anchor setups and field studies. Based on those results, design recommendations and construction guidelines will be produced for at least one method.

TxDOT Study 0-4124, "Methods to Develop Composite Action in Non-Composite Bridge Floor Systems," has seven project tasks as stated in the project proposal[1]:

1. Perform a literature review and summary of composite action design and behavior. Previously utilized connections between steel and

---

[1] Engelhardt, M. D. and Klingner, R. E., Proposal for TxDOT Study 4124.

concrete will be researched as well as mechanisms to transfer shear force.

2.  Conduct a survey of existing TxDOT bridges that are non-composite steel girder and concrete bridge decks.

3.  Identify methods for post-installing shear connectors based on the results of the first two tasks.  These methods will be judged based on expected structural performance, constructability, and cost.

4.  Conduct push-out tests in order to obtain the basic load-deformation behavior of the post-installed methods.

5.  Perform large-scale tests on composite beams utilizing post-installed shear connectors in order to verify previously observed behavior and to further evaluate the constructability of the method.

6.  Develop design procedures and recommendations for the post-installed shear connectors.

7.  Prepare a project report based on the results of all the previous tasks.

Task (4) has been modified since the proposal was written.  Direct shear tests will be performed on individual shear connectors in order to obtain the load-deformation behavior of a single connector.  Fatigue testing will also be carried out on single connectors to understand individual connector response under cyclic loading.  Standard push-out tests will then be performed on the connection methods that perform well structurally on an individual-connector basis.

## 1.3   SCOPE OF THIS THESIS

This paper addresses Task (2) and portions of Task (1), Task (3), and Task (4).  Tasks (1) and (3) relate in part to the literature review of post-installed shear-connection methods, and the modified Task (4) deals with testing of shear

3

connectors under static loading. Some types of connectors are addressed in this thesis; and the rest are addressed in Schaap (2004). Task (2) concerns a survey of existing bridges, and is discussed here in its entirety.

Task (1) deals with a literature review of composite design and previously developed connections between concrete and steel. Current design guidelines in the AASHTO Standard Specifications and the AASHTO LRFD design manuals are reviewed and summarized, along with portions of the AISC design manual and the Eurocode pertaining to shear stud design and the standard push-out test. A wide variety of cast-in-place and post-installed connections between concrete and steel are examined, including traditional and innovative methods.

Field investigations of existing bridges are performed as indicated in Task (2). Several bridges are identified by TxDOT as possible candidates for strengthening with post-installed shear connectors. Six of those candidate bridges are inspected, and their geometry, site layout, and structural condition are recorded.

Task (3) concerns the structural performance and constructability of the possible connection methods between concrete and steel. Several post-installed shear-connection methods are selected based on expected structural performance and constructability. Structural performance is evaluated in terms of the load-slip behavior of individual connectors, using criteria of initial stiffness, ultimate capacity, ductility, and failure mode. Connector performance is compared to that of cast-in-place welded studs.

Additional research discussed in this thesis includes tests to determine the coefficient of static friction between in-service steel girders and bridge decks, and an initial study to propose ways of determining maximum slip demand. By comparing the slip demand with observed capacity, relatively well-performing retrofit connection methods can be identified.

4

## 1.4  OBJECTIVES OF THIS THESIS

The primary objective of this thesis is to determine if using post-installed shear connectors to create composite action is a viable way of strengthening an existing bridge.  If so, it is then necessary to determine which of the post-installed shear-connector methods studied here should be tested further.

# CHAPTER 2

# Fundamental Shear-Transfer Mechanisms

## 2.1 CHAPTER OVERVIEW

In this chapter, terms related to connections between steel and concrete are defined, and placed in the context of this project. To fulfill this study's primary objective of developing a method of shear transfer that is structurally adequate, constructible and cost-effective, this chapter also includes a preliminary discussion of possible methods of shear transfer and the fundamental mechanisms underlying their structural action, as described by load-slip behavior.

## 2.2 CONNECTION DEFINITIONS

The term "connection" (Figure 2.1) refers to the entire assemblage of an attachment, concrete, and anchors (fasteners). The "attachment" is the structural or mechanical element to be connected to the concrete. The "anchor," or "fastener," is defined as the piece connecting the attachment to the concrete (Klingner 2003). An anchor may be cast-in-place or post-installed, and post-installed anchors may be classified as either mechanical anchors or bonded anchors (Klingner 2003).
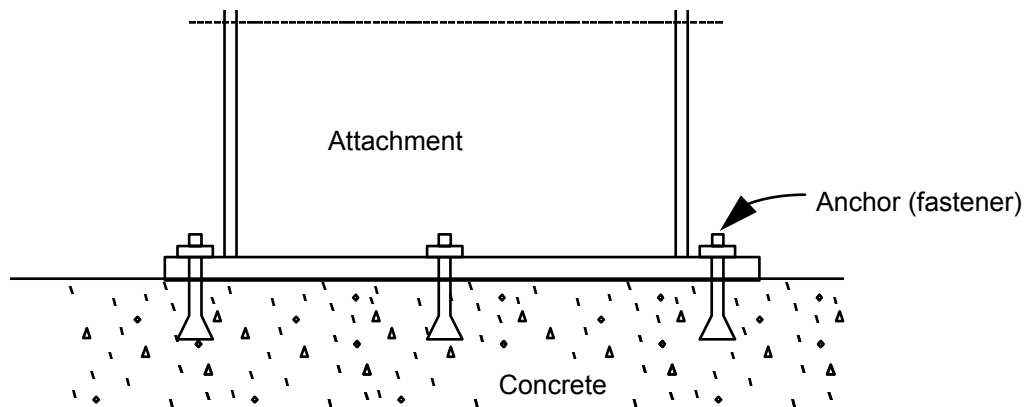
*Figure 2.1: Schematic of a connection*

In this thesis, the term "shear connection" defines the particular assemblage of the steel girder (attachment), concrete, and the method of shear transfer between the concrete and steel. The "method of shear transfer" is either an anchor (also referred to as a "shear connector"), or a pure adhesive.

## 2.3 FUNDAMENTAL CATEGORIES OF SHEAR TRANSFER

Two fundamental categories of shear transfer are considered here.

o    In the first category, which may be described as "embedded-depth transfer," shear is transmitted at some depth within the concrete rather than at the steel-concrete interface. One example of embedded depth-transfer is the common welded shear stud.

o    In the second category, which may be described as "interface transfer" shear force is transmitted directly at the concrete-steel interface by friction or adhesion.
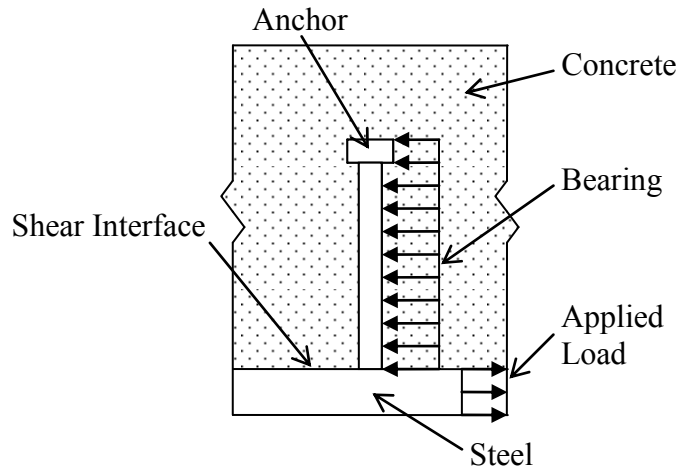
***Figure 2.2: Embedded-depth transfer of shear force***
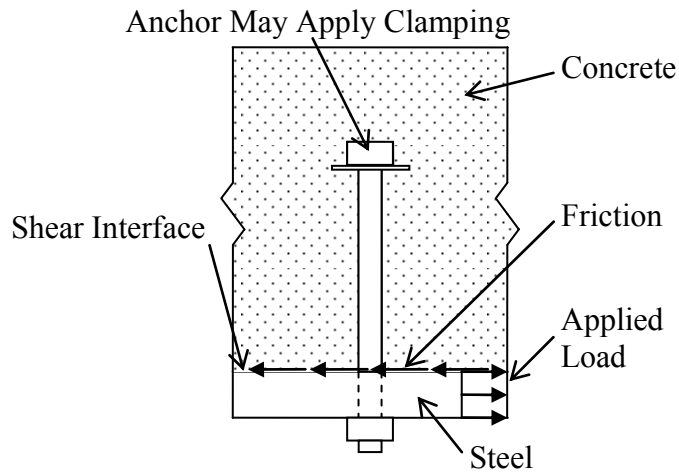


***Figure 2.3: Interface transfer of shear force***

Each of these two categories involves one or more fundamental resistance mechanisms. As shown in Figure 2.2 and Figure 2.3, embedded-depth transfer occurs by the fundamental resistance mechanism of bearing of the anchor against the concrete; and interface transfer can occur by the fundamental resistance

mechanisms of adhesion, static friction or dynamic friction, individually or in combination.
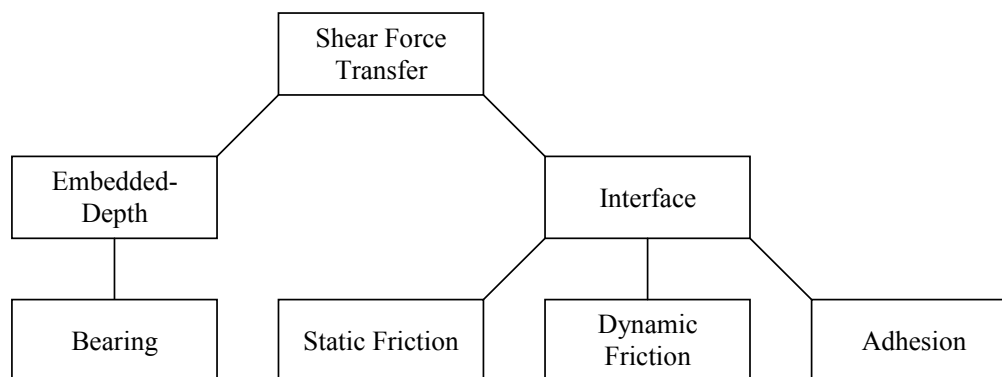


*Figure 2.4: Hierarchy of categories and fundamental mechanisms of shear-force transfer*

In this thesis, the term "primary mechanism of shear-force transfer" refers to the resistance mechanism that is first engaged when a shear force is applied to the connection. The term "secondary mechanism of shear transfer" refers to the resistance mechanism engaged after the primary transfer mechanism has been overcome. A secondary mechanism does not exist in all connections; it is typically present only as bearing after static friction, or as dynamic friction after static friction. To be identifiable, the secondary force-transfer mechanism must provide greater load resistance than the primary force-transfer mechanism.

Tertiary force-transfer mechanisms are also possible. For example, an anchor could initially transfer load by static friction, then by dynamic friction, and finally by bearing. Dynamic friction is typically ignored in design, and is not considered here as a viable method of force transfer.

## 2.4   POSSIBLE METHODS OF SHEAR TRANSFER

Several post-installed methods of shear transfer are commonly used as connectors between concrete and steel.  The relationship among all divisions of shear transfer is shown in Figure 2.5.  Table 2.1 displays the possible methods of shear transfer along with their structural identifications such as name, installation, type of shear-transfer method, and mechanism of shear transfer.
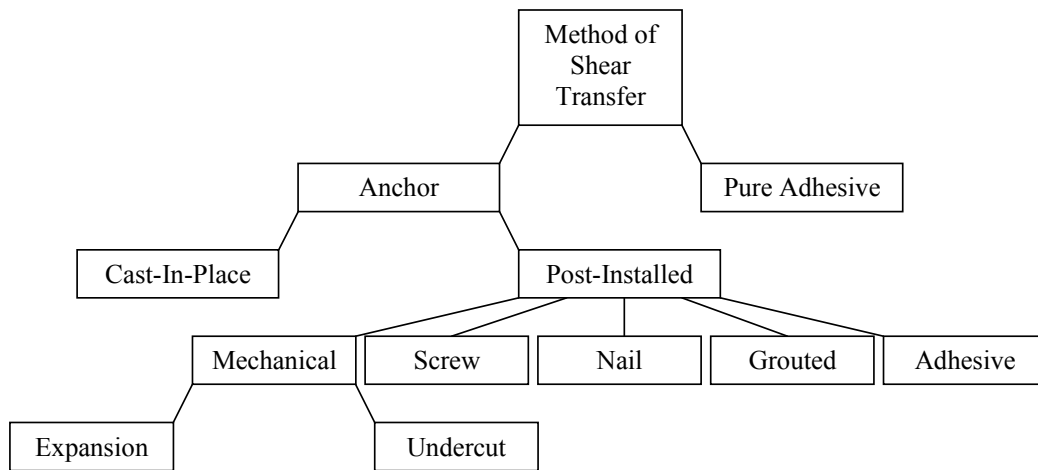
*Figure 2.5: Categorization of methods of shear transfer*

*Table 2.1: Possible methods of shear transfer and their structural identifications*

| Name | Method of Installation | Type of Shear-Transfer Method | Primary Mechanism of Shear-Force Transfer | Secondary Mechanism of Shear-Force Transfer |
|---|---|---|---|---|
| Cast-In-Place Welded Stud | Cast-In-Place | Anchor | Bearing | None |
| Expansion Anchor | Post-Installed | Anchor | Static Friction | Bearing |
| Undercut Anchor | Post-Installed | Anchor | Static Friction | Bearing |
| Screw Anchor | Post-Installed | Anchor | Bearing | None |
| Nail | Post-Installed | Anchor | Bearing | None |
| Grouted Anchor | Post-Installed | Anchor | Static Friction/ Bearing | Bearing/ None |
| Adhesive Anchor | Post-Installed | Anchor | Static Friction | Bearing |
| Pure Adhesive | Post-Installed | Pure Adhesive | Adhesion | None |

# CHAPTER 3

# Expected Load-Slip Demand

## 3.1 PRELIMINARY REMARKS ON LOAD AND SLIP DEMAND

This chapter includes a general discussion of terms related to composite action, and a thorough explanation of the current AASHTO procedure for the design of fully composite and partially composite bridges, including the requirements of the AASHTO LRFD and of the AASHTO Standard Specifications, which include allowable stress design and load factor design provisions. The chapter concludes with a discussion of models for determining load-slip demand and response.

## 3.2 DEFINITIONS RELATED TO COMPOSITE ACTION

In general, composite action occurs when two or more components (for example, a concrete bridge deck and a steel girder) act as a single structural element. In the specific context of steel and concrete elements, a composite member may be defined as fully composite or partially composite.

o    The flexural strength of a fully composite member is governed by the capacity of either the concrete slab or the steel girder.

o    The flexural strength of a partially composite member is governed by the ultimate strength of the shear connectors.

In describing how two elements act together, it is also useful to introduce the term "interaction," or the amount of discontinuity in the strain diagram

12

resulting from slip at the concrete-steel interface. Interaction may be defined as full or partial, as depicted in Figure 3.1.

o       A composite member with full interaction between concrete and steel has no discontinuity in the strain diagram at the interface, and hence no slip there. This condition may be attained by static friction or adhesion.

o       A composite member with partial interaction has a strain discontinuity at the concrete-steel interface as the result of slip there. Because (as discussed later in this thesis) traditional welded shear studs have some slip even at very small shear loads, they provide partial interaction.
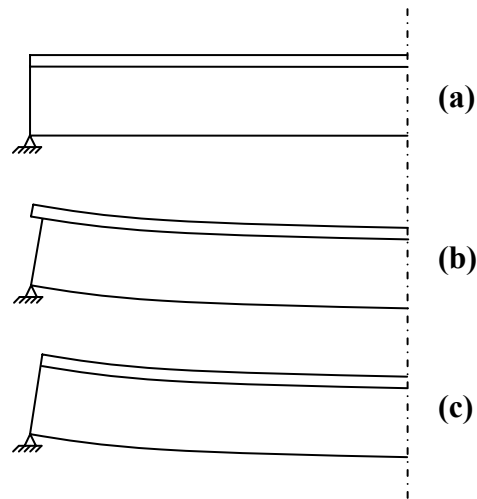


*Figure 3.1: (a) Undeformed shape of half of a simply supported beam; (b) deformed shape of a composite member with partial interaction; (c) deformed shape of a composite member with full interaction*

13

**3.3    CURRENT DESIGN PROCEDURES FOR COMPOSITE MEMBERS**

For composite design of bridges, the AASHTO design specifications (AASHTO 2002 and AASHTO 1998) are the standard; for buildings, the AISC design specification is used (AISC 2002). Cast-in-place welded shear stud are used for both. In bridge design, the shear stud diameter, spacing, and pitch are selected to satisfy fatigue requirements, and the resulting design is then checked for ultimate strength. The current AISC design manual allows partial composite design; the AASHTO design manuals do not.

In this thesis, the *AASHTO LRFD Bridge Design Specifications*, 2nd Edition (1998) is referred to in shorthand form as "AASHTO LRFD" and are referenced as (LRFD). The *AASHTO Standard Bridge Design Specifications*, 17th Edition (2002) are referred to in shorthand form as the "AASHTO Standard Specifications." Allowable-stress design provisions in the *AASHTO Standard Bridge Design Specifications*, 17th Edition (2002) are referred to in shorthand form as "AASHTO ASD," and are referenced as (ASD). The load factor design provisions in the *AASHTO Standard Bridge Design Specifications*, 17th Edition (2002) are referred to in shorthand from as "AASHTO LFD," and are referenced as (LFD).

**3.3.1    Composite Design Using the LRFD Bridge Design Specifications**

The AASHTO LRFD is currently in its 2nd Edition. Load and resistance factor design (LRFD), a relatively new design approach, is an attempt to account more directly than previous design approaches for the statistical variability of loads and element capacities. The sections in the LRFD most relevant to the design of shear connectors are the following:

o    "COMPOSITE SECTIONS" (LRFD 6.10.3.1 pg. 6-57 to 6-60)

14

o        "SHEAR CONNECTORS" (LRFD 6.10.7.4 pg. 6-95 to 6-100)

In the AASHTO LRFD, the nominal capacity of a shear stud is given in LRFD 6.10.7.4.4c (repeated here as Equation 3.1), based on the work of Ollgaard *et al.* (1971).

$$Q_n = 0.5 A_{sc} \sqrt{f_c' E_c} \leq A_{sc} F_u \qquad \textit{(Equation 3.1)}$$

where

$Q_n$ = nominal shear capacity of a shear stud (kips)

$A_{sc}$ = cross-sectional area of a shear stud (in.$^2$)

$f'_c$ = specified compressive strength of concrete at 28 days (ksi)

$E_c$ = modulus of elasticity of concrete (ksi)

$F_u$ = specified minimum ultimate tensile strength of a shear stud (ksi)

Requirements for concrete cover, spacing, edge distance, general connector requirements, and flexural capacity calculations in the AASHTO LRFD are the same as those contained in the AASHTO Standard Specifications except where otherwise noted in this chapter.  The AASHTO LRFD does not permit partial composite design.

**3.3.2   Composite Design Using the Standard Specifications for Highway Bridges**

The AASHTO Standard Specifications are discussed at length in this chapter.  The current AASHTO Standard Specifications, the 17$^{th}$ Edition, permits design by either of two sets of design provisions, termed working stress design or allowable stress design (ASD), and load factor design (LFD).  This thesis deals primarily with AASHTO design requirements (either ASD or LFD) related to

15

strength. Serviceability-related requirements (primarily fatigue) are discussed in Schaap (2004).

### 3.3.2.1 AASHTO Allowable Stress Design (ASD)

In AASHTO Allowable Stress Design (ASD), structural elements are designed by comparing stresses due to loading combinations against allowable stresses for the material. The section in the AASHTO ASD most relevant to the design of shear connectors is "COMPOSITE GIRDERS" (ASD 10.38 pg. 303-307)

The AASHTO ASD provisions address fatigue design (ASD 10.38.5.1.1 and 10.38.5.1.3), and require a strength check using the reduced ultimate strength of a shear stud (ASD 10.38.5.1.2). The ultimate strength of a single welded shear stud whose length exceeds 4 diameters is given in ASD 10.38.5.1.2, and repeated here as Equation 3.2.

$$S_u = 0.4d^2 \sqrt{f_c' E_c} \le 60,000 A_{sc} \qquad \textbf{\textit{(Equation 3.2)}}$$

where

$S_u$ = ultimate strength of an individual shear stud (lb)

d = diameter of shear stud (in.)

$f_c'$ = specified compressive strength of concrete at 28 days (psi)

$E_c$ = modulus of elasticity of the concrete (psi)

$A_{sc}$ = cross-sectional area of a shear stud (in.$^2$)

### 3.3.2.2 AASHTO Load Factor Design (LFD)

The AASHTO Load Factor Design (LFD) provisions address strength, serviceability, durability, control of permanent deformation due to overload, and fatigue and live-load deflection under service loading are considered as well. The

sections in the AASHTO LFD most relevant to the design of shear connectors are the following:

o        "COMPOSITE SECTIONS" (LFD 10.50 pg. 323-326)

o        "SHEAR CONNECTORS" (LFD 10.52 pg. 328)

o        "FATIGUE, Composite Construction" (LFD 10.58.2 pg. 335)

The AASHTO LFD 10.50 includes the flexural capacity of composite cross-section based on a fully-plastic stress distribution. The AASHTO LFD 10.52 and 10.58 refer to AASHTO ASD 10.38.5.1.2 for strength and AAHSTO ASD 10.38.5.1.1 for fatigue design of shear connectors. This point is very important when partial composite design is discussed later in this chapter.

### 3.3.3    AASHTO Requirements for Concrete Cover, Spacing, and Edge Distance

AASHTO requirements incorporate several basic restrictions regarding shear connector location and geometry that are the same for LRFD, and for ASD and LFD.

o        The minimum concrete cover above the top of a shear connector must be 2 in. (ASD 10.38.2.3 and LRFD 6.10.7.4.1d).

o        The maximum pitch (longitudinal spacing between anchors) is 24 in. (ASD 10.38.5.1, LFD 10.52.3, and LRFD 6.10.7.4.1b), and the minimum center-to-center spacing between adjacent connectors is 4 diameters (ASD

10.38.2.4). In contrast, the AASHTO LRFD requirements for the minimum center-to-center spacing in the longitudinal and transverse directions are 6 diameters and 4 diameters, respectively (LRFD Articles 6.10.7.4.1b and 6.10.7.4.1c).

o    The minimum distance allowed between edge of shear connector and edge of the girder flange is 1 in. (ASD 10.38.2.4 and LRFD 6.10.7.4.1c), and AASHTO specifications also requires that the ratio of the height to the diameter of the shear stud not be less than four (ASD 10.38.5.1.2 and LRFD 6.10.7.4.1a).

### 3.3.4   General AASHTO Requirements for Shear Connectors

The general shear connector requirements are also the same for ASD and LFD. The AASHTO Standard Specifications define shear connectors in ASD 10.38.2.1 as a "…mechanical means used at the junction of the girder and slab for the purpose of developing the shear resistance necessary to produce composite action…"

This definition implies the use of bearing or friction as mechanisms of shear transfer; adhesion would not apply. Section 29 of the AASHTO Standard Specifications addresses embedment anchors, and that definition may apply to a post-installed shear connector. The description of the scope of the section states that cast-in-place, grouted, adhesive-bonded, expansion, and undercut steel anchors are covered by the section.

The shear connector must resist horizontal as well as vertical movement (ASD 10.38.2.1 and LRFD 6.10.7.4.1a). Shear connectors are designed for fatigue, and that design is checked for strength (ASD 10.38.5.1 and LRFD

6.10.7.4.1b). Fatigue typically controls the design, and the strength calculation is a formality. Composite design requires that shear connectors be located only in positive-moment regions, although they are suggested to be used the entire length of the bridge in continuous spans (LRFD 6.10.7.4.1). If they are placed only in positive-moment regions, the region is permitted to be designed as simply supported. Shear connectors are required in negative-moment regions only when the reinforcing steel in the concrete slab is considered part of the composite section (ASD 10.38.4.2, LFD 10.52.1, and LRFD 6.10.7.4.1). The connectors are permitted to be placed at regular or variable intervals (ASD 10.38.4.2 and LRFD 6.10.7.4.1), but the spacing is limited by the calculated required pitch, and by the maximum and minimum spacing requirements noted earlier.

### 3.3.5   AASHTO Requirements for Calculating Flexural Capacity

All AASHTO design provisions require full composite action when designing the flexural capacity of a cross-section, and the composite moment of inertia method is used to calculate the stresses in the composite slab and girder in all AASHTO design methods. It is preferred that composite sections be designed so that the neutral axis lies below the top surface of the steel girder, to use the full compressive capacity of the concrete. The design procedure varies slightly in positive and negative moment regions, but the flexural design strength using LFD and LRFD provisions is calculated assuming the development of the full plastic capacity of the reinforced concrete slab and the steel girder (Figure 3.2).
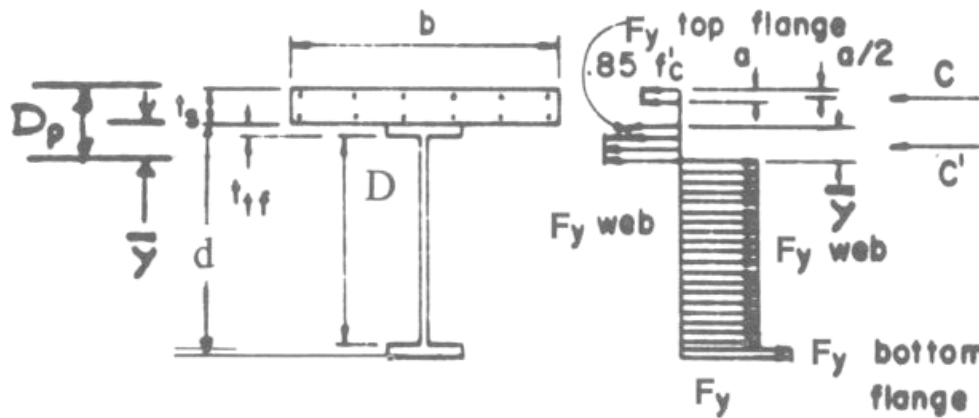
***Figure 3.2: Composite cross section and plastic stress distribution as defined in AASHTO LFD provisions***

Also with respect to flexural capacity, the all AASHTO design methods require additional connectors as anchorages at dead-load points of inflection when no connectors are placed in the negative moment region of the span (ASD 10.38.4.2 and LRFD 6.10.7.4.1).

In the author's opinion, two concerns exist with current AASHTO design procedures.

o      First, calculated flexural capacity is based on a plastic stress distribution that may not be attainable because another failure mode such as lateral-torsional buckling may occur first.  As a result, an excessive number of shear studs may be required according to design calculations.

o      Second, although partially composite design was apparently permitted in prior editions of the AASHTO LFD, the current edition contains no provisions explicitly permitting partially composite design.  The history associated with this is thoroughly discussed in the next section.

### 3.3.6 Historical Review of AASHTO Treatment of Partial Composite Design

As noted in earlier in the chapter, partial composite design would permit member capacity to be governed by the shear capacity of the studs. Although exhaustive demonstration of this is not within the scope of this thesis, partial composite design often permits a much smaller number of shear studs (and hence much more economy), at the cost of only slight decreases in flexural capacity. This is particularly relevant for this study, because partial composite design could make retrofit options more feasible.

In conducting the preliminary literature review for this study, it was noted that while the 15th Edition of the AASHTO *Standard Specifications for Highway Bridges* (1992) contained an equation apparently used for partial composite design, that equation did not appear in the 16th Edition of the same provisions (1996), nor in subsequent and current editions.

This matter was therefore investigated further. The design equation that apparently allowed partial composite design existed in LFD Article 10.50.1.1 of the 1992 AASHTO *Standard Specifications for Highway Bridges,* 15th Edition. A corresponding equation did not exist in the ASD section of that document. The partial composite design equation in the AASHTO LFD provisions was removed prior to the 1996 *Standard Specifications,* 16th Edition. Further investigations revealed that the Section C10.50.1.1.1 of the *Commentary* to the 1995 *Interim Specifications for Division I-Design* discussed the removal of the equation: "It is proposed that Equation (10-124) [in the LFD section] be eliminated."

In the 15th Edition of the *Standard Specifications*, in calculating the ultimate flexural capacity, the design compressive force in the concrete slab, C, was calculated by Equation (10-124) in Article 10.50.1, repeated here as Equation 3.3,

21

$$C = \Sigma Q_u \qquad \textit{(Equation 3.3)}$$

where $\Sigma Q_u$ was the sum of the ultimate strengths of the shear connectors between the cross-section under consideration and the section of zero moment. This equation apparently would have controlled if partial composite design had been used. As noted in the Commentary to the 15th Edition, "This equation is redundant because the sum of the shear stud capacities must equal or exceed the forces given by Equations (10-122) and (10-123)…" In the 15th Edition, Equation (10-122) was used to calculate the resultant of the fully plastic stress distribution of the concrete slab, and Equation (10-123) was used to calculate the resultant of the fully plastic stress distribution of the steel girder. The Commentary to the 15th Edition continues, "…according to the design provisions specified for shear studs in Article 10.38.5.1.2 [in the ASD section]."

Again in the 15th Edition, Article 10.38.5.1.2 *Ultimate Strength* in ASD states that "The number of connectors so provided for fatigue [ASD 10.38.5.1.1] shall be checked to ensure that adequate connectors are provided for ultimate strength." The article continues with several equations used to calculate the required number of shear connectors based on the force in the concrete slab and the ultimate strength of a shear connector. The force in the concrete slab, at points of maximum positive moment, is again the lesser of the resultants of the fully plastic stress distribution of the steel girder and the fully plastic stress distribution of the concrete slab. There is no equation for the summation of ultimate strengths of the shear connectors.

Based on that literature search, it was concluded that in the 15th Edition of the *Standard Specifications*, ultimate flexural strength is permitted to be calculated using LFD, but the number of shear connectors must be determined by ASD (LFD 10.52.2). This explains why ASD 10.38.5.1.2 supersedes any value

calculated from Equation (10-124) in LFD 10.50, and why that equation was subsequently removed.

Although a superficial reading of AASHTO design provisions might indicate that partial composite design was briefly allowed in bridge design, closer inspection showed that it in fact has never been permitted. The 1995 Interim Commentary Section C10.50.1.1.1 concludes with the following: "Equation (10-124) may control when utilizing partial composite action; however, partial composite action is not currently permitted by AASHTO. Removal of this equation eliminates an unnecessary step in the design of composite beams and girders."

In considering possible reasons for the prohibition of partial composite design from the AASHTO *Standard Specifications for Bridges* and the LRFD Bridge Design Specifications, the author notes that partial composite design requires that some shear connectors undergo inelastic deformation near ultimate capacity. This could cause connectors to fail in fatigue. In the author's opinion, the history of this issue is worth investigating further.

## 3.4   DISCUSSION OF MODELS FOR CALCULATING LOAD-SLIP DEMAND

As a composite member is loaded, the load-slip demand on the shear connectors sustaining that composite action can be predicted using analytical equations based on engineering mechanics, empirical relationships, and more recently on finite-element analyses. The analytical models can calculate load-slip demand in two ways:

o       the demand on the anchor is calculated from the applied load, taking into account the behavior of the entire composite member; or

o      the demand on the anchor is calculated from the applied load based on engineering mechanics, and that demand is related to the response of the entire composite member in an iterative process.

Load-slip demands may also be determined through finite element modeling. Material models used in a serviceability analysis may be considered linear-elastic because the response of the structure to the applied loads does not exceed the elastic range. Nonlinear springs whose load-slip behavior is set to match experimentally determined behavior, can be used to model the exact load-slip behavior of a shear connector. This approach is especially effective in the determination of force and slip demands under service loads. This approach is thoroughly discussed in Chapter 7.

The slip of a connector at the ultimately capacity is important only when considering the ultimate limit state of the bridge, and the ultimate limit state provision is not as significant in bridge design as the serviceability limit state. This relationship is demonstrated in the procedure for the composite design of bridges, where fatigue requirements typically control the design of shear connectors. Fatigue requirements and allowable deflections are both limit states that are considered in investigating slip under service loads.

## 3.5   DISCUSSION OF MODELS FOR CALCULATING LOAD-SLIP RESPONSE

The load-slip response of the shear connectors sustaining the composite action is primarily predicted using empirical equations. The predictive models are based on the ultimate strength limit state.

The most common relation for the ultimate capacity of a welded shear stud is the empirical equation developed by Ollgaard *et al.* (1971), using a curve-fit to the results of a series of push-out tests (Figure 3.3) on welded shear studs.
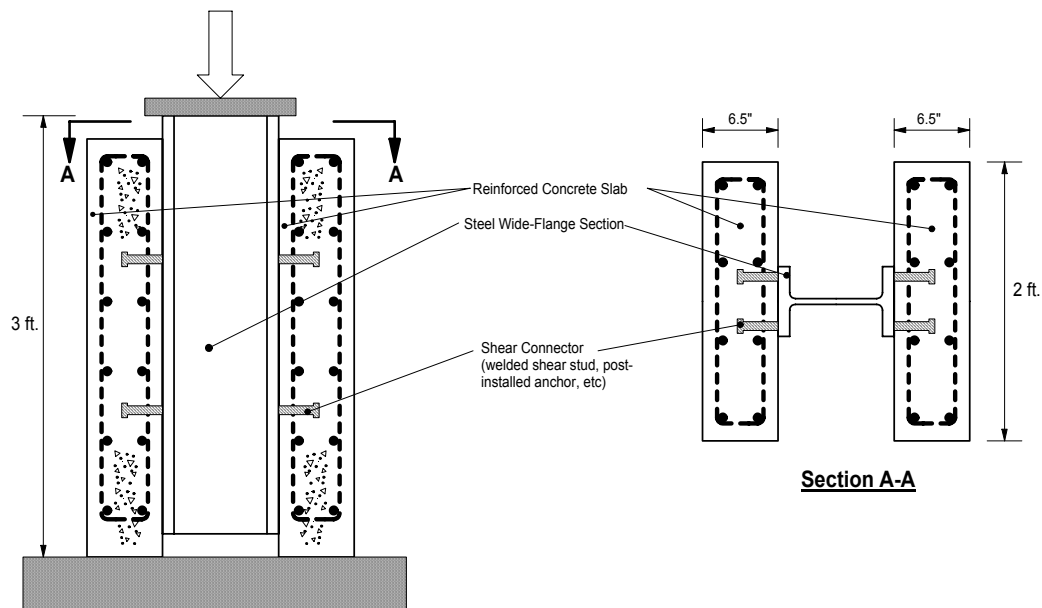
*Figure 3.3: Schematic of a typical push-out test*

In push-out tests a compressive force is applied to a steel wide-flange section that is connected on each flange to two concrete specimens. Each half of the test setup has four shear connectors between the concrete and steel. The load-slip behavior of a single connector is developed using the applied load divided by eight, and the measured displacement of the steel section relative to the concrete section.

The tests performed by Ollgaard *et al.* (1971) varied the compressive strength of the concrete, the diameter of the shear stud, and the number of shear studs in a specimen. The empirical strength equation so developed is discussed in detail later in this thesis. It involves relatively few variables, and has been used successfully in design by the AISC LRFD provisions (buildings) and the AASHTO LRFD provisions (bridges).

This empirical equation for ultimate strength may also be used in conjunction with another empirical equation developed by Ollgaard *et al.* (1971) to describe the complete load-slip behavior of a shear stud.

# CHAPTER 4

# Preliminary Studies and Results

## 4.1    PRELIMINARY REMARKS

This chapter includes a discussion of the results of inspections of representative central Texas bridges that were selected as potential prototypes for retrofitting for composite action.  Based on those inspections, an idealized prototype bridge is created, and used to develop a test setup for obtaining the load-slip behavior of single connectors, for performing preliminary design and cost analyses, and for modeling load-slip limits in finite-element analyses.

Because several retrofitting methods for composite action use static friction as the primary mechanism of shear-force transfer, determination of an appropriate design value for the coefficient of static friction is very important.  As described in this chapter, based on the variability of the surface conditions at the concrete-steel interface, it was judged useful to perform tests to measure the coefficient of static friction.  Those tests are explained in detail here.

## 4.2    BRIDGE INSPECTIONS

### 4.2.1    General Description

This research study required identification and site-specific observations of typical prototype bridge structures that would be candidates for retrofitting by the addition of shear connectors.  These observations were necessary to understand such prototype structures in general, and also get a better idea of the field variability of support conditions, expansion joints, structural elements, and interface conditions.  Six candidate bridges located on the north side of San

27

Antonio, Texas were selected for their geographic proximity to Austin, Texas and to each other. Corresponding bridge numbers are given in Table 4.1, and locations highlighted in Figure 4.1. The bridges were inspected on March 22, 2003.

*Table 4.1: Numerical identification of 6 bridges identified as potential*
*prototypes and examined in field study*

| Bridge Name | Bridge Number | Traffic Carried | Year Built | Year Reconstructed |
|---|---|---|---|---|
| Huebner Road | 12 and 13 | IH-10 Eastbound and Westbound | 1961 | 1994 |
| Honeysuckle Lane | 10 and 11 | IH-410 Eastbound and Westbound | 1961 | 1976 |
| Walzem Road/FM 1976 | 15 | IH-35 Southbound | 1962 | 1983 |
| Binz-Engelman Road | 17 and 18 | IH-35 Northbound and Southbound | 1962 | N/A |
| Southern Pacific Railroad and FM 78 | 31 | IH-410 Southbound | 1953 | 1994 |
| Southern Pacific Railroad and IH-35 Northbound | 20 | IH-410 Connection to Freeway | 1964 | 1989 |
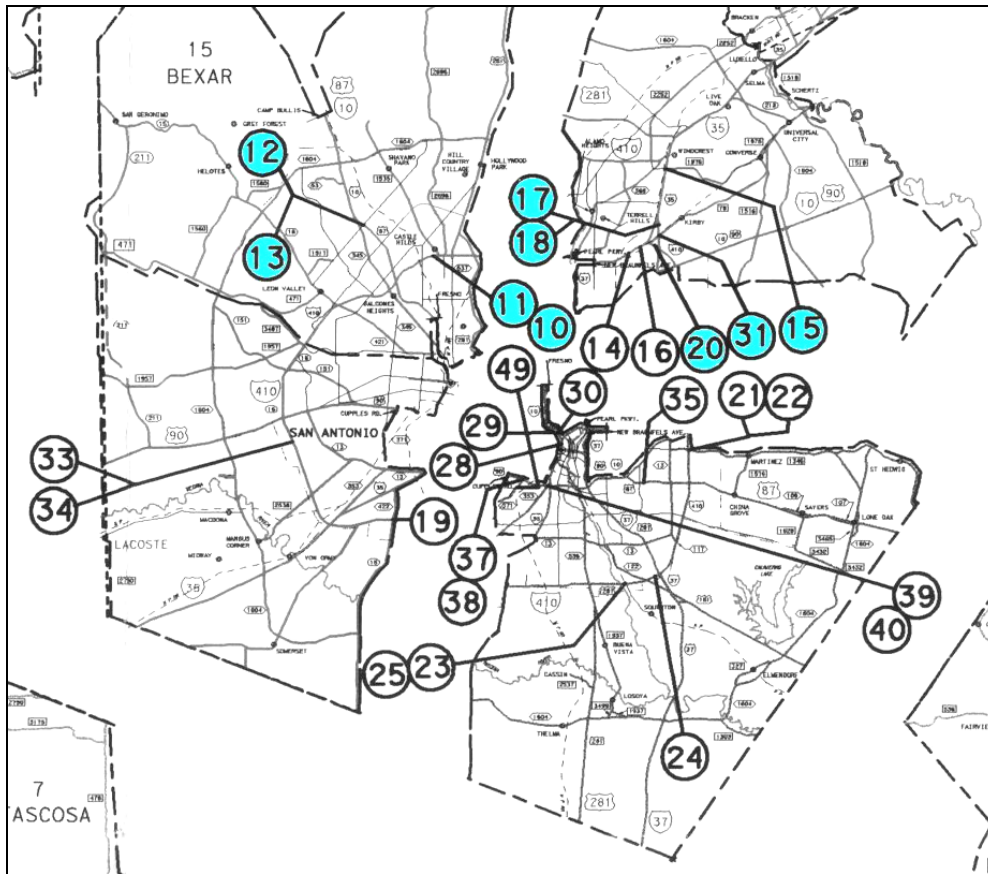
*Figure 4.1: Map of TxDOT bridges near San Antonio, showing bridges identified as potential prototypes and examined in this study*

The weather on March 22 was fair during inspections of the first 4 bridges, and light rain for the last 2 bridges. The rain gave an excellent opportunity to examine for water penetration to the underside of the bridge decks.

### 4.2.2   Characteristics and Ages of Identified Bridges

All six inspected bridges crossed interstate highways, heavily traveled roads in urban areas, and railroad tracks. The bridges carried major interstate traffic, implying that lane closures would result in significant direct and indirect costs. An example of this heavy traffic is shown in Figure 4.2 for the Huebner

Road bridge. It would therefore be a considerable benefit if a proposed retrofitting scheme did not require lane closures. Because of heavy surrounding urban traffic, any retrofitting work performed underneath the bridge would probably need to be done from a snooper or a platform supported over ground-level traffic. Because some of the bridges are quite high (Figure 4.3), the platform would probably have to be supported from the bridge itself rather than the ground.



*Figure 4.2: Urban traffic at Huebner Road bridge*

*Figure 4.3: Southern Pacific Railroad and FM 78 bridge, showing typical high clearance*

Most of the bridges examined in the field portion of this study had been constructed in the early sixties, and were reconstructed within the last twenty years. These bridges are in relatively good condition because of their relatively recent construction, and even more so because of their relatively recent reconstruction. As a result, TxDOT is very interested in keeping the existing structural components, and in investigating post-installed shear connectors as an alternative to removing the concrete deck or replacing the girders.

### 4.2.3 Structural Layout and Dimensions of Potential Prototype Bridges

Table 4.2 indicates the basic configurations of the bridges examined in the field portion of this study. Span lengths range from 50 to 60 ft, and the transverse girder spacings from 6.75 to 8 ft. The span length determines the minimum number of connectors. Based on a maximum center-to-center connector spacing

of 2 ft as specified in AASHTO and a span of 50 ft, the minimum number of shear connectors is 25.

The maximum number could also be affected by span. AASHTO ASD and LFD provisions allow a minimum pitch (center-to-center longitudinal spacing) of 4 in., while the AASHTO LRFD provisions allow 6 in. For a 50-ft span, these requirements result in maxima of 150 and 100 shear connectors respectively.

*Table 4.2: Configurations of potential prototype bridges examined in field study*

| Bridge Number | Span Type | Number of Spans | Maximum Clear Span (ft) | Girder Spacing (ft) |
|---|---|---|---|---|
| 12 and 13 | Continuous | 4 | 60 | 8 |
| 10 and 11 | Continuous | 4 | 60 | 8 |
| 15 | Continuous | 4 | 55 | 7 |
| 17 and 18 | Continuous | 4 | 55 | 7 |
| 31 | Continuous | 9 | 50 | 6.75 |
| 20 | Continuous | 9 | 60 | 7 |

All six investigated bridges were continuous across interior supports except the 9-span bridges, which had an expansion joint at an intermediate support. All bridges had roller-rocker supports at abutments.

*Figure 4.4: Continuous structure over interior supports on Southern Pacific Railroad and IH-35 Northbound bridge*

*Figure 4.5: Expansion joint at an interior support on the Southern Pacific Railroad and FM 78 bridge*



*Figure 4.6: Roller-rocker support at abutment of Huebner Road bridge*

TxDOT bridge decks have a typical minimum design thickness of 7 in. Several field measurements of the bridges examined in this study showed slab thicknesses from 8 to 9 in. This excess thickness is usually due to transverse slopes for drainage and variations in slab elevation at vertical curves. The minimum specified slab thickness of 7 in. determines the maximum height of the shear connector, because current AASHTO provisions require a 2-in. cover between the roadway surface and the top of the shear connector. The resulting maximum height of the connector is 5 in.

As shown in Table 4.3, for bridges examined in the field portion of this study, the steel girders ranged in depth from about 28 to 36 in. This dimension is important because it determines the vertical clearance available for tools and retrofitting operations when working from the bottom of the top flange. The flange width and thickness were also of particular interest because these dimensions are critical to the design of individual post-installed shear connectors.

***Table 4.3: Dimensions of steel girders in potential prototype bridges examined***
***in this study***

| Bridge Number | Height (in.) | Web Depth (in.) | Web Thickness (in.) | Flange Width (in.) | Flange Thickness (in.) | Cover Plates (Y/N) |
|---|---|---|---|---|---|---|
| 12 and 13 | 32-1/4 | 31-1/4 | 1/2 | 11-1/2 | 7/8 | N |
| 10 and 11 | 36 | 34-1/4 | 3/4 | 12 | 7/8 | Y |
| 15 | 27-1/2, 33 | 25-1/2, 31-1/8 | 9/16, 3/4 | 14-1/8, 11-1/2 | 1-1/8, 7/8 | N |
| 17 and 18 | 33 | 31-1/8 | 3/4 | 11-1/2 | 3/4 | N |
| 31 | 29-3/4 | 28-1/4 | 3/4 | 10-1/4 | 3/4 | N |
| 20 | 36 | 34 | 5/8 | 12-1/4 | 1 | N |

Flange widths ranged from about 10 to 14 in. Current AASHTO provisions require 1 in. between the edge of the girder flange and the edge of the connector, and impose a minimum center-to-center transverse spacing of 4 in. This allows two or three connectors to be placed transversely on a girder flange. For the example of a 3/4-in. diameter anchor, the maximum number of connectors that can be placed transversely in each row depends on whether the flange width is less than or greater than 10.75 in.
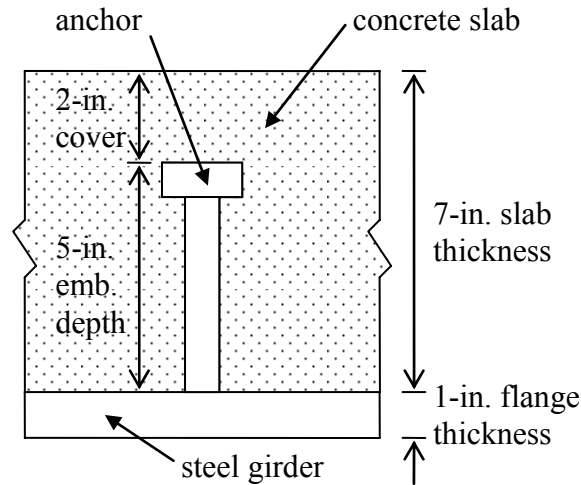
*Figure 4.7: Idealized girder flange, concrete slab, and anchor dimensions*

Measured flange thicknesses ranged from 3/4 to 1-1/8 in. This dimension combined with the maximum allowable embedment depth of 5 in., determined that the maximum length of the shear connector from the bottom edge of the flange as 6 in. This length is used in sizing anchors through the flange.

### 4.2.4    Development of Idealized Prototype Bridge

Using the dimensions of typical bridges studied in the field inspections, an idealized prototype bridge was developed for this study. The idealized prototype was intended as the basis for the single-anchor test setups, and for calculations of slab bending stiffness and tributary dead weight, for finite-element analyses, and for preliminary cost comparisons.

The idealized prototype bridge is a simply supported 50-ft span, with a 7-ft transverse spacing between steel girders. The girders are connected to a 7-in. concrete deck with shear connectors spaced at the maximum permitted pitch of 2 ft. The resulting concrete slab tributary volume was 7 ft wide, 2 ft long, and 7 in. thick. The steel girder was 36 in. high with a flange width of 1 ft, and 1-in. web and flange thicknesses.
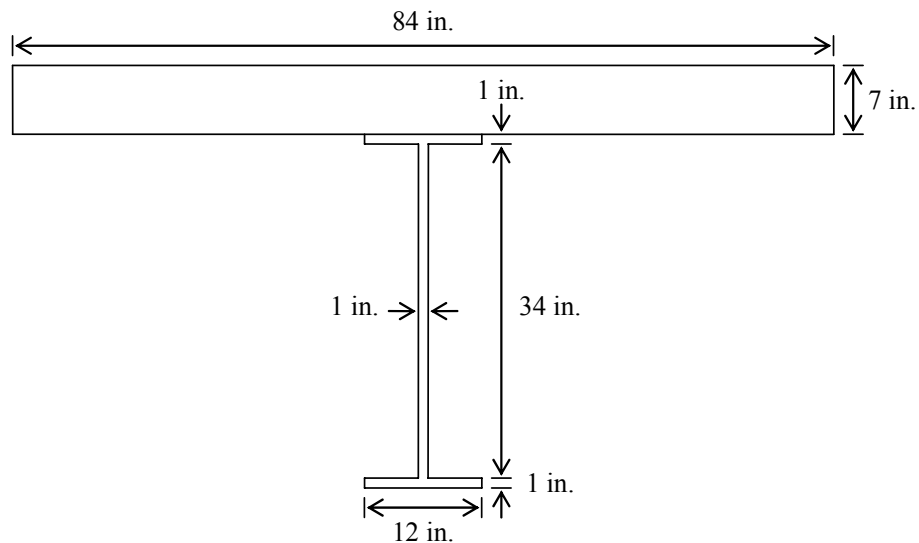
*Figure 4.8: Cross-section of idealized prototype bridge*

### 4.2.5 Physical Condition of Observed Bridges

#### 4.2.5.1 General Remarks on Physical Condition

All observed bridges were in good overall condition; their concrete decks were in excellent shape and the steel girders were well painted and largely rust-free. The bridges appeared relatively new, and it was very clear why TxDOT prefers to keep the existing structural components.

The top flange of the outermost girders was typically embedded in the underside of the deck concrete. Although this was probably done to reduce weathering of the concrete-steel interface, it did not always appear to accomplish this objective, judging by the example shown in Figure 4.9.

*Figure 4.9: Spalling and rust at interface near abutment of Binz-Engleman Road bridge*

Several bridges had minor rusting where paint had worn away from the surface. Nearly every bridge had significant rusting at diaphragms and expansion joints (for example, Figure 4.10). In several bridges, the concrete at expansion joints had cracked and spalled due to excessive rusting (for example, Figure 4.11).

***Figure 4.10: Expansion joint gap, rust at interface, and peeling paint near
abutment of Walzem Road/FM 1976 bridge***

### 4.2.5.2   Concrete Cracking and Spalling

In general, most concrete spalling in the inspected bridges occurred
adjacent to a steel flange, probably as a result of rusting of the steel reinforcement
in the concrete due to penetration of water through cracks in the concrete, and to
water trapped between the slab and the girder.  These conditions may have caused
lamellar rusting of the upper surface of the top flange of the girder.  A substantial
amount of water entered through expansion joints like the one pictured in Figure
4.10.

*Figure 4.11: Extensive spalling and rust at interface of the slab and girder near the abutment of Southern Pacific Railroad and IH-35 Northbound bridge*



*Figure 4.12: Close-up of spalling and rust shown in Figure 4.11*

Any loss, cracking or deterioration of concrete would have been significant concerns in evaluating the probable performance of a retrofitting method using post-installed shear connector. Such conditions were rare in the inspected bridges, however.

### 4.2.5.3 Rust

For the inspected bridges, significant rust was generally present at lateral bracing locations. The rust creates a stain extending the full depth of the girder from the point where the bracing is welded to the top flange of the girder (Figure 4.13 and Figure 4.14)



*Figure 4.13: Extensive rust at lateral bracing on Southern Pacific Railroad and IH-35 Northbound bridge*

*Figure 4.14: Rust at lateral bracing on Binz-Engleman Road bridge*

This rust was observed to penetrate the concrete-steel interface at some lateral bracing locations. Such rusting may be a concern for methods where welding or friction is used, because major efforts may be required to clean the rust away to create a suitable surface for welding. Also, the coefficient of friction is likely to be highly variable if the rust has created distinct lamellar layers, as observed in some bridges.

*Figure 4.15: Expansion joint at abutment, rust, and pouring water on Southern Pacific Railroad and IH-35 Northbound bridge*

On one particular bridge (Southern Pacific Railroad and IH-35 Northbound), water was seen at the interface of the concrete and steel. This created clearly visible rust layers in addition to rust from lateral bracing and possibly to reinforcement. The water probably had entered the interface via the expansion joints. In one location on this bridge, where there was a considerable separation between the concrete and steel, water was visibly ejected from the concrete-steel interface each time a vehicle passed overhead.

## 4.3    FIELD STUDIES OF THE COEFFICIENT OF STATIC FRICTION

### 4.3.1    Preliminary Remarks

Because many of the methods investigated in this study for increasing composite action depend primarily on shear transfer by static friction, it is important to have reliable values, under probable field conditions, for the coefficient of static friction between steel and concrete cast against the steel. Although a value of 0.7 is indicated by Section 11.7.4.3 of ACI 318-02 as a coefficient of static friction between rolled steel and cast concrete, that value may not be applicable to the interface conditions observed in the bridge inspections described earlier in this chapter.

To determine reliable values under probable field conditions, a portable test setup was devised and constructed for measuring the coefficient of static friction in the field.  As shown in Figure 4.19, it applied a known horizontal force to a concrete block of known weight placed on the upper surface of the flange of a steel girder.  The coefficient of static friction was calculated as the quotient of the horizontal force at first slip of the block, divided by the block's weight.  Using this apparatus, 24 friction tests were performed on July 28, 2003 on four steel girders from the prototype bridge over Honeysuckle Lane in San Antonio, Texas. This bridge, shown in Figure 4.16, was undergoing demolition during this study, and the situation offered the opportunity to determine the coefficient of static friction on aged steel girders removed from a typical prototype bridge.   The underside of the bridge deck before demolition is shown in Figure 4.17.   The girders had been removed from their locations in the bridge, exposing the upper surfaces of the top flanges.

*Figure 4.16: Honeysuckle Lane bridge during demolition*



*Figure 4.17: Typical conditions on underside of Honeysuckle Lane bridge*

### 4.3.2 Field Conditions for Tests to Determine the Coefficient of Static Friction

Friction tests were performed on four girders previously removed (from unknown locations) on this bridge. The first girder was tested at both ends and the middle. The next two girders were tested at the one end and the middle ends, and the last girder was tested at one end only. At each location selected for test, the smaller region at which the coefficient of friction was evaluated was selected to permit measurement on a wide range of surface conditions.

The surface conditions of the steel girders varied greatly, from areas nearly untouched by rust, to areas with flaky layers of rust. Tests were conducted in areas throughout the range between these two extremes. An area of relatively severe rusting is pictured in Figure 4.18.



*Figure 4.18: Surface conditions of steel girder and base of concrete test block*

### 4.3.3 Details of Test Apparatus for Measuring the Coefficient of Static Friction

The test apparatus for measuring the coefficient of static friction is shown in Figure 4.19. Shown in the right-hand side of that figure is a 10- x 8- x 3-1/2 in., normal-weight concrete block. To attain an interface roughness similar to that between a concrete deck cast on a steel girder, the block was cast against the upper surface of a steel plate. To have a means of pulling the block horizontally, an eyebolt was cast in the middle of one side. The concrete block and eyebolt weighed 20.06 lb.
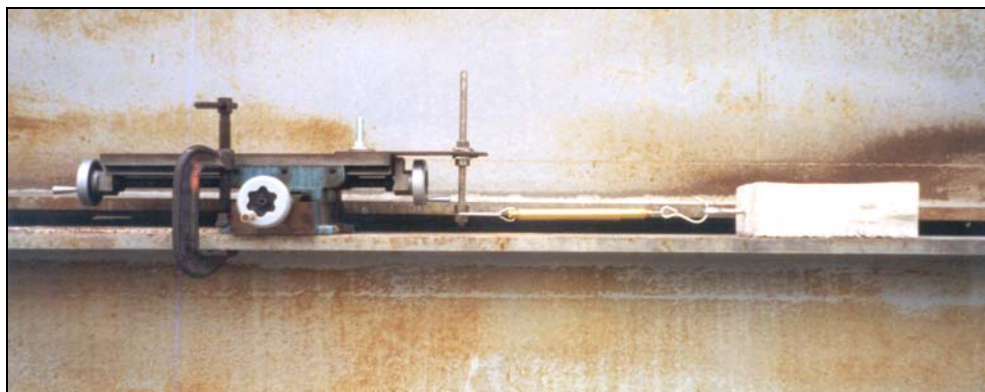


*Figure 4.19: Side view of test setup to measure the coefficient of static friction*

A horizontal force was applied to the block, parallel to the girder axis, using a cross-slide milling table whose base was clamped to the girder, and which could slide in those lubricated tracks on that base in response to rotation of a geared dial. Rotation of the dial applied a gradually increasing horizontal force to the concrete block. The horizontal force was transmitted through a threaded rod connected to a 50-lb spring scale. Nuts on either side of the hook to the spring scale ensured that the hook did not move vertically relative to the threaded rod during testing, and also permitted fine vertical adjustment to position the spring

49

parallel with the girder surface.  The spring was hooked to the eyebolt in the concrete block.

To measure the longitudinal inclination (if any) of the upper surface of the top flange of the girder, this inclination was measured with a T-square and a pendulum (Figure 4.21).  A T-square was fitted with a protractor, and weights hanging from a string were attached at the origin of the protractor.  The weights always hung straight down, while one leg of the T-square was placed longitudinally on the upper surface of the top flange of the girder.  The value of the angle of inclination was read from the protractor (Figure 4.21).
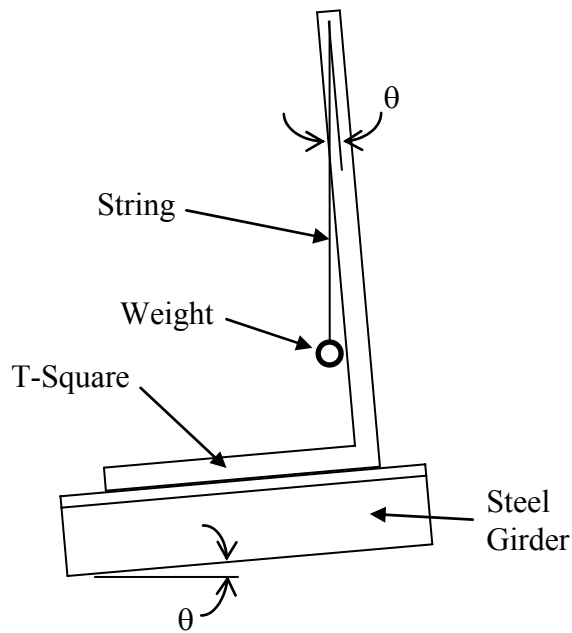


***Figure 4.20: T-square and pendulum device***

*Figure 4.21: Use of T-square and pendulum to determine longitudinal inclination of girder during tests to determine static coefficient of friction*

### 4.3.4    Test Procedure to Determine Static Coefficient of Friction

Each test to determine the static coefficient of friction was performed as follows:

o       The longitudinal inclination of the upper surface of the top flange of the girder surface was measured with the T-square and pendulum device.

o       The nuts on the threaded rod were adjusted so the spring scale would be parallel with that upper surface.  The dial on the cross-slide milling table was turned slowly and smoothly to apply a gradually increasing force parallel to the girder axis.  When the block slipped, the force in the scale was read to the nearest 0.25 kg.

The coefficient of static friction, $\mu$, was calculated as follows, using the free-body diagram of Figure 4.22.

51
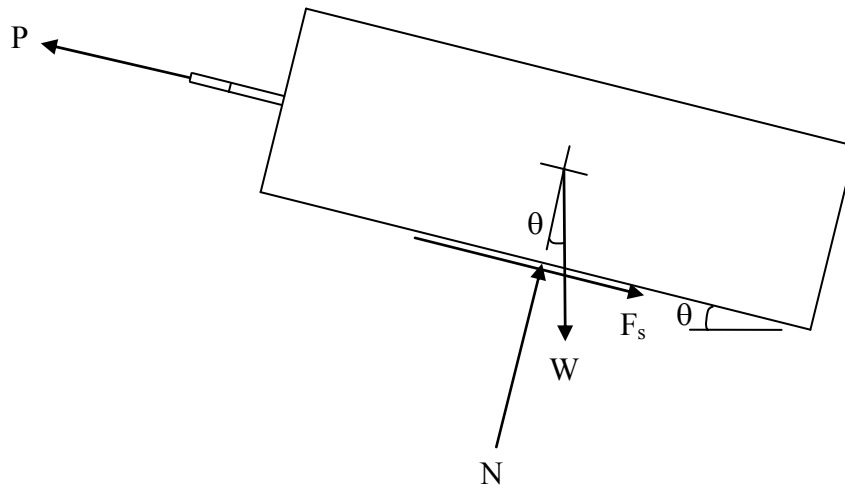
*Figure 4.22: Free-body diagram of the concrete block*

In that figure,

$F_s$ = static friction force

P = applied force at slip, parallel to the girder surface

W = weight of the concrete block

N = normal force of girder surface on concrete block

$\theta$ = horizontal inclination of girder axis

The static friction force was calculated by Equation 4.1.

$$F_s = P - W \cdot \sin(\theta)$$                    *(Equation 4.1)*

The normal force was calculated by Equation 4.2.

$$N = W \cdot \cos(\theta)$$                    *(Equation 4.2)*

The coefficient of static friction was then given by Equation 4.3.

$$\mu = \frac{F_s}{N}$$                    *(Equation 4.3)*

### 4.3.5 Results of Tests to Determine the Coefficient of Static Friction

The results of tests to determine the coefficient of static friction are summarized given in Table 4.4 and presented graphically in Figure 4.23. Results of all friction tests are given in Appendix A.

*Table 4.4: Summary of tests to determine coefficient of static friction*

| Maximum | 0.77 |
|---|---|
| Mean | 0.63 |
| Minimum | 0.50 |
| Coefficient of Variation | 0.10 |
| Precision | 0.04 % |
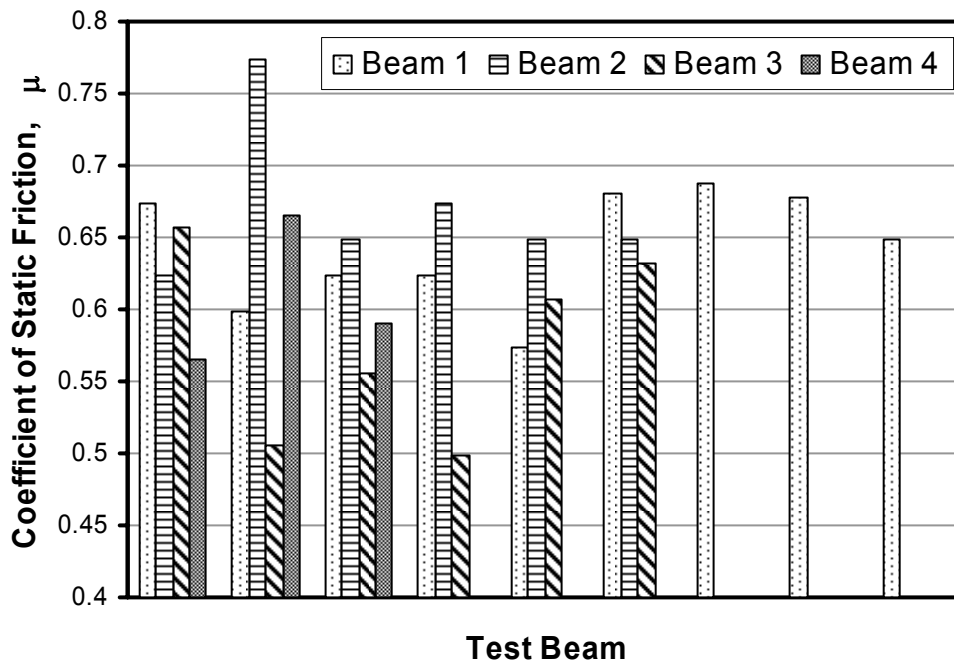
*Figure 4.23: Results of tests to determine the coefficient of static friction*

The mean of the results of the tests to determine the coefficient of static friction was relatively close to, yet lower than, the coefficient value of 0.7 as indicated in Section 11.7.4.3 of ACI 318-02. The lower coefficient was expected because of the adverse conditions of the concrete-steel interface.

Three concerns beyond the mean computed value of the friction coefficient must be considered when determining the coefficient of static friction used in design. First, the minimum computed value of the coefficient of static friction was 0.50, over 20% less than the mean. Second, although the conditions under which the friction tests were performed were considered to be representative of all possible prototype bridges, interface conditions may possibly be worse in other bridges, and that possibility must be taken into consideration. Third, conservatism must be entered in the selection of the coefficient for design

purposes. Therefore, given the mean coefficient, the minimum computed coefficient, variable concrete-steel interface conditions, and conservatism in design, the coefficient of static friction used for design is suggested to be 0.4.

# CHAPTER 5

# Load-Slip Tests

## 5.1 PRELIMINARY REMARKS

To determine the basic load-slip behavior that could later be used to evaluate possible retrofitting methods, two basic test setups were investigated: push-out test setups and direct-shear setups. In this chapter, each setup is described; their advantages and disadvantages are noted; and reasons are presented for selecting the direct-shear setup. The direct-shear setup is then described further, along with the post-installed shear connectors to be tested using that setup. Finally, test procedures, instrumentation and data acquisition are described.

## 5.2 POSSIBLE TEST SETUPS FOR INVESTIGATING LOAD-SLIP BEHAVIOR OF SHEAR CONNECTORS

### 5.2.1 Push-Out Test Setup

Starting with the tests of Ollgaard *et al.* (1971), shear connectors have traditionally been evaluated using push-out tests. While this test method (and its associated test setup) has not been published as an ASTM standard, other documents such as the Eurocode (ENV 1994-1-1:1992) include specific requirements for the test setup (Figure 5.1). Both setups have traditionally used 4 connectors per side, as shown in that figure.
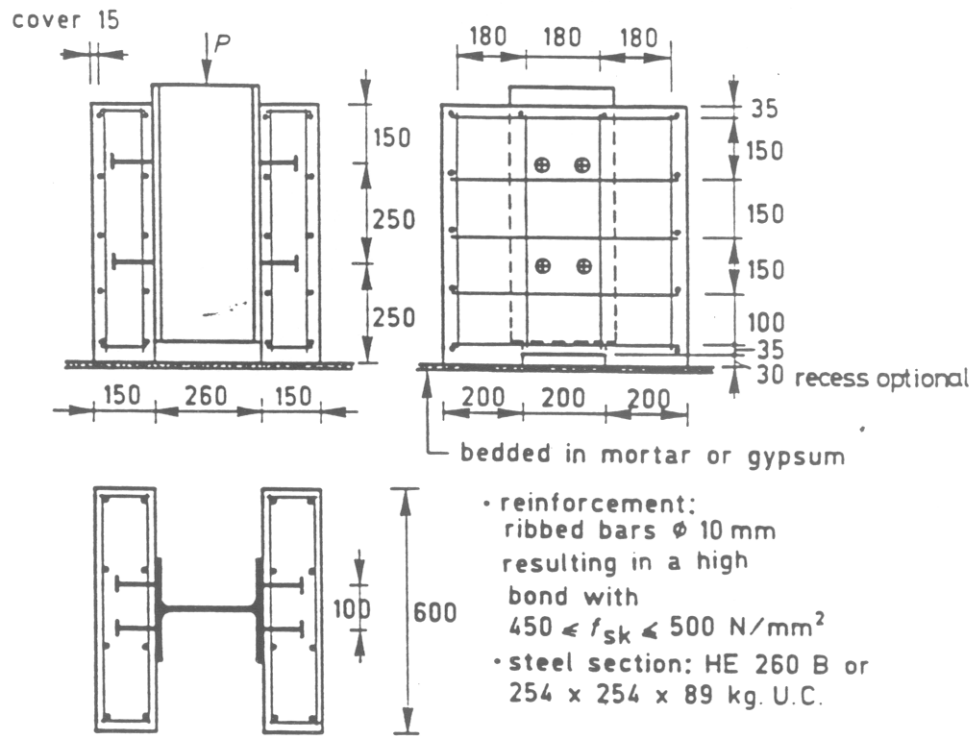
*Figure 5.1: Standard dimensions for the push-out test setup according to the Eurocode (SI units)*

The push-out test setup depicted in Figure 5.1 is used for what is termed a "fixed-base push-out test" because the bases of the concrete elements are embedded in mortar or gypsum, and cannot move horizontally. This setup effectively represents a finite-depth beam with pin supports at each end. The condition of zero longitudinal displacement at each support requires inward horizontal reactions, shown in Fig. 5.2(a). As shown in Figure 5.2, equal and opposite horizontal reactions at the pin supports are necessary to maintain the condition of zero horizontal movement of the two supported points.

57
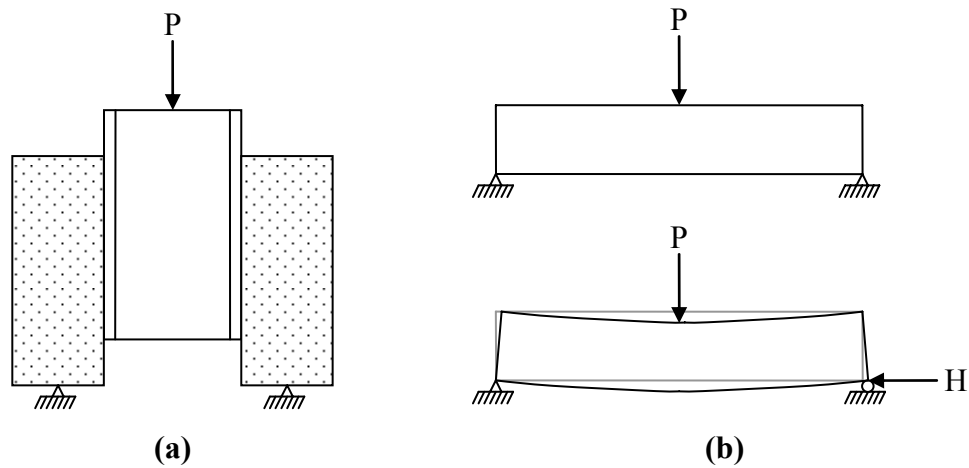
***Figure 5.2: (a) Model of a typical push-out test; (b) horizontal force resulting from a pin-pin support condition***

These horizontal reactions must be equilibrated at the steel-concrete interface by moments. These are not present in general in the prototype beam that the push-out test is intended to represent. They could be expected to reduce the observed shear capacity of the shear connector, and therefore are undesirable in a test method intended to establish load-slip behavior under pure shear.

These undesirable horizontal reactions can be eliminated using a variant of the push-out test (Figure 5.3(a)), termed the "roller-base" push-out test (Figure 5.3(b)). Even though this setup involves no external horizontal reactions, it still introduces tension in the anchor, as a result of bending moments in the specimen.

**(a)**                                 **(b)**
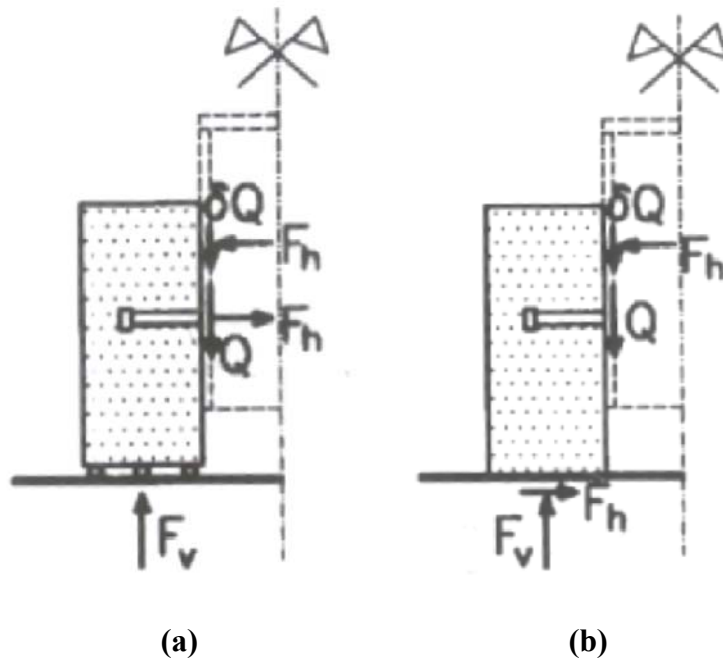
*Figure 5.3: (a) Forces on half of the fixed-base push-out test; (b) forces on half of the roller-base push-out test*

As shown in Figure 5.4 and Figure 5.5, both push-out test setups introduce tension in the connector, because both have moments at the centerline of the wide-flange section. These are resisted by tension in the connector, compression at the interface, and (for the fixed-base setup) inward horizontal reactions at the base.
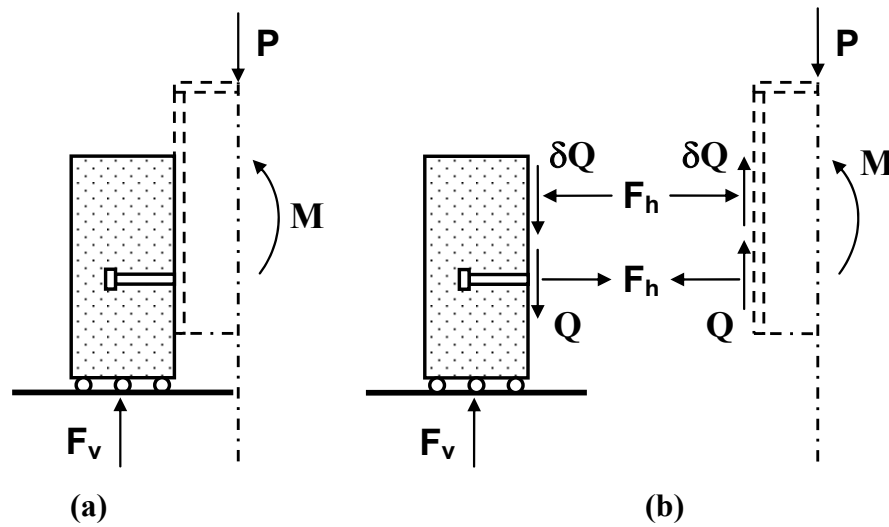
*Figure 5.4: (a) Free body diagram of half of the roller-base push-out test; (b) free body diagrams of the concrete-anchor and the steel wide flange for half of the roller-base push-out test*
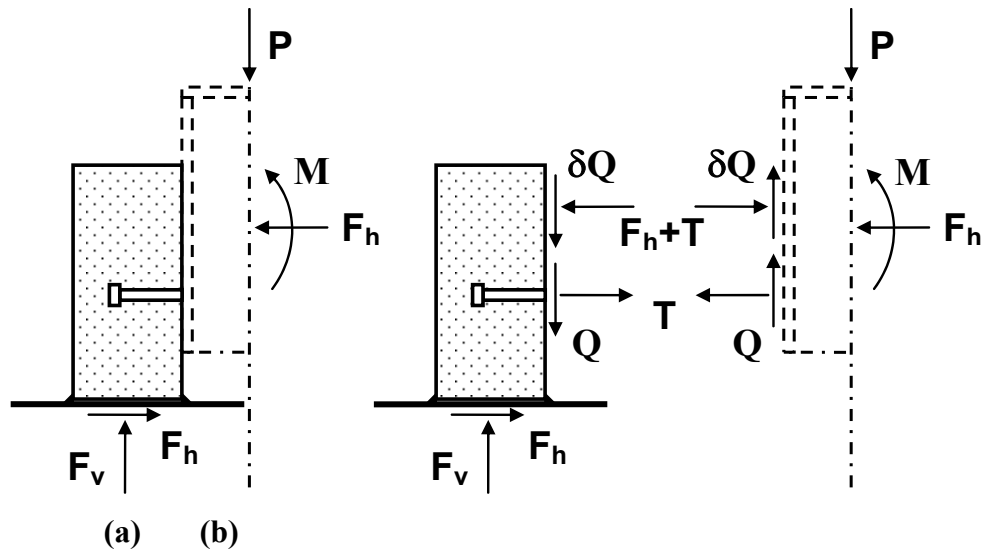


*Figure 5.5: (a) Free-body diagram of half of the fixed-base push-out test; (b) free-body diagrams of the concrete-anchor and the steel wide flange for half of the fixed-base push-out test*

The moment at the centerline of the wide-flange section is equal to the vertical reaction on each side of the specimen, multiplied by the horizontal eccentricity between that vertical reaction and the centerline of the wide-flange section (Figure 5.6).
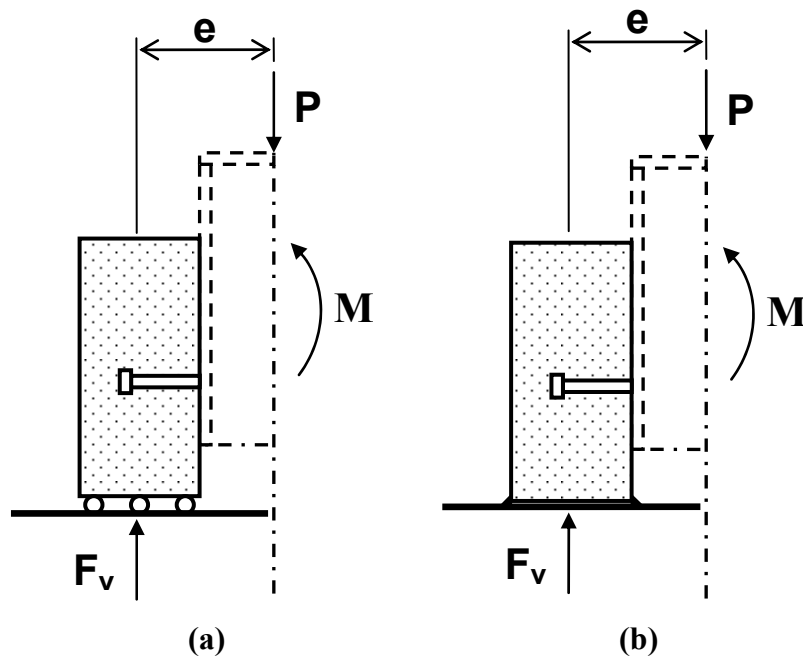


***Figure 5.6: Eccentricity of reaction relative to the applied load produces moment in both (a) the roller-base push-out test and (b) the fixed-base push-out test***

The vertical reaction on each side is presumed to act through the center of each concrete block, so the eccentricity is simply the one-half the horizontal distance between the centers of the concrete blocks. In the push-out test setup of Ollgaard *et al.* (1971), the eccentricity was 7.13 in.; in the Eurocode test setup (ENV 1994-1-1:1992) it is 130 mm plus 75 mm, or 205 mm (8.07).

In each setup, using 4 anchors per side, for example, a 200-kip applied load (nominally 25 kips per connector) produces moments of 178 kip-in. and 202 kip-in. in the setups of Ollgaard *et al.* (1971) the Eurocode, respectively. This moment must be resisted by the couple produced by a pair of equal and opposite horizontal forces, $F_h$ , separated by an internal eccentricity. To calculate the magnitude of those horizontal forces, it is necessary to know the vertical eccentricity between them. While that eccentricity depends on the relative stiffnesses of the different elements of the test setup, it can reasonably be assumed as at least equal to the vertical distance between the anchors.

Using that assumption, it is possible to estimate the significance of the tensile force introduced into the connectors by the roller-base push-out setup.

o    For example, for a roller-based setup with the dimensions of that of Ollgaard *et al.* (1971), loaded by 200 kips, the moment of 178 kip-in., divided by the vertical distance between the connectors (12 in.), and then divided by 2 (the number of connectors in each line), gives a tensile force per connector of 7.42 kips, about 30% of the nominal shear force of 25 kips per connector.

o    For a roller-based Eurocode setup, also loaded by 200 kips, the moment of 202 kip-in., divided by the vertical distance between the connectors (250 mm, or 9.84 in.), and then divided by 2 (the number of connectors in each line), gives a tensile force per connector of 9.05 kips, about 36% of the nominal shear force of 25 kips per connector.

In the fixed-based setup that Ollgard *et al.* (1971) actually used, the tensile forces would be less, because they would be reduced by the moment produced by the

inward horizontal base reactions.  In any event, however, it is clear that traditional push-out tests setups probably introduce connector tensions that are a significant percentage of the anchor shears.  It is also clear that these connector tensions are equilibrated by compressive forces at the steel-concrete interface, which, multiplied by the coefficient of friction there, can introduce significant resisting shears, and significantly reduce the shear experienced by each anchor.

Another problem of the push-out test is that the shear force acting on each individual connector is unknown during the test.  One critical connector must fail before the rest of the connectors.  It is unknown when this failure occurs, and which connector is critical.

To avoid these inherent difficulties with the traditional push-out test setup, it was decided to investigate conducting the load-slip tests of this study using a direct-shear setup.  In the next section, that setup is described.

### 5.2.2   Direct-Shear Test Setup

The direct-shear test setup is shown in Figure 5.7.  Though structurally very similar to the roller-base push-out test, it creates less moment at the shear plane, because it reduces the eccentricity between the applied load and the reaction in the concrete.  The structural similarity is displayed in Figure 5.8 and Figure 5.9.
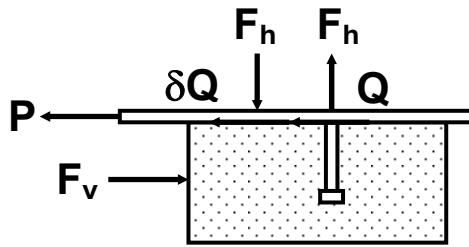
*Figure 5.7: Direct-shear test setup*
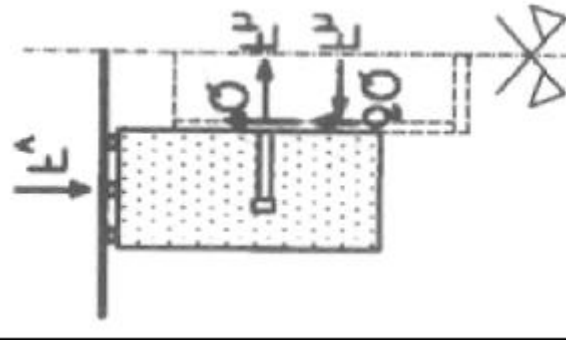


*Figure 5.8: Figure 5.3(b) rotated 90 degrees clockwise and flipped vertically to show similarity between direct-shear and push-out tests*
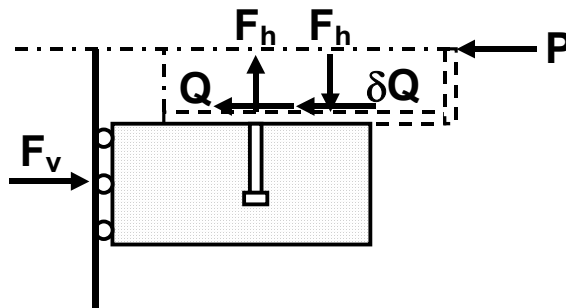


*Figure 5.9: Figure 5.8 redrawn with the applied load "P," showing similarity between direct-shear and push-out tests*

In this study, the direct-shear test setup was designed so that the longitudinal axis of the hydraulic actuator (the line of action of the applied force) would lie in the interface between the concrete block and the steel plate. This was

intended to minimize the eccentricity of the applied load relative to the shear plane. As is discussed subsequently in this thesis, however, the eccentricity of applied load was later found to be reduced but not eliminated by this design.

At this stage, in any event, it is useful to study the direct-shear test setup in more detail, to investigate the forces produced by it in the concrete block and the connectors. In a typical direct-shear setup, shown in Figure 5.10 below, the dimension "i" represents the spacing of the shear connectors in the direction of load (pitch). The vertical reactions $R_1$ and $R_2$ of that must be supplied in any actual test setup. In the direct-shear setup used in this study, those reactions are provided by two sets of two 3/4-in. threaded rods, spaced horizontally at 2 ft in the direction of applied load. In the direct-shear setup, a shear force Q is applied at the concrete-steel interface, as indicated in Figure 5.10(d).
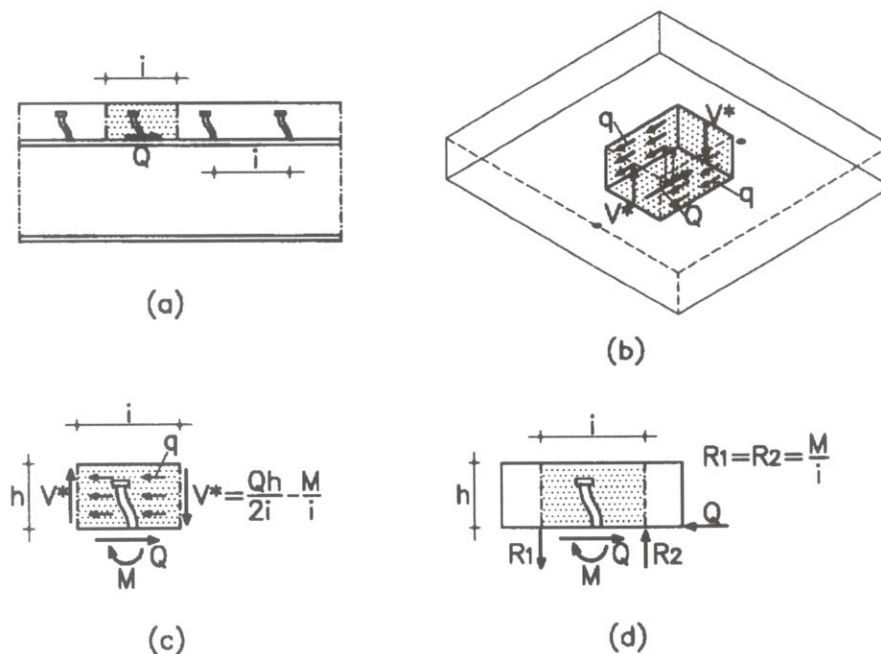


*Figure 5.10: Applied forces and reactions associated with direct-shear test setup: (a) element in the beam; (b) concrete element in three-dimensional view; (c) forces acting on the element; (d) forces acting on the specimen*

65

For convenience, push-out tests are usually conducted in compression using a universal testing machine. Direct-shear tests, in contrast, are conducted by applying tension to the steel plate, thereby avoiding potential buckling of the plate. By requiring less material and a simpler concrete-casting procedure, the direct-shear test can save material and time. These savings are partially offset by the need for a frame to hold the concrete block, however.

Calculations similar to those for the push-out tests can be conducted to determine the extraneous forces acting on the specimen in the direct-shear test setup. A load of 200 kips produces a moment of 112.5 kip-in. on a single connector. The moment must be divided by the vertical distance between the connectors (use 250 mm, or 9.84 in., from the Eurocode setup), and then divided by 2 (the number of connectors in each line), to give a tensile force per connector of 5.72 kips, about 23% of the nominal shear force of 25 kips per connector. This is 13 percentage points lower than the corresponding percentage in the Eurocode test setup.

In view of its greater degree of static determinacy, lower level of extraneous connector tension, and lower cost, the direct-shear test setup was selected for determining the load-slip behavior of connectors investigated in this study.

### 5.2.3 Single-Connector Test versus Group-Connector Test

After deciding to use a direct-shear setup, it was necessary to choose whether to test a single connector at a time, or multiple connectors. In this section, the advantages and disadvantages of each type of test are discussed.

In a single-connector test, the behavior of the single connector being tested is obviously known. In a group-connector test, elastic and inelastic distributions of load among connectors are unknown, and consequently the load-slip behavior

66

of individual connectors is also unknown.  Load-slip results from group tests are averages only.  For these reasons, it was decided to use single-connector tests in this study.

## 5.2.4  Details of Direct-Shear, Single-Connector Test Setup Used in this Study

The setup used in this study to conduct static loading tests on single connectors in direct shear consists of two components:  the first, for load application, includes the reaction frame, a 100-kip hydraulic actuator, and clevis; and the second, for data, includes instrumentation and data acquisition.  The test setup is shown schematically in Figure 5.11 and Figure 5.12, and in photographs in Figure 5.13 and Figure 5.14.
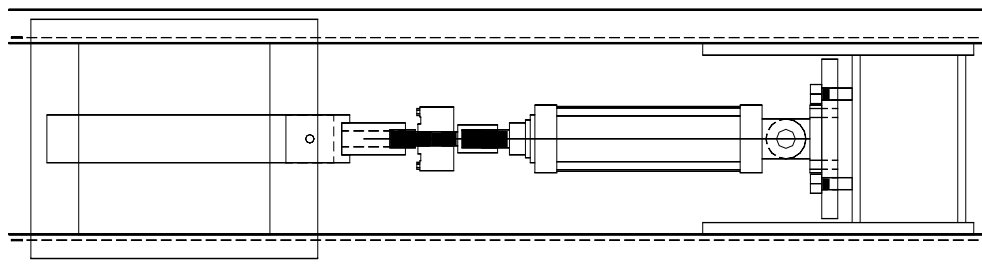


*Figure 5.11: Schematic of test setup (plan view)*
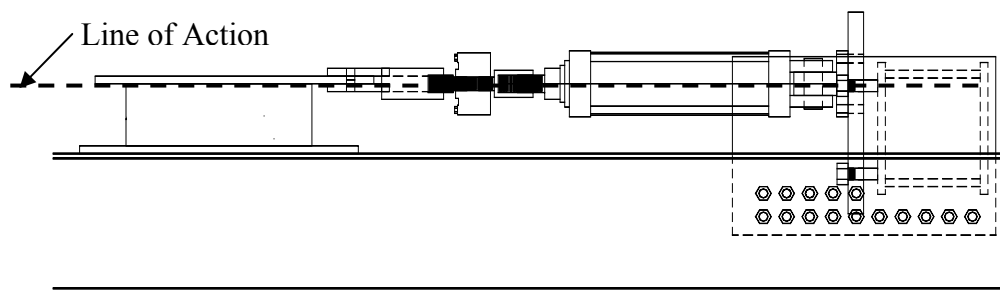


*Figure 5.12: Schematic of test setup (side view)*

67

***Figure 5.13: Reaction frame, hydraulic actuator and clevis of direct-shear setup
used for single-connector tests in this study***

In the following subsections, the components of this test setup are
described in more detail.

### 5.2.4.1   Reaction Frame

The reaction frame, adapted from one used in a previous test program,
consists of two 24- x 14-in. built-up steel bulkheads connecting two 23-ft long
stiffened MC18x58 channels.  A 2-in. thick steel adapter plate connects four 1-3/8
in. diameter bolts welded to the bulkhead and the base plate of the hydraulic
actuator.  The weight of the actuator is supported by the connection to the adapter
plate at its base, and by a wide-flange section at its other end.  Using a female
thread, one end of the load cell attaches to the male-threaded actuator shaft.  The

other side of the load cell, having a male thread, attaches to the male-threaded rod eye using a male-male threaded adapter.

The steel test plates have a 1-5/16 in. diameter hole that fits into the mouth of the clevis, and the two members are joined by a 1-1/4 in. diameter A490 bolt. The steel test plate is attached to the concrete test block by the shear connector being tested.



*Figure 5.14: Test setup with reaction frame and concrete block restraint*

The concrete test block rests on a 1-in. thick base plate welded on either side to the channels. The base plate is a 30- x 24-in. steel plate with two 18- x 7-in. sections removed from the middle along two opposite edges. This shape of the base plate allows space for the stirrups protruding from the top of the concrete blocks when the concrete block is turned over.
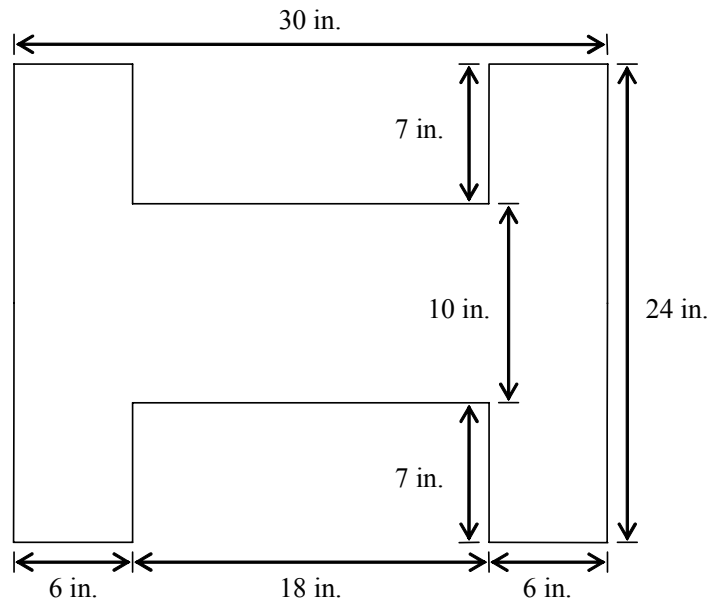
***Figure 5.15: Base plate***

The channels complete the load path to the bulkhead. The concrete block is kept from sliding by a 6- x 6- x 1-in. angle welded across the front of the base plate. The gap between the concrete block and the front angle is eliminated by filling it with hydrostone poured into plastic storage bags. Neoprene pads measuring 4 in. square were placed at the four corners on top of the concrete block. Two lengths of 6- x 6- x 1-in. angle were tightened across the top of the block by anchored 3/4-in. threaded rods to restrain the block vertically.

## 5.2.5 Development of Direct-Shear, Single-Connector Test Specimens Used in this Study

The direct-shear, single-connector test specimens used in this study were developed based on the idealized prototype bridge developed from the bridge investigations. Field investigations revealed that for typical bridges that might be retrofitted in this manner, prototype the slab was 7-in. thick, and girders had a 1-ft flange width and a 1-in. flange thickness. TxDOT indicated that the rolled steel

70

girders used in bridges constructed during the time were A36 steel. A 36- x 6- x 1-in. steel test plate was selected for use in the test specimen because it represented one-half of the top flange of a steel girder from the idealized prototype bridge. Only half the top flange is used because all investigated methods may have a shear connector installed on both sides of the beam web.
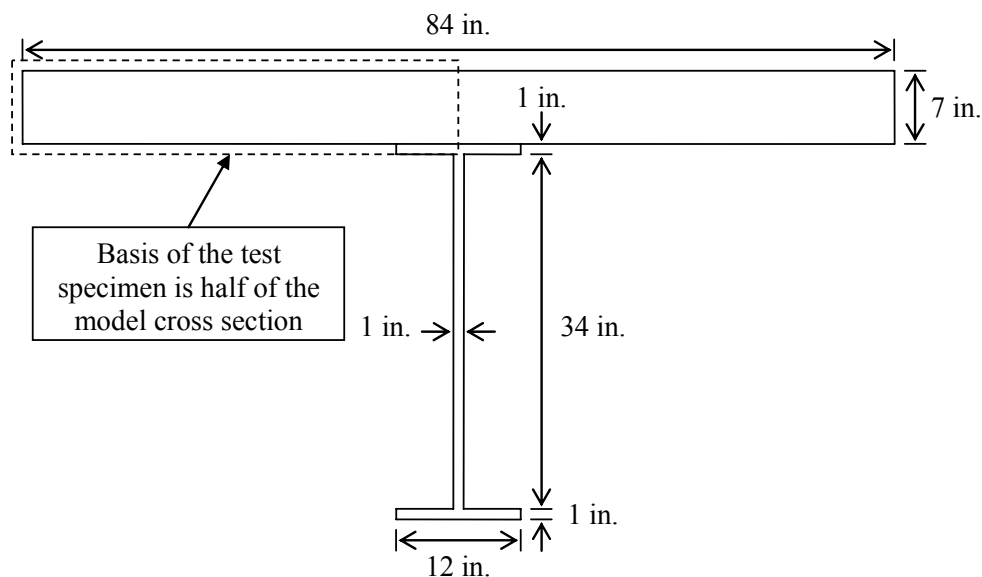


*Figure 5.16: Cross-section of the prototype composite bridge used to develop the direct-shear test specimens of this study*

In a prototype bridge, shear connections would experience the dead load from the overlying bridge deck. For convenience in testing, in the test setup the vertical position of the deck and the steel plate were reversed, with the latter on top. Because of this, a dead weight on top of the steel plate was used to simulate the dead load from the slab. The dead weight represents the weight of a 3-1/2 ft x 2-ft x 7-in. volume of the concrete bridge deck that would be tributary to each anchor. This assumes a girder spacing of 7 ft, a concrete bridge deck thickness of 7 in., and a given anchor spacing of 2 ft. Figure 5.17 and Figure 5.18 display the prototype bridge layout and tributary volume of the concrete bridge deck.

71
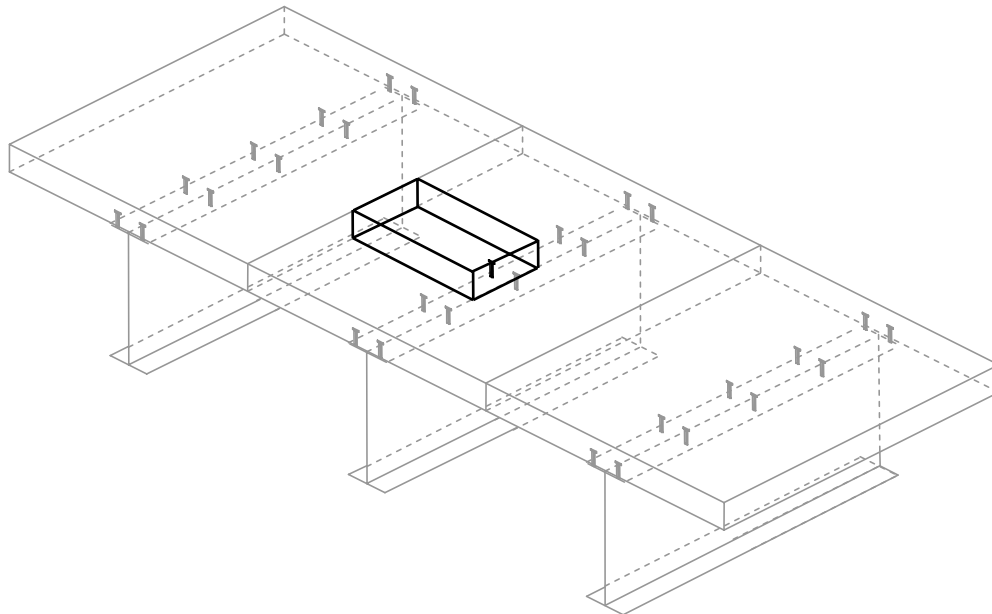
*Figure 5.17: Prototype bridge layout with tributary volume highlighted*



7 in.

3.5 ft

2 ft
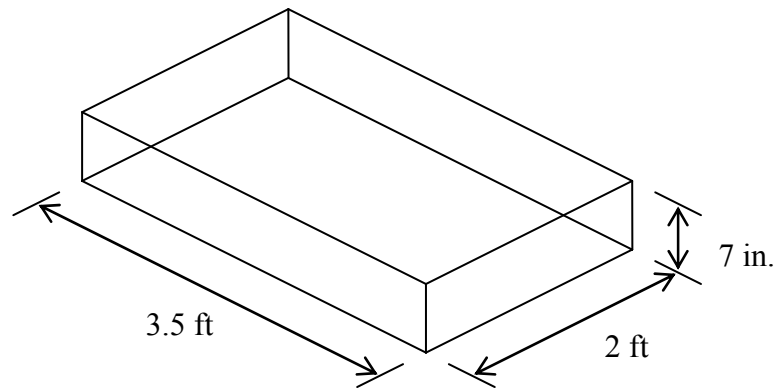
*Figure 5.18: Tributary volume of concrete bridge deck*

These values are consistent with field investigations, TxDOT design drawings, and discussions with TxDOT engineers. The calculated weight of this tributary volume of concrete is 612.5 lb. The test dead weight, created using three large blocks of scrap steel welded together, weighed 585 lb, and was placed concentrically with the anchor.

*Figure 5.19: Complete test setup with dead weight*

### 5.2.5.1 Concrete Test Blocks

Concrete test blocks were cast using fiberglass waffle-slab forms, measuring 23-1/2 in. square by 12 in. deep. While these forms had a higher initial cost ($56 each) than wooden forms, they saved substantial time that would have been spent constructing wooden forms, and will be reused for future specimens.

The concrete test blocks were cast using the inside of the form (Figure 5.20(a)) rather than outside (the originally intended orientation). Four 4-3/8 in. tall plastic reinforcing chairs were placed inside the form (Figure 5.20(b)) on which a 22-1/4 x 22-1/4 x 5/8-in. piece of plywood was set (Figure 5.20(c)). Sealant was placed around the edge of the plywood to ensure a watertight fit (Figure 5.20(d)). The cage was placed on 1-1/2 in. reinforcing chairs in the

remaining space (Figure 5.20(e)). The form created a concrete block measuring 22-1/4 to 23-1/2-in. square, and 7 in. thick (Figure 5.20(f)).
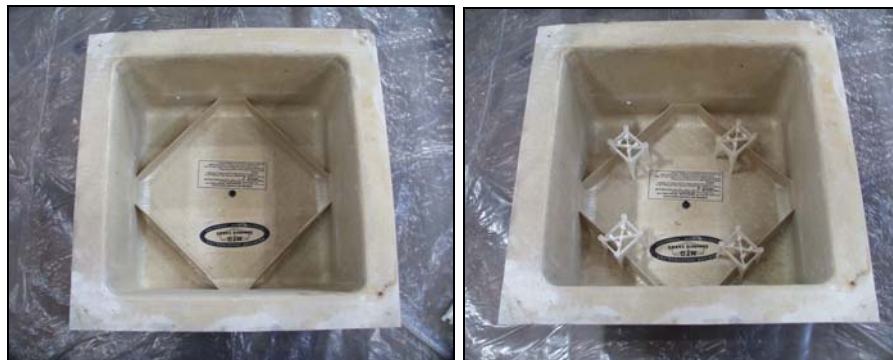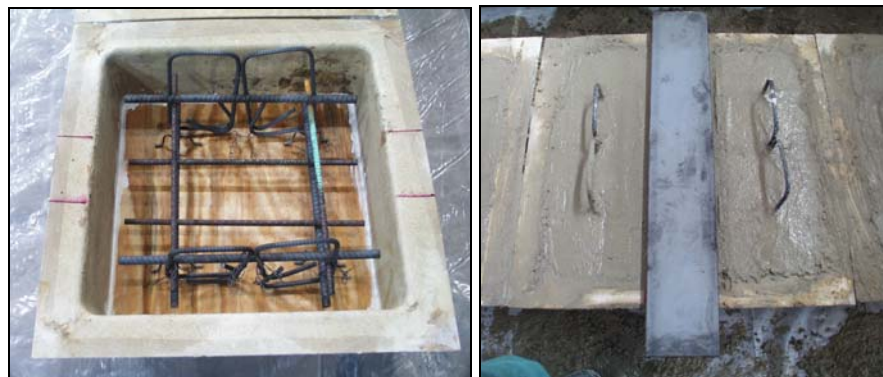
***Figure 5.20: (a) Empty waffle slab form; (b) form with plastic reinforcing chairs; (c) form with plywood; (d) form with plywood and caulk; (e) form with reinforcing cage; (f) cast concrete with steel test plate***

The reinforcing cage was composed of two layers of reinforcement tied to four #3 stirrups located at the corners. Each layer consisted of two #4 bars and two #5 bars in each the longitudinal and transverse directions. The configuration and dimensions are shown in Figure 5.21 through Figure 5.24.
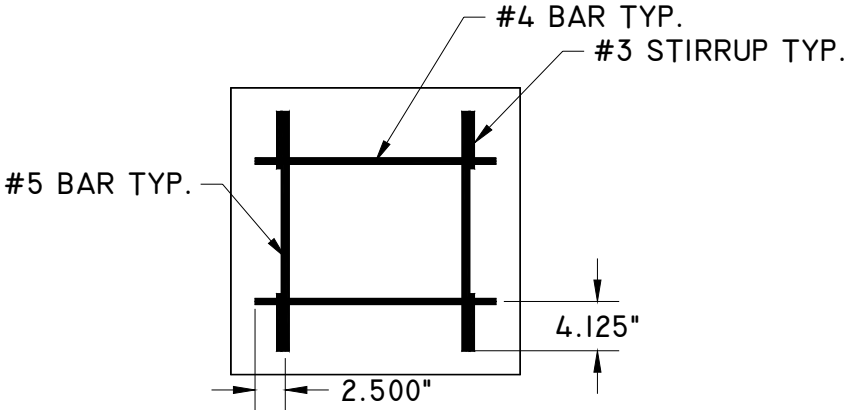


*Figure 5.21: Reinforcing cage, top view, top layer*
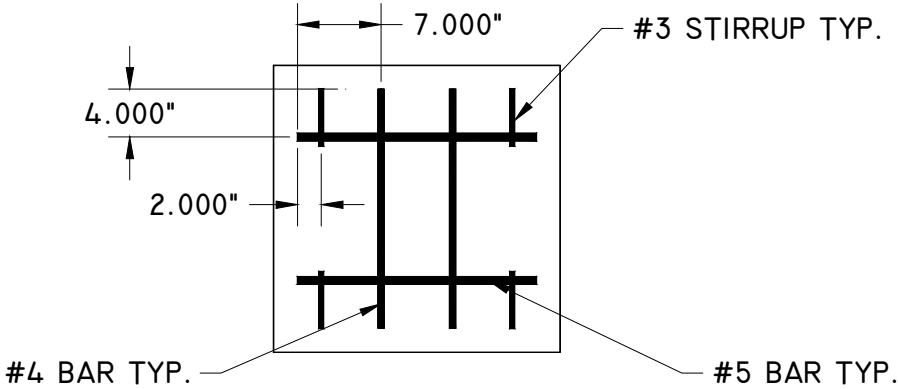


*Figure 5.22: Reinforcing cage, top view, bottom layer*
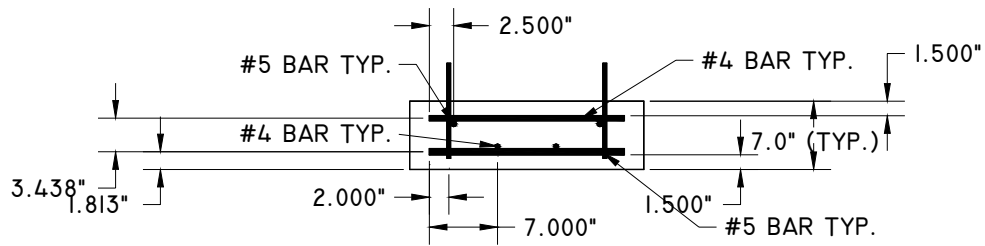
*Figure 5.23: Reinforcing cage, front view*
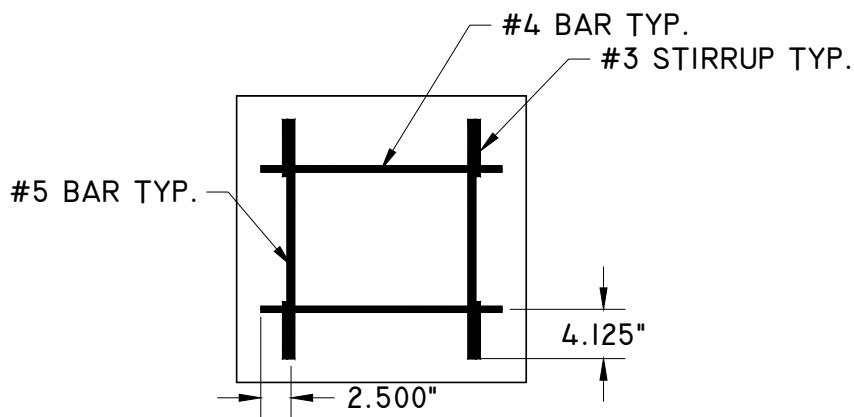


*Figure 5.24: Reinforcing cage, side view*

Reinforcement was included in the concrete block for several reasons, even though the blocks were too small to permit development of the tensile capacity of that reinforcement. The reinforcement was intended to mimic the size and layout of reinforcement used in prototype bridges, and thereby makes the test specimen as realistic as possible. It was also intended to attach the lifting stirrups and hold the concrete test block together, even after severe cracking.

Fifty concrete specimens and 30, 6- x 12-in. cylinders were cast at 8 am on July 11, 2003, using 5 cubic yards of concrete with a specified 28-day compressive strength of 3000 psi.

77

*Figure 5.25: Concrete specimens as cast*

The concrete was ordered as Mix Design #261 from Capitol Aggregates in Austin, Texas, and had the mixture design shown in Table 5.1.

*Table 5.1: Concrete mix components and their weights*

| Concrete Mix Component | Weight (lb) |
|---|---|
| Portland Cement | 1875 |
| 3/4-in. size river aggregate | 9620 |
| sand | 1875 |
| water | 742 |
| 100XR retarder | 28 |
| TOTAL | 14140 |

The cast blocks were covered with plastic and sprinkled with water twice daily for 5 days after casting. Test cylinders were covered with plastic and kept

next to the test blocks. To determine compressive strength, cylinder tests were performed at 7, 14, 21, and 28 days, and on four later occasions during static testing. Results are shown in Figure 5.26. The average compressive strength at 28 days was 2960 psi.
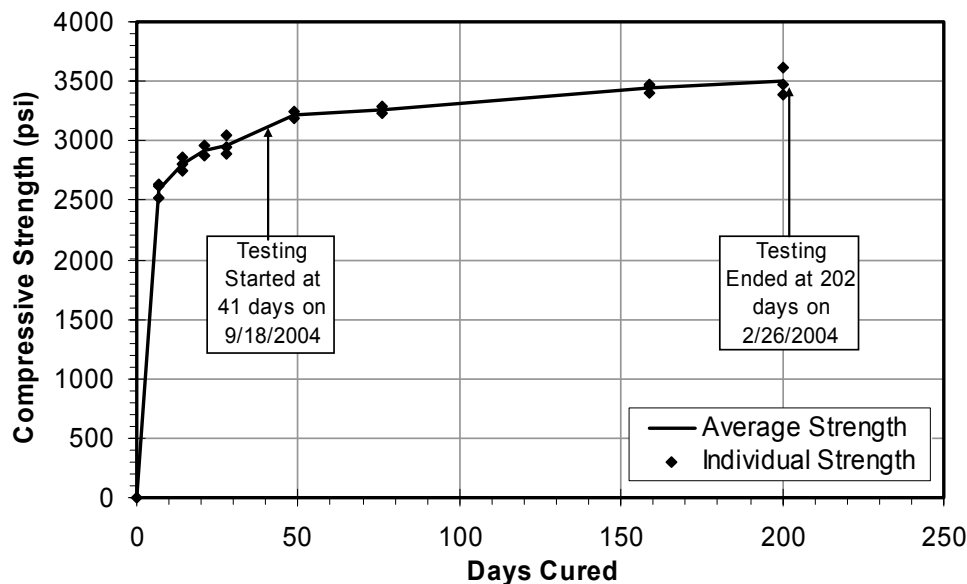


*Figure 5.26: Concrete compressive strength of test specimens versus time*

The 3-ft steel plates were placed on top of the concrete blocks immediately after casting, so that the surface of the concrete blocks would have interface conditions similar to those of the prototype bridges. After the concrete had cured, the concrete-steel interface was closely examined; it was concluded that too much cement paste had come to the top surface of the concrete block, and some of the plates were not completely flush with the concrete. Because that surface of the concrete did not seem suitable to be placed against the anchor plates, a decision was made to turn the blocks over, placing their bottom surface (originally in contact with the plywood) against the steel plate during testing. It was also thought that the concrete density and coarse aggregate distribution on the

bottom of the concrete test block would be more representative of prototype conditions. This is important because the local stiffness of the concrete has a direct effect on the stiffness and strength of the shear connection, and this local stiffness depends on the local distribution of the aggregate.

### 5.2.5.2 Steel Test Plates

Fifty 36- x 6- x 1-in. A36 steel plates were ordered for the test specimens. A 1-5/16 in. diameter hole centered 2-1/2 in., from one end was drilled in each plate for the attachment with the clevis. ASTM A370 coupon testing was performed on a sample test plate to determine the material properties of the steel (Figure 5.27). The average static yield strength was 39.9 ksi; the average dynamic yield strength, 43.0 ksi; and the average ultimate tensile strength, 66.9 ksi. The calculated modulus of elasticity was 29,400 ksi.
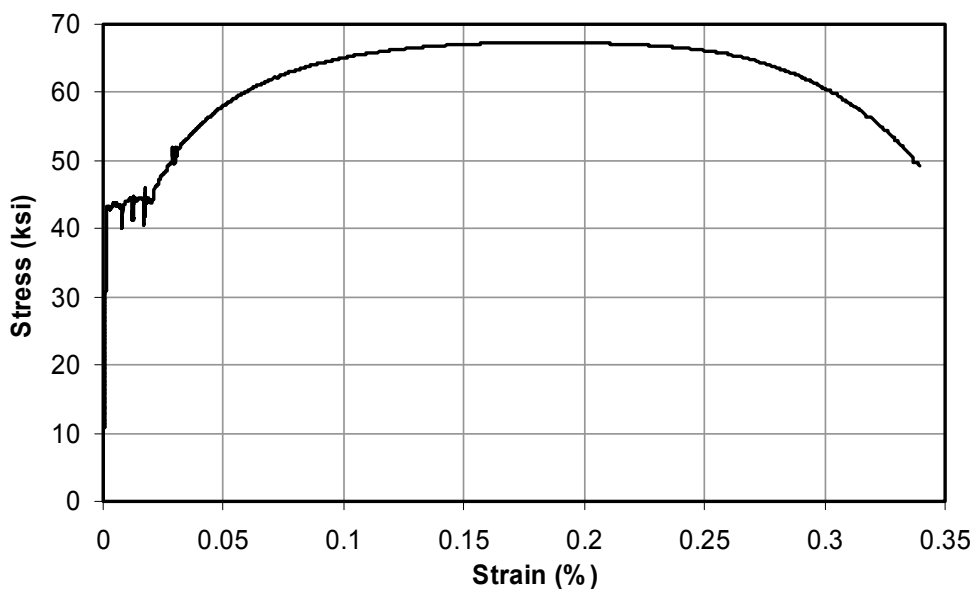


*Figure 5.27: Results of tensile tests on steel plate coupons*

### 5.3 POST-INSTALLED SHEAR CONNECTORS INVESTIGATED IN THIS STUDY

#### 5.3.1 Connectors Considered in this Study but Not Tested

In the beginning phases of this study, a wide variety of possible shear connectors was considered. Some of these were eliminated from further consideration for various reasons. In subsequent sections, the eliminated connectors are briefly described, and the reasons for eliminating them are presented.

##### 5.3.1.1 Rivet

The drive rivet, shown in Figure 5.28, is basically a large nail that is sprung open at its base when the pin at the head of rivet is struck.



***Figure 5.28: Drive Rivet in initial and installed positions***

It was thought that this could be used as a quickly installed bearing device. A preliminary investigation of the Rivet was performed to determine if a drive rivet may work as a shear connector. After some discussion, it was decided that the drive rivet would cause significant damage to the concrete, even if it were inserted into a pre-drilled hole in the concrete. Other potential problems included fatigue and low capacity, because the maximum diameter of rivet available was only 3/8-in. For these reasons, the Rivet was not considered further.

##### 5.3.1.2 Powder-Actuated Fasteners

Powder-actuated fasteners, shown in Figure 5.29 are a simple way to connect concrete and steel.
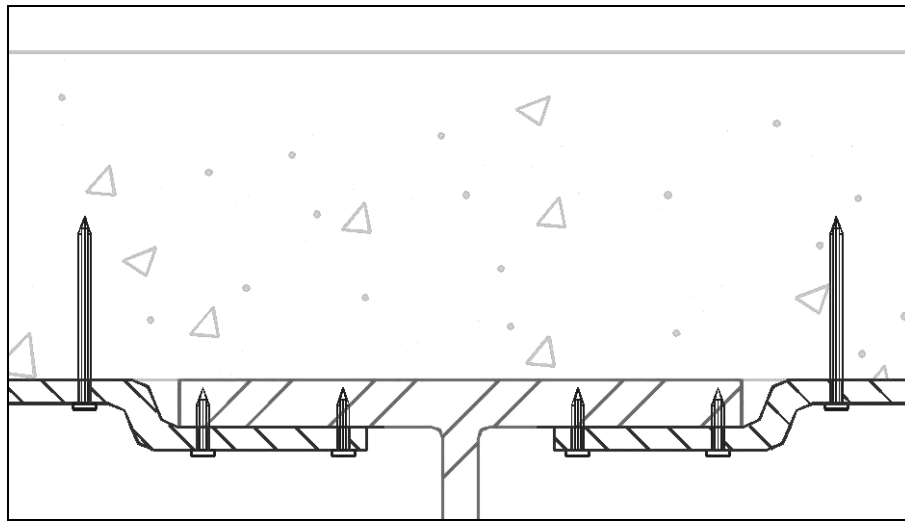
***Figure 5.29: Potential application of Powder-Actuated Fasteners in bridge retrofitting***

For use in bridge retrofitting, as shown in that figure, a bent steel plate would be attached to the top flange of the girder by fasteners driven into predrilled holes. The other side of the plate would be attached to the underside of the concrete deck by fasteners as well. To reduce damage to the concrete and increase the reliability of the connection, it might be necessary to pre-drill holes in the underside of the deck as well. The maximum available size of a powder-actuated fastener was only 3/8-in. diameter, associated with a relatively low design shear capacity.

Despite some concerns that this connection might be too flexible parallel to the girder flange, a preliminary design was performed using 0.3 kips as the typical shear capacity of a powder-actuated fastener in concrete. It was determined that several thousand fasteners would be needed to transfer the required shear in a single bridge span. This number would be further increased by the fact that many of the fasteners do not correctly embed in the concrete, requiring a significant over-design. It was also thought that the Powder-Actuated

Fastener, like the Rivet, would perform poorly in fatigue. For these reasons the Powder-Actuated Fasteners were eliminated from further consideration.

### 5.3.1.3  Saw-Tooth Connection

The Saw-Tooth connection, shown in Figure 5.30, was an intriguing concept in which matching grooves are created in a steel plate connected to the girder and on the bottom of the concrete bridge deck. The concept has been proven in new construction such as in the anchoring of cables on bridge decks. The Saw-Tooth connection works because the grooves interlock, producing friction on a macroscopic scale. The geometry of the teeth is determined by possible inclinations of the compression field and aggregate size.
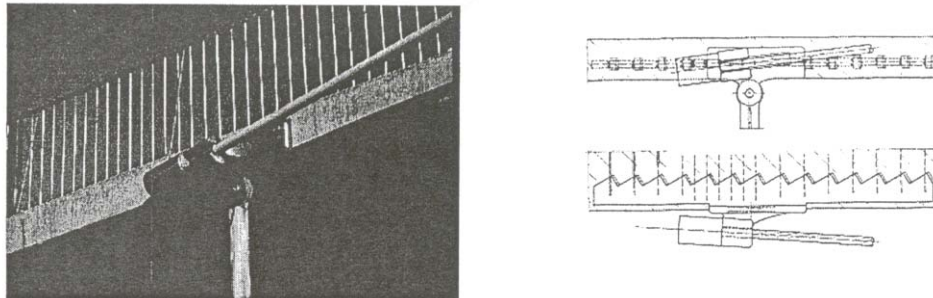


*Figure 5.30: Saw-Tooth Connection in a bridge cable anchor*

The Saw-Tooth connection is most valuable when large shear forces exist at the interface, but there is little depth of concrete for anchor embedment. No reasonable construction method was devised to create the necessary ridges in the concrete and matching ridges in the steel plate, however. For this reason, the Saw-Tooth connection was not considered further.

### 5.3.2　Connectors Tested in this Study

#### *5.3.2.1　Cast-In-Place Welded Shear Stud (CIPST)*

The Cast-In-Place Welded Shear Stud, shown in Figure 5.31, was not a post-installed method.
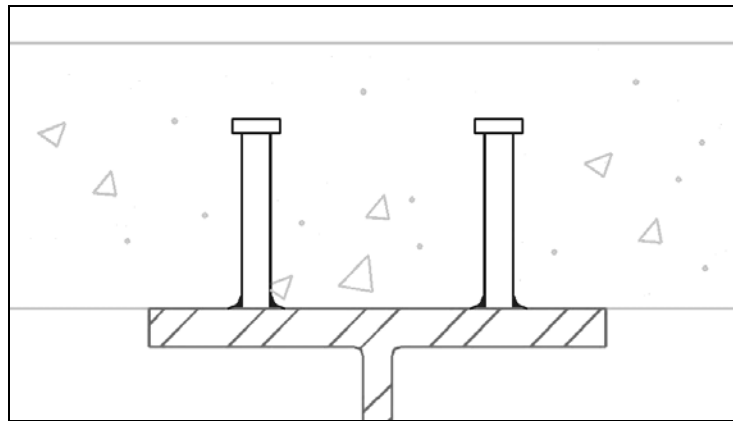


*Figure 5.31: Cast-In-Place Welded Shear Stud*

A traditional welded stud was welded to the steel test plate and then was cast in the concrete block as a complete test specimen. The vast majority of shear connector research has been performed on welded shear studs resulting in numerous empirical equations. Results of this study were applied to these equations to verify the test specimen setup as well as the validity of the test setup as a whole. The welded stud was the benchmark against which the rest of the post-installed methods were compared.

The Cast-In-Place Welded Stud is an embedded-depth transfer method. The steel test plate transmits load to the stud by means of the weld at the base of the stud. The stud transmits the resulting force to the concrete through bearing of the shank of the stud on the surrounding concrete.

The welded studs were attached to the test plates with a standard stud welding gun at Alpha Stud Weld in Houston, Texas. The 3/4-in. diameter Welded

Shear Stud was formed of AISI C-1015 carbon steel. It had a minimum specified yield strength of 50 ksi (manufacturer's tested value 53.1 ksi), and a minimum specified ultimate tensile strength of 60 ksi (manufacturer's tested value 66.2 ksi). The stud was 5-3/16 in. long before welding, and 5 in. after. To confine the weld pool, a ceramic washer was placed around the base of the stud before welding, and removed afterwards.

The Welded Shear Stud and test plate were placed across the top middle of a cast concrete test block from edge to edge of the form. The stud was fully embedded, and the concrete was further vibrated to ensure that the stud would be completely surrounded by concrete.

### 5.3.2.2   Welded Threaded Rod (POSTR)

The Welded Threaded Rod, shown in Figure 5.32, used the static friction mechanism initially, and bearing was used as a secondary load transfer mechanism.
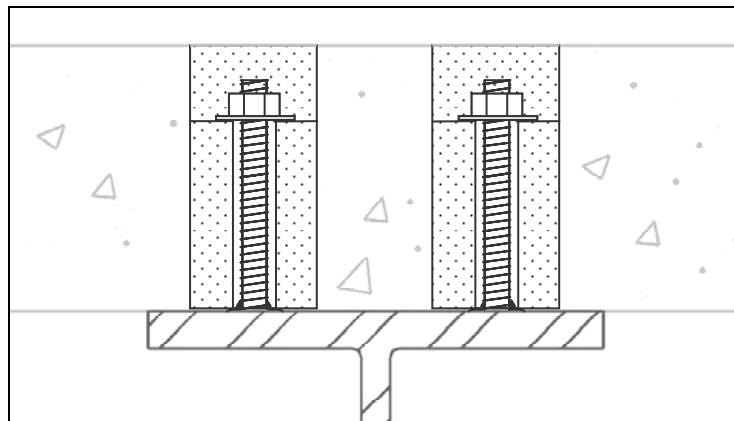


*Figure 5.32: Welded Threaded Rod*

The Welded Threaded Rod was a 3/4-in. fully threaded rod, 6-3/16 in. long before welding and 6 in. after. The steel was AISI C-1018 zinc-plated

carbon steel with a minimum specified ultimate tensile strength of 60 ksi and a minimum tested ultimate strength 61 ksi.

Several concrete test blocks were cast with a 7-in. length of 3-1/2 in. outer diameter PVC pipe placed vertically in the middle of the form. The pipe left a void in the concrete, making it unnecessary to core a hole in the block after the concrete had cured. The dimension of the hole was controlled by the requirement that a 3-1/4 in. diameter nozzle of a stud-welding gun fit in the hole. The test plates were laid across the form of the concrete test block immediately after casting.

A sheath was placed around the threaded rod to keep the grout that would be used to fill the hole away from the threads. If the grout had been allowed to penetrate the space between the threads, it would not have been possible to tighten the rod to create a clamping force at the interface of the concrete and steel. To compare their ease of removal, two types of sheaths were used: a PVC tube and a brass tube. Both had a 7/8-in. inner diameter and a 1-1/16 in. outer diameter, and both were lubricated with silicone spray before use.

A non-shrink grout ("Five Star Highway Patch") was used to fill the hole around the threaded rod. The compressive strength of the grout as given by the manufacturer was 2000 psi at 2 hours, 5000 psi at 1 day, and 7000 psi at 7 days. The grout was proportioned and mixed in plastic buckets according to the manufacturer's recommendations. The water and grout were mixed gradually using a Black & Decker Industrial Heavy Duty electric drill connected to a 3-ft mixing wand attachment with an 8-1/2 x 4-in. mixing blade. The drill had to be powerful (450 rpm, 120 V, 7 amp) to mix the grout thoroughly.

The grout was poured in the concrete hole around the sheath within 1-1/4 in. of the top of the threaded rod, and the grout surface was then hand-leveled. The sheaths were removed from the specimen when the grout was partially cured

because it would have been more difficult to remove them later. The remaining gap between the threaded rod and grout was attempted to be filled with an adhesive ("Five Star RS Anchor Gel"). One 22-fluid ounce, dual-cartridge unit was used and dispensed with a mixing nozzle. The application was unsuccessful, because even after repeated efforts it was not possible to force the adhesive into the gap left by the sheath.

As shown in Figure 5.33, Hilti HIT HY 150 adhesive was used to create a more level surface on which to tighten the washer on test specimen POSTR02. The hex nut was tightened to a torque of 200 ft-lb, using a torque wrench with a maximum capacity of 250 ft-lb and a 1-1/8 in. socket.



***Figure 5.33: Welded Threaded Rod with HY 150 adhesive beneath the washer***

The Welded Threaded Rod had a few advantages and several disadvantages.

Its advantages include its ability to be quickly welded to the steel with a standard stud-welding gun, and then to be tightened to create static friction at the concrete-steel interface.

Its disadvantages include the need to fill, with grout, the void left by coring in the concrete, and to place and later remove a sheath around the rod. It is also necessary to fill with grout to a precise level, leaving a sufficient length of threaded rod above the grout on which to place the washer and nut. The grout must be allowed time to cure. The nut needs to be tightened against a relatively flat surface so that stress is evenly distributed below the washer; such a surface is not easily formed. After the rod is tensioned, the space remaining above it must be filled with grout. Attempts to fill the space left by the sheath between the rod and the grout were unsuccessful, and the threaded rod was able to slide a significant distance into bearing. This construction sequence was complex and imprecise.

### 5.3.2.3  HAS-E Adhesive Anchor (HASAA)

The Hilti HAS-E Adhesive Anchor, shown in Figure 5.34, uses static friction as an initial load-transfer mechanism, and bearing as secondary mechanism.
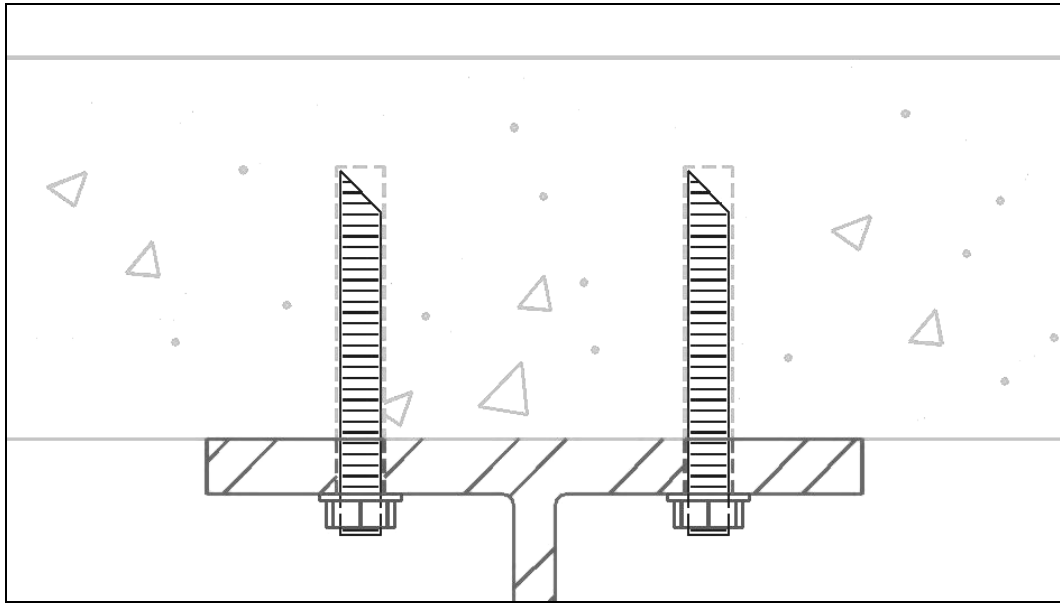
*Figure 5.34: HAS-E Adhesive Anchor*

The Hilti HAS-E Adhesive Anchor, shown in Figure 5.35, was ISO 898 Class 5.8 zinc-plated steel.



*Figure 5.35: Hilti HAS-E Adhesive Anchor*

The 3/4-in. diameter anchor had a minimum specified yield stress of 58 ksi and an ultimate tensile stress of 72.5 ksi. This was an ultimate anchor shear capacity of 14.4 kips. The anchor had a 10-in. total length with 6-3/4 in. from the beveled tip to the transition shank (a discontinuity in the threads, 1/8-in. long and 5/8-in. in diameter). The transition shank was the portion of the anchor intended to be in the shear plane. Another 3-1/8 in. of threaded rod was available after the transition shank. Unlike the HITTZ, HAS-E threaded rods are available in

89

diameters up to 1-1/4 in.  This is significant, because it offers the possibility of higher shear strengths, and more cost-effective retrofitting.

A 13/16-in. diameter hole was drilled through the steel test plate with a high-speed annular cutter and a Jancy magnetic-base drill press.  The plate was wiped clean of oil and debris with a clean cotton rag and acetone.

A 5-1/2 in. deep hole was drilled in the concrete with a 13/16-in. carbide drill bit and a Hilti TE-55 rotary hammer drill.  A Hilti TE-52 rotary hammer drill or similar drill may be used as well.  It was necessary that the drill bit have at least a 6-1/2 in. usable length to pass through the hole in the steel plate and drill the full depth in the concrete.  The hole was to be cleaned with a wire brush and compressed air.  A hand-held pump may also be used.



*Figure 5.36: Hilti HIT HY 150 adhesive*

Hilti HIT HY 150 adhesive, shown in packaged form in Figure 5.36, was used to attach the connector to the concrete.  HY 150 contains portland cement, and had excellent maintenance of strength at high temperature.  An 11.1-fluid ounce dual-cartridge pack (one part resin and one part hardener) was sufficient to install several anchors.  HY 150 adhesive has manufacturer's specified ultimate compressive strength of 10.42 ksi, ultimate tensile strength of 2.31 ksi, and modulus of elasticity of $1.02 \times 10^3$ ksi.  The dual-cartridge pack was dispensed

with a Hilti HIT-MD 2000 manual dispenser (Figure 5.37) fitted with a static mixing nozzle.  The mixing nozzle served to mix the resin and hardener, provide a precise outlet from which to apply the adhesive, and act as a seal for the remaining adhesive in the cartridge.



*Figure 5.37: Hilti HIT-MD 2000 manual dispenser*

The HAS-E Adhesive Anchor was installed in the laboratory setting with the concrete block below the steel plate as shown in Figure 5.38, and using the following steps:

o      Place the mixing nozzle on the dual cartridge pack and discard the first two trigger pulls of the adhesive.  This initial amount is not correctly proportioned, and it should not be used.

o      Inject the adhesive with the tip of the nozzle at the base of the hole (the bottom in the down-hole application of this test program).

o        Insert the threaded rod while rotating it in the same direction as when screwing it in, to ensure that the adhesive fills the threads.  Wipe excess adhesive from the edge of the hole.

o        Do not move the anchor after the specified gel time.



*Figure 5.38: Typical installation of a post-installed anchor*

The finished installation is shown in Figure 5.39.
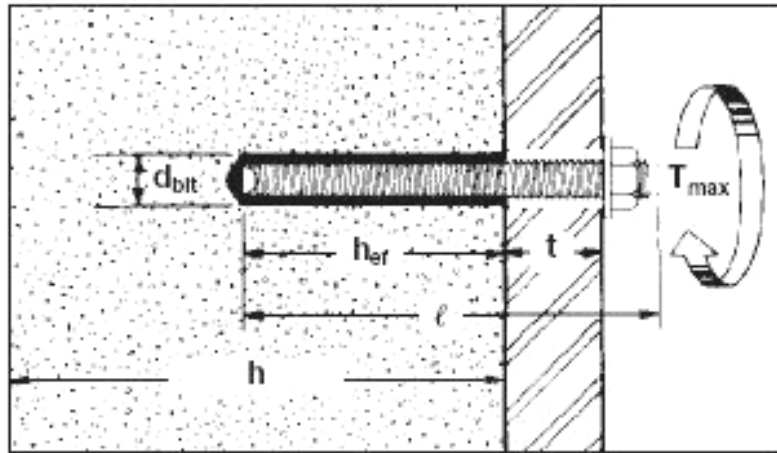
*Figure 5.39: Installation of an HAS-E Adhesive Anchor*

The HY 150 adhesive has a gel time of 6 minutes at 68 F and 4 minutes at 86 F.  It has a cure time of 50 minutes at 68 F and 40 minutes at 86 F (Figure 5.40).

## Open Gel Time Table (Approximate)[1]

| Base Material Temperature | | HIT HY 150[2] | HIT-ICE |
|---|---|---|---|
| °F | °C | | |
| -10 | -23 | – | 1.5 hrs |
| 0 | -18 | – | 1.5 hrs |
| 23 | -5 | 25 min | 40 min |
| 32 | 0 | 18 min | 26 min |
| 41 | 5 | 13 min | 11 min |
| 68 | 20 | 5 min | 4 min |
| 86 | 30 | 4 min | 1.5 min |
| 104 | 40 | 2 min | – |

## Final Cure Time Table (Approximate)[1]

| Base Material Temperature | | HIT HY 150[2] | HIT-ICE |
|---|---|---|---|
| °F | °C | | |
| -10 | -23 | – | 24 hrs |
| 0 | -18 | – | 24 hrs |
| 23 | -5 | 6 hrs | 6 hrs |
| 32 | 0 | 3 hrs | 4 hrs |
| 41 | 5 | 90 min | 2 hrs |
| 68 | 20 | 50 min | 1 hrs |
| 86 | 30 | 40 min | 30 min |
| 104 | 40 | 30 min | – |

1. Product temperatures must be maintained above 41°F (5°C), with the exception of HIT-ICE which must be above 0°F (-18°C).
2. Use of HIT HY 150 and HIT-TZ rods must be installed in base material temperatures ≥ 40° F (5° C).

*Figure 5.40: Gel and cure time tables for Hilti HY 150 adhesive (Hilti 2002)*

If this anchor were used in a real retrofit application, overhead installation would be required. The installation sequence would involve more steps than in the down-hole application of the test specimen. Steps would be as follows:

o    Cover the hole in the steel flange with a piece of duct tape, with a small slit cut in it to allow the mixing nozzle to pass through.

94

o        Perform a test application of the HY 150 adhesive in a test container. The test container should have the same volume as the anchor hole in the steel and concrete. Count the number of trigger pulls necessary to fill the container 1/2 to 2/3 full. This is the number of trigger pulls necessary to place the correct amount of adhesive in the tape-covered hole.

o        Place the mixing nozzle on the dual cartridge pack and discard the first two trigger pulls of the adhesive. This initial amount is not correctly proportioned, and it should not be used.

o        Inject the adhesive with the tip of the nozzle at the base of the hole (the top in an overhead application).

o        Insert the threaded rod while rotating it in the same direction as when screwing it in, to ensure that the adhesive fills the threads. Wipe excess adhesive from the edge of the hole.

o        Do not move the anchor after the specified gel time.

After the adhesive had cured, the anchor was tightened to 150 ft-lb after the adhesive had cured.

The HAS-E Adhesive Anchor has several potential advantages for the purposes of this study:

95

o       It is available in diameters up to 1-1/4 in. and in high-strength ASTM A193 Grade B7 steel, permitting large shear capacities in static friction after pre-tensioning, and large bearing capacities even if slip should occur.

o       It exhibits zero slip into bearing in both the steel and concrete holes because the adhesive fills the gap between the anchor shank and the edge of the hole.

o       HY 150 adhesive is virtually odorless because it contains no styrene, and maintains its strength well at the temperatures expected on the underside of bridge decks in Texas in the summer (about 110 F).  Its allowable bond strength at 110 F is 97% of its peak strength at room temperature (Figure 5.41).

## Influence of Temperature on Bond Strength
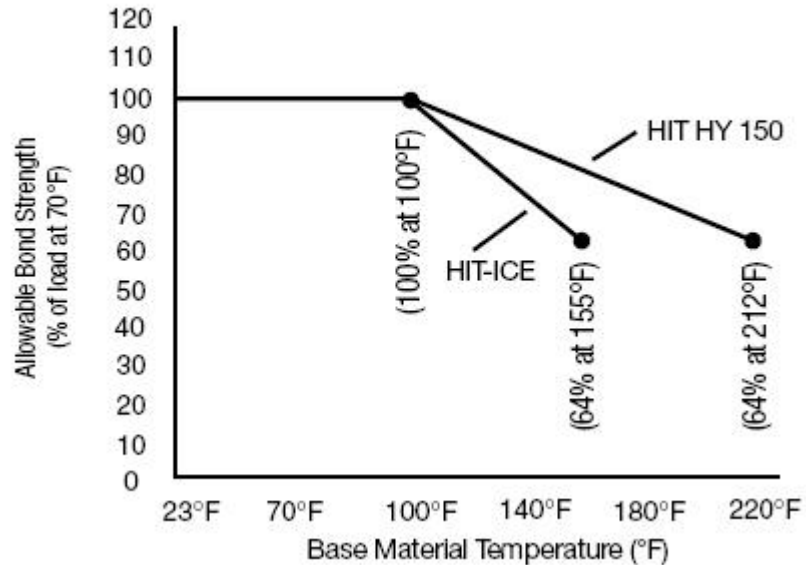


*Figure 5.41: Influence of temperature on the bond strength of HY 150 adhesive (Hilti 2002)*

Disadvantages of this connection method include the increased complexity and difficulty associated with using it in overhead construction. Extra steps are required in installation, and air voids can remain at the top of the hole. Also, the recommended embedment depth of 6 in. for the 1-1/4 in. diameter anchor would not be possible in the candidate bridges, and the anchor capacity less than the maximum available values. Because the adhesive must not be disturbed between the gel time and the cure time, the bridge might need to be closed to traffic during and for a time after anchor installation. In addition, the curing time is significant (about 50 minutes), and represents most of the time required for installation. This does not adversely increase total construction time, however, because while the first anchor is curing, subsequent anchors can be installed. Although the workers tightening the anchors would work considerably later than those installing the

97

adhesive and placing the anchors, very little time would actually be wasted during curing.

### 5.3.2.4  HIT-TZ Adhesive Anchor (HITTZ)

The Hilti HIT-TZ Adhesive Anchor, shown in Figure 5.42, used static friction as an initial load-transfer mechanism, and bearing as the secondary mechanism.  The primary mechanism acted when the steel test plate transferred load by static friction to the concrete.
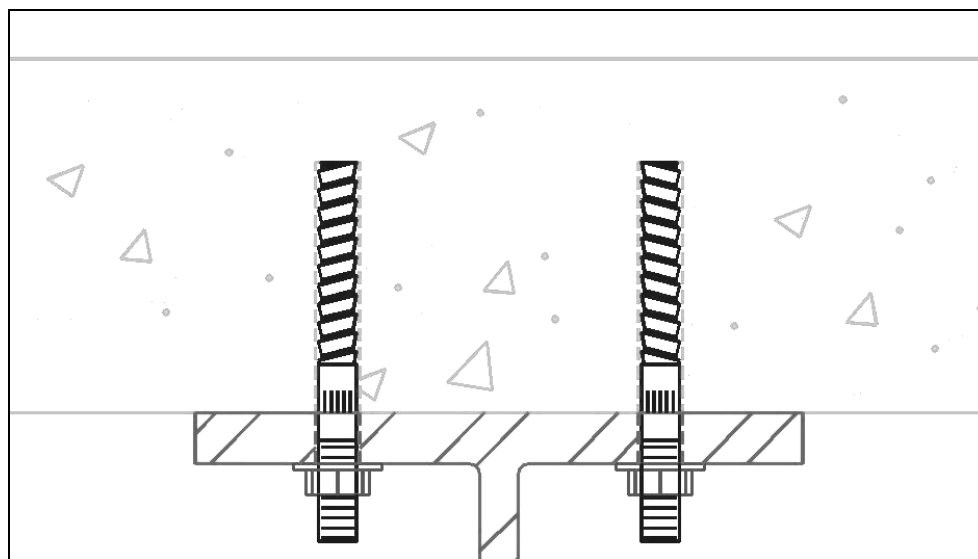


*Figure 5.42: HIT-TZ Adhesive Anchor*

The 3/4-in. diameter Hilti HIT-TZ Adhesive Anchor was made of ASTM A510 carbon steel with zinc plating.  The minimum specified yield strength was 70 ksi and the ultimate tensile strength was 87 ksi.  The manufacturer-specified ultimate shear strength of the anchor was 17.3 kips.

As shown in Figure 5.43, the anchor has a total length of 8-1/2 in., 3-3/4 in. of which consists of coarse, wedge-like threads intended to be inserted into the adhesive, and 3-1/4 in. of which consists of fine threads intended to hold a hex nut.  The HIT-TZ is not available in diameters greater than 3/4 in.

*Figure 5.43: Hilti HIT-TZ Adhesive Anchor*

The HIT-TZ anchor transfers force to the concrete differently than the HAS-E anchor. The coarse, wedge-like threads on the embedded end of the HIT-TZ anchor are coated with a bond-breaking coating, and de-bond from the surrounding adhesive when the anchor is tightened. The anchor transfers load to the surrounding adhesive through wedging action of the threads, rather than adhesion. This wedging action forces the pieces of adhesive against the inside of the hole.

The HIT-TZ Adhesive Anchor used the same HIT HY 150 adhesive as the HAS-E Adhesive Anchor, and was installed almost the same, with two key differences.

o    The hole did not need to be cleaned, because the anchor works by wedging of adhesive rather than by bond between the adhesive and the anchor shank and surrounding concrete.

o    In addition, the hole could readily be checked for the proper depth by able to be checked by placing the anchor in the hole, and verifying that only the fine threads were visible (Figure 5.44).
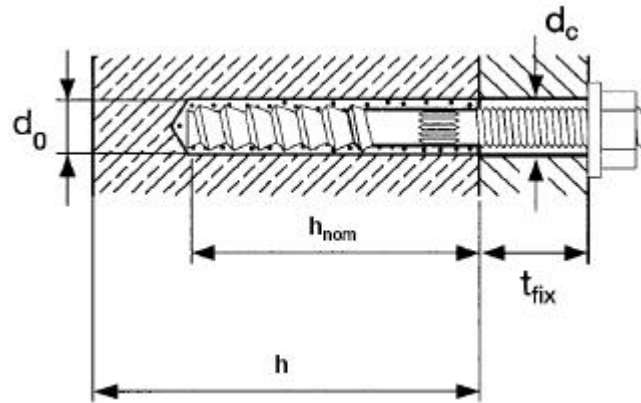
*Figure 5.44: Installation of an HIT-TZ Adhesive Anchor*

The HIT-TZ Adhesive Anchor has advantages and disadvantages similar to those of the HAS-E anchor. Both use the Hilti HY 150 adhesive, and they share its benefits. The HIT-TZ has two additional advantages over the HAS-E for this study. First, the HIT-TZ does not depend on adhesive bond to transfer the tension load from the anchor to the concrete, and consequently can be installed in an uncleaned hole, or even in standing water. Second, because of the higher capacity of the adhesive in wedging rather than adhesion, a HIT-TZ anchor can develop the same capacity as a HAS-E anchor of the same diameter with 20% less embedment depth.

The key disadvantage, however, is that the HIT-TZ is not available in diameters greater than 3/4 in. This is important because a larger anchor diameter generally means larger capacity, fewer required anchors, and lower retrofitting costs.

### 5.3.2.5  HY 150 Plate (HY150)

A shear connector idea was devised in which the test plate would be attached to the concrete by a layer of adhesive between the two components. This idea was tested using a single specimen, with HIT HY 150 adhesive. To conserve

specimens, the adhesive was applied evenly to the entire surface of a previously used test plate, which was then placed on the concrete block, at room temperature, under pressure from the deadweight, and allowed to cure for 2 hours prior to testing.  Only one test was performed on this method.

### 5.3.2.6   *Wedge-Bolt Concrete Screw (WEDGB, WEDGG, WEDGS)*

The Powers Fasteners Wedge-Bolt Concrete Screw used the bearing mechanism to transmit load between the steel and concrete (Figure 5.45).
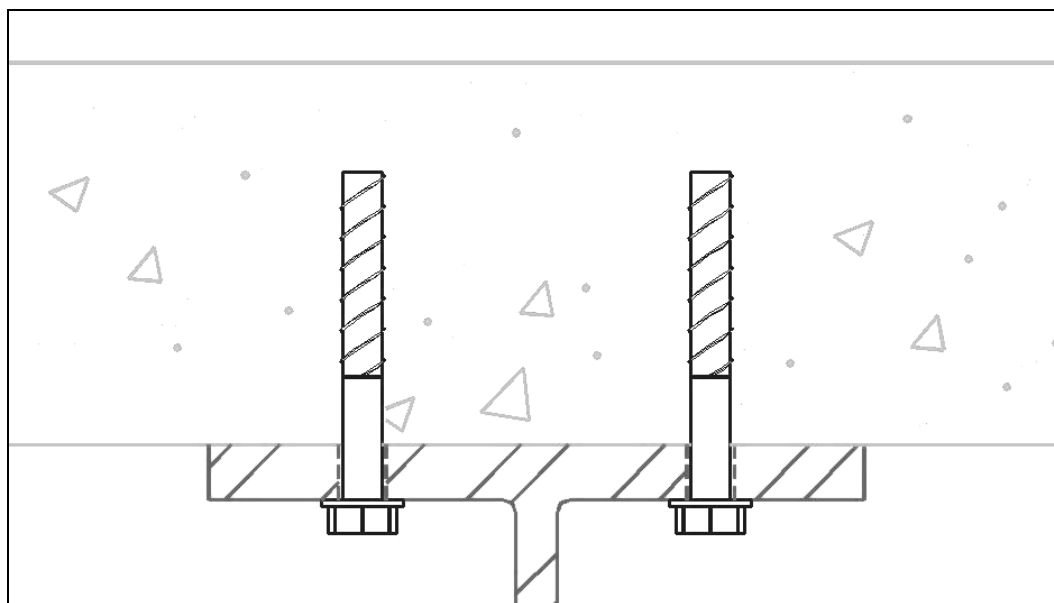


*Figure 5.45: Wedge-Bolt Concrete Screw*

The Wedge-Bolt, pictured in Figure 5.46, was made of AISI 1020/1040 zinc-plated carbon steel, with minimum specified yield and ultimate strengths of 36 and 58 ksi, respectively.

*Figure 5.46: Powers Wedge-Bolt Concrete Screw*

The anchor has a total length of 6 in., of which 3-3/4 in. is threaded (with a 3/4-in. diameter), and 2-1/4 in. is smooth (with a 0.7-in. diameter). The Wedge-Bolt was available only in diameters up to 3/4 in.

The hole was drilled through the steel test place with a Jancy magnetic-base drill press fitted with a 13/16-in. diameter annular cutter. After drilling, the plate was wiped clean of oil and debris with a cotton rag. The hole in the concrete was made with a Hilti TE-55 rotary hammer drill fitted with an adapter that permitted a SDS-Plus Wedge-Bit to be used.



*Figure 5.47: SDS-Plus special matched-tolerance drill bit*

The SDS-Plus Wedge-Bit, shown in Figure 5.47, was a special carbide steel drill bit with a matched tolerance range of 0.720 to 0.725 in. to accompany the 3/4-in. Wedge-Bolt. The drill bit had an 8-in. total length and a 6-in. usable length, allowing the bit to pass through the 1-in. hole in the steel test plate and drill the 5-3/4 in. deep hole in the concrete. Although the anchor has an embedment of only 5 in. in the concrete, the hole must be drilled deeper than that embedment because some debris clogs the bottom of the hole as the anchor is installed. After drilling, the hole was cleaned with a hand-held compressed-air nozzle and then vacuumed.

The WEDGS test was performed with a sheath that filled the gap between the smooth shank of the screw and the surrounding surface of the hole in the steel plate (Figure 5.48).



*Figure 5.48: Wedge-Bolt sheath installed*

After investigating several alternatives, it was determined that electrical metal conduit would be the best material for this sheath. Steel electrical metal tubing, or EMT, was made with galvanized, high-grade mild strip steel. The geometry of the screw shank and the diameter of the hole in the steel plate determined the required size of tubing. The sheaths are shown in Figure 5.49.
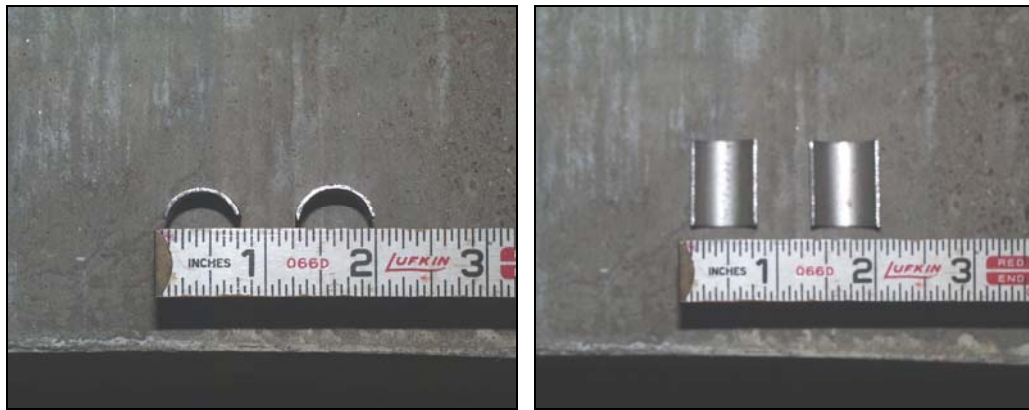
*Figure 5.49: Wedge-Bolt sheaths made from EMT*

Sheaths were made from 1/2- and 3/4-in. EMT, the tubing was cut in half longitudinally with a hacksaw or a pneumatic rotary saw, and then cut to the correct length (1 in.). The result was approximately two halves of a 1-in. length tube. The 1/2-in. sheath was easier than the 3/4-in. sheath to fit to the surface of the anchor, because the 1/2-in. diameter was originally too small and needed to be bent outward. With the 3/4-in. diameter, in contrast, extra material needed to be removed. The 1/2-in. tubing had a nominal thickness of 0.042 in., and was cut with a hacksaw to minimize the material lost in cutting. The 3/4-in. tubing was molded to the anchor after removing excess circumferential material, and its thickness was a tighter-fitting 0.049 in. The 3/4-in. tubing was cut longitudinally with a rotary saw because the wider blade used in that method would remove more of the excess circumference. The 3/4-in. tubing was ultimately used for the sheaths in the WEDGS specimens because it filled the gap more completely than the 1/2-in. tubing.

For the WEDGG specimens, attempts were made to fill the gap between the anchor shank and the plate with Five Star RS Anchor Gel, a high-strength viscous adhesive used in structural applications.

The Wedge-Bolt Concrete Screw was installed by placing it in the hole in the steel. One individual pressed down on the top of the torque wrench placed on the head of the anchor. This was necessary in order to apply sufficient axial compression to the anchor to cause the first few threads to engage the concrete when twisted. Another individual twisted the screw into place with the torque wrench set to the manufacturer's maximum recommended torque for the given strength of the concrete (in our case, 200 ft-lb for 3000-psi concrete). It was important to not over-tighten the screw, first because there would be no purpose to this (no static friction was intended to be developed), and second because over-tightening could strip the threads, making the anchor useless. Though the anchor could be inserted and tightened very quickly, the twisting was sometimes more difficult when a thread encountered aggregate in the concrete.

The bearing sheaths of 3/4-in. EMT needed to be lubricated before placement to minimize their twisting due to friction as the anchor was twisted into place. They were placed around the anchor in the steel hole before the head of the anchor had been drawn down against the plate. It was desirable to position the sheaths so that the gaps between the sheath halves were oriented perpendicular to the direction of the applied force. The screw continued to be twisted and the sheaths were pushed into place. The installation process was over when the underside of the washer head was firmly against the steel plate.

It was important that the washer head be contact with the steel plate so that no lift and bending deformation of the anchor would occur. The head of the anchor was not in contact in the WEDGG tests when Five Star RS Anchor Gel was used to try to fill the gap between the anchor and the hole in the steel. This condition is shown in Figure 5.50. In these cases, the hole was not drilled deep enough for the hex-washer of the Wedge-Bolt to be flush with the steel test plate.

Three tests were performed in each the WEDGB and WEDGG methods, and one test was performed on the WEDGS method.
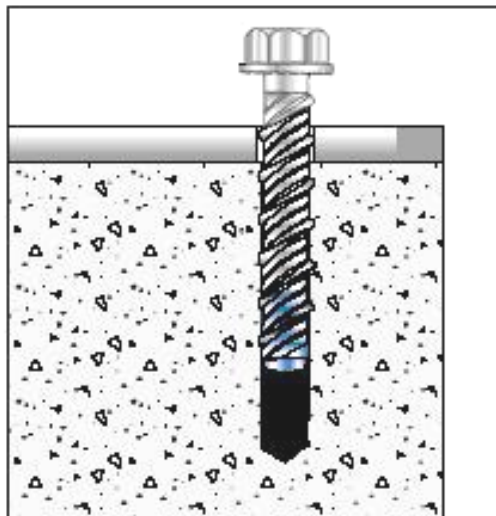


*Figure 5.50: Incomplete anchor installation*

The Wedge-Bolt Concrete Screw has many advantages. The Wedge-Bolt had the simplest and fastest installation of any anchor investigated in this study. No installation work would be required from the top of the bridge deck, permitting the bridge to remain open to traffic. The anchor could be loaded immediately after installation. Because the Wedge-Bolt is a screw, its behavior is commonly understood by designers and installers. Its one-piece design leaves no chance of lost parts or incorrect assembly, and its length and diameter are clearly stamped on the top of the hex washer head for inspection (Figure 5.51). The Wedge-Bolt itself is stiffer and ultimately stronger than a traditional welded shear stud under similar loading conditions. A concrete screw may be removed and reused if incorrectly installed. Finally, this anchor costs less than or the same as other anchors tested, and it has a clean finished appearance when installed.
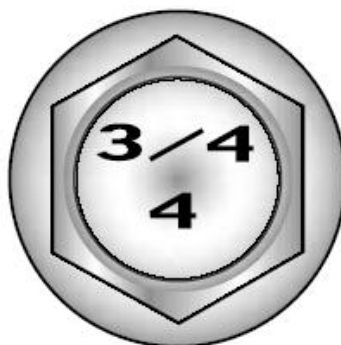
***Figure 5.51: Wedge-Bolt diameter and length stamped on top of the hex washer head***

Disadvantages of the Wedge-Bolt include the fact that its primary load-transfer mechanism is bearing, so fatigue may be a concern.  The anchor behaves poorly if the gap between the anchor shank and the hole in the steel is not filled, or if the washer head of the screw is not tightened to the point of contact with the steel.  The gap between the anchor and the plate needs to be filled, and a reasonable way of doing this was with a two-part sheath, cut from electrical metal tubing and placed in halves around the anchor where it passed through the steel plate.  Also, if the installation torque applied to the anchor was not carefully limited by a torque wrench or other similar device, it would be possible to strip the anchor in the concrete, making it useless.

### 5.3.2.7   *Epoxy Plate (3MEPX, 3M24H, 3MSTS, 3MCNS)*

The Epoxy Plate method was the only method other than the HY 150 test to use the adhesion mechanism.  The steel test plate was adhered directly to the surface of the concrete as shown in Figure 5.52.
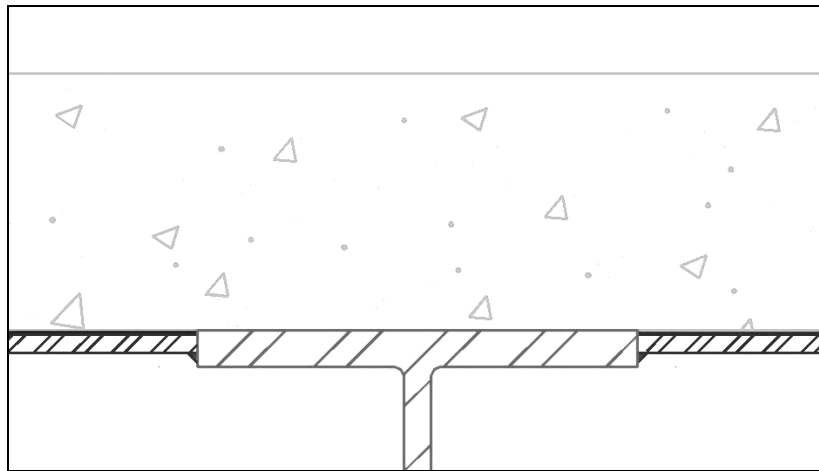
***Figure 5.52: Epoxy Plate***

After considerable study, the 3M DP-460 NS Epoxy was selected as the adhesive: it has a very high shear strength; it is very rigid after curing; and it maintains its strength well at high temperatures. Its shear capacity is 4650 psi at 73 F and 1360 psi at 180 F, both easily greater than the estimated shear-friction capacity of the concrete.

A 7-in. swath along the middle of the concrete test block was measured and marked along its length as the area where the plate would lie on the block. A 7-in., 6000-rpm DeWalt angle sander with a 6-in. diameter spinning wire brush was used to grind the concrete surface within that marked area. It was important to use a brush that was not very worn; the wire threads must be loose and bristling as pictured in Figure 5.53.

***Figure 5.53: Epoxy Plate prepared concrete surface with newer brush***

The surface paste may be brushed away with only a few passes of the sander as long as the aggregate is clearly visible. If the wire threads are nearly solid, the grinding will wear away the concrete paste as well as the aggregate as pictured in Figure 5.54.

*Figure 5.54: Epoxy Plate prepared concrete surface with worn brush*

In these tests, it was originally thought that the most effective bond with the epoxy could be obtained by grinding the surface concrete relatively deeply, removing considerable paste between the surface aggregate. This preparation was used in the 3MEPX, 3M24H, and 3MSTS tests.

The 3MCNS tests, in contrast, used a less complete preparation of the concrete surface, involving only a few passes of the grinder on the concrete surface. This less-complete surface preparation was actually found to be better than the deeper preparation. To obtain the most effective performance of the epoxy, it was best to grind only the surface layer of concrete paste, without dislodging the aggregate close to the surface. After grinding, the prepared concrete surface was blown free of dust and debris with a high-pressure air hose.

*Figure 5.55: Epoxy Plate prepared steel surface*

Cleaning of the steel plate was also important. The surface of the steel plate was wiped clean of oil and debris with a clean cotton rag, and its surface was scoured with 3M Scotch-Brite Heavy Duty Scour Pads, and then wiped with 91% isopropyl alcohol on a clean cotton rag. The 3MSTS tests were intended to investigate the differences, if any, of cleaning the steel surface less extensively. The steel surface-preparation process was performed only once on the 3MSTS tests but repeated twice more for the 3MEPX, 3M24H 3MCNS tests. After this preparation, the steel surface was wiped with a dry, clean cotton rag.

The epoxy was applied to the concrete surface using a 3M DP Manual Applicator II (Figure 5.56) with a 3M mixing nozzle. The process was slow, and it could not be hurried. If the trigger on the manual applicator was squeezed too hard, the epoxy would leak out the rear of the cartridge rather than passing through the mixing nozzle. This would create a mess and ruin the applicator. The application had to be completed within the working time for the adhesive: 60 minutes at room temperature, but only 40 minutes or less on a hot summer day. The after application, the epoxy was spread evenly on the surface using a rubber-gloved finger. Eight 27-mL, two-part cartridges were required produce enough

111

adhesive to completely cover the 22- x 6-in. area between the concrete and steel, with an average adhesive thickness of less than 1/8 in.



*Figure 5.56: 3M DP Manual Applicator II with epoxy cartridge*

The steel plate was placed level on the adhesive-covered area of the concrete block, with the prepared surface downward; it was pressed down by hand, lifted back up, and checked to ensure that the epoxy was in contact with the entire surface of the plate. If not, additional epoxy was applied to the concrete and the steel plate was checked again.

Once full contact was attained, the dead load was placed on the steel test plate to apply the manufacturer's minimum recommended contact pressure of approximately 1 or 2 psi (Figure 5.57). This contact pressure only served to force the epoxy into the microscopic surface roughnesses of the concrete and steel; it did not affect the curing process.

*Figure 5.57: Epoxy Plate specimen with contact pressure applied*

Most specimens were cured at room temperature. The 3MEPX tests were cured at higher temperatures, using space heaters placed next to the specimens (Figure 5.58). In these specimens, steel plates were positioned so as to nearly surround the epoxy surface and hold in the heat. The heaters were left on nearly half the time during the four days of curing, with most of the time being in the first three days. While the heaters were on, temperatures surrounding the epoxy surface varied from 100 to 150 F. Otherwise, room temperature varied from approximately 45 to 65 F. The cure time for the 3MEPX specimens was four days.

The 3M24H tests were intended to determine the difference, if any, of only 24 hours of curing time. The 3MSTS and 3MCNS tests were performed after two days of curing. Three tests were performed in the 3MEPX series, and two tests were performed in each of the 3M24H, 3MSTS, and 3MCNS series.

*Figure 5.58: Heat-cured Epoxy Plate specimen*

If the Epoxy Plate method were used in the field, the construction sequence would have to vary significantly from that used in the laboratory and described above. First, steel plates would need to be fabricated at the specified design size, and holes would need to be predrilled for injection and outlet of adhesive as well as for temporary anchors. Each plate would need to be lifted into position, held with temporary anchors, and its edge welded to the edge of the top flange of the girder. After the plate had cooled, a perimeter seal would have to be applied to the plate; the epoxy would be injected into inlet holes, and inspected for its exit through one or more outlet holes. This process is illustrated in Figure 5.59.

*Figure 5.59: Epoxy injection in building retrofit*

The connection would need to cure for at least 1 day, with no traffic permitted on the bridge during that time. After that time, the temporary anchors could be removed for reuse.

The main advantages of the Epoxy Plate method are its very high expected shear capacity, and its zero slip under load. Design capacity can be increased significantly by simply using a larger plate, with very little associated increase in difficulty of installation. Potential concerns about incomplete injection of epoxy, temperature effects, or the non-ductile failure mode may be easily addressed by over-designing the connection. The application is fairly simple: although it involves several steps, none is sophisticated. No detailed measurements are necessary, and the process may be inspected with ease.

Disadvantages of the Epoxy Plate method include the multi-step nature of the construction procedure. Holes may be required for injection and exit of epoxy, and also for monitoring. The epoxy injection must be closely supervised. Even so, some voids may remain between the steel and the concrete. The 3M epoxy is also somewhat expensive: the 27-mL cartridge costs $10, and seven or eight cartridges were needed to cover a 22- x 6-in. area. This cost may be reduced

115

by bulk application, however. Although this could be debated, it is probable that no traffic would be allowed on the bridge until the adhesive cured, because deflections and vibrations produced by traffic might reduce the adhesive bond. Finally, the Epoxy Plate method fails in a brittle manner, permitting no redistribution of stress. As a result, a high factor of safety would be required for design, but this could be easily achieved by increasing the plate size.

### 5.3.3 Summary of Post-Installed Connector Methods Tested in this Study

The post-installed connector methods tested in this study were group according to primary methods, under which some secondary variations were investigated. In this study, 16 primary connection methods were investigated. Those methods, including some that were not tested, are described in previous sections of this thesis.

The methods tested in this study are summarized in Table 5.2. In that table, each primary method and its secondary variations (if any) are grouped together, and variations are denoted by asterisks. As shown in that table, 13 primary methods were tested; 5 of these had variations. The number of primary methods and variations totaled 22.

With the number of replicates shown in Table 5.2, this gave 22 primary methods or variations, and 50 specimens. Of these, 12 primary methods or variations (CIPST and below in Table 5.2) are discussed in this thesis. The rest are discussed in Schaap (2004).

## Table 5.2: Primary methods and variations tested in Study 0-4124

| Primary Methods (Label) | Replicates |
|---|---|
| Hilti Kwik Bolt II Expansion Anchor (KWIKB) | 1 |
| *Hilti Kwik Bolt II w/ Grout (KWIKG) | 1 |
| Drillco Maxi-Bolt Undercut Anchor (MAXIB) | 3 |
| *Drillco Maxi-Bolt Undercut Anchor, High Strength (MAXIG) | 1 |
| *Drillco Maxi-Bolt Undercut Anchor, HS, RS Anchor Gel (MAXIG) | 1 |
| Post-Installed Welded Stud (POSST) | 3 |
| High-Tension Friction Grip Bolt (HTFGB) | 3 |
| *1.25-in. High-Tension Friction-Grip Bolt (HTFAT) | 3 |
| Double-Nut Bolt (DBLNB) | 3 |
| Stud Welded to Plate (STWPL) | 3 |
| Cast-In-Place Welded Stud (CIPST) | 3 |
| Welded Threaded Rod (POSTR) | 2 |
| Hilti HAS-E Adhesive Anchor (HASAA) | 3 |
| Hilti HIT-TZ Adhesive Anchor (HITTZ) | 3 |
| Hilti HY 150 Adhesive Plate (HY150) | 1 |
| Powers Wedge-Bolt Concrete Screw (WEDGB) | 3 |
| *Powers Wedge-Bolt with Sheath (WEDGS) | 1 |
| *Powers Wedge-Bolt with RS Anchor Gel (WEDGG) | 3 |
| 3M DP-460 NS Epoxy Plate (3MEPX) | 3 |
| *3M DP-460 NS Epoxy Plate, 24-Hour Cure (3M24H) | 2 |
| *3M DP-460 NS Epoxy Plate, Steel Surface (3MSTS) | 2 |
| *3M DP-460 NS Epoxy Plate, Concrete Surface (3MCNS) | 2 |
| TOTAL | 50 |

## 5.4    INSTRUMENTATION AND DATA ACQUISITION

The instrumentation and data acquisition system consists of the hydraulic actuator load cell for measuring applied load, a load washer for measuring anchor tension, and two linear variable differential transformers (LVDT), for measuring slip.

The hydraulic actuator load cell had a 100-kip capacity. The measurement output was given to the nearest pound and was accurate to within 0.5%, based on a statistical evaluation of the output. The hydraulic actuator is located in the test setup between the hydraulic actuator and the clevis.

Several setups included a 7/8-in. diameter load washer, intended to measure anchor clamping force. The load washer measurement was given to the thousandth of a pound, but it was only accurate to within 20% of the output in the experiments, based on the same statistical evaluation.



*Figure 5.60: Load washer*

The LVDTs are actually direct current differential transformers (DCDT) that receive a DC input, convert that input to AC within the device, and then

convert the output signal back to DC. The LVDT has a precision of 0.0001 in., and it was accurate to 0.2% of the displacement reading, based on the same statistical analysis.
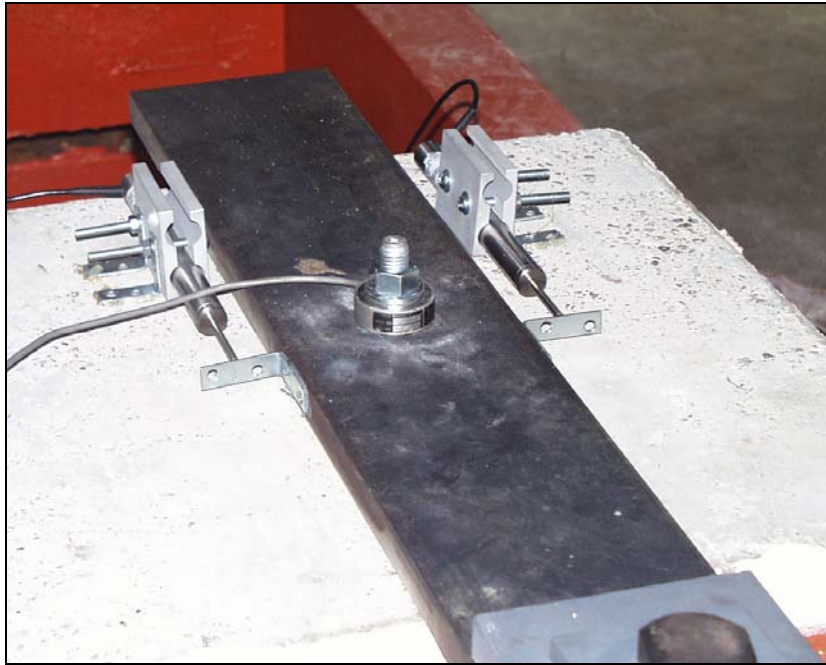


*Figure 5.61: LVDTs and load washer*

The LVDTs were aligned parallel to the steel plate using aluminum spacer blocks, and were fitted to brackets attached with epoxy to each side of the concrete block. Two more brackets were fastened to the steel plate with the same epoxy. The arrangement was such that the displacement wand extended in the direction of displacement. This ensured that the LVDTs would not be damaged by a sudden large displacement.

Instrumentation was connected to a standard bridge completion box, scanner, and personal computer. LabVIEW 7 Data Acquisition software was used to continuously obtain input every half-second while testing.

## 5.5 PROCEDURE USED FOR DIRECT-SHEAR, SINGLE-CONNECTOR SHEAR TESTS OF THIS STUDY

The direct-shear, single-connector shear tests of this study were carried out using the following sequence of steps:

1) The steel test plates were connected to the concrete test blocks by the shear connectors, and the concrete test blocks were restrained by the reaction frame.

2) The hydraulic actuator, whose capacity was 100 kips, was operated using a 10,000-psi capacity pneumatic oil pump and a manual regulator to apply load to the steel test plates at rates ranging from 0.1 to 0.3 kips per second.

3) Load was applied until the connector failed or the concrete test block had developed a significant crack through its entire section.

# CHAPTER 6

# Results of Load-Slip Tests

**6.1  PRELIMINARY REMARKS**

In this chapter, load-slip behavior and failure modes of post-installed anchors in direct shear are described. To the extent possible, typical behavior is briefly described in an initial section. In subsequent sections, the load-slip behavior and failure modes of individual connection methods are discussed in more detail.

**6.2  LOAD-SLIP BEHAVIOR AND FAILURE MODES OF SHEAR CONNECTORS TESTED IN THIS STUDY**

**6.2.1  Typical Load-Slip Behavior and Failure Mode of Shear Connectors**

Although the load-slip behaviors of each type of shear connector varied in many respects, all load-slip curves shared a few common characteristics, shown in Figure 6.1 for a post-installed anchor.
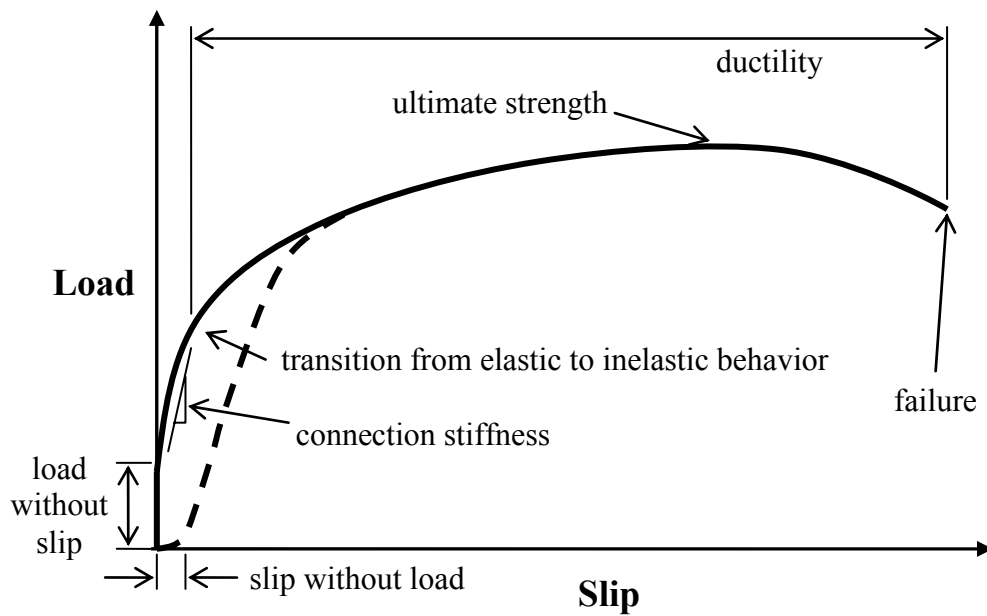
*Figure 6.1: Typical characteristics of a load-slip curve for an anchor*

The typical characteristics of a load-slip curve for an anchor are the following:

o      slip without load

o      load without slip

o      connection stiffness

o      ultimate strength

o      ductility

o      failure

An anchor may have load without slip if it has initial pre-tension. An anchor may have slip with nearly zero load if a gap exists between the anchor and the concrete or steel. The connection stiffness is the stiffness of the anchor-concrete system after the anchor has slid into bearing. The ultimate strength of the anchor is the maximum load experienced by the anchor. After a typical short descending branch, failure of the anchor marks the end of load-slip response. The ductility of the anchor is defined as slip at failure divided by slip at the transition from elastic to inelastic behavior divided by.

The failure modes observed for the connection methods of this thesis are summarized in Table 6.1.

***Table 6.1: Summary of failure modes observed for each connection method***
***discussed in this thesis***

| Test Name | Failed Component | Failure Mode | Failure Location |
|---|---|---|---|
| CIPST01 | Anchor | Shear-Tension | Above Weld Pool |
| CIPST02 | Anchor | Shear-Tension | Above Weld Pool |
| CIPST03 | Anchor | Shear-Tension | Above Weld Pool |
| POSTR01 | Anchor | Shear-Tension | Above Weld Pool |
| POSTR02 | Anchor | Shear-Tension | Above Weld Pool |
| HASAA01 | Anchor | Shear-Tension | Concrete-Steel Interface |
| HASAA02 | Anchor | Shear-Tension | Concrete-Steel Interface |
| HASAA03 | Anchor | Shear-Tension | Concrete-Steel Interface |
| HITTZ01 | Anchor | Shear-Tension | Root of Inclined Thread |
| HITTZ02 | Anchor | Shear-Tension | Concrete-Steel Interface |
| HITTZ03 | Anchor | Shear-Tension | Concrete-Steel Interface |
| HY15001 | Adhesive | Shear-Tension | Concrete-Steel Interface |
| WEDGB01 | Anchor | Shear-Tension | Root of Inclined Thread |
| WEDGB02 | Anchor | Shear-Tension | Root of Inclined Thread |
| WEDGB03 | Anchor | Shear-Tension | Root of Inclined Thread |
| WEDGS01 | Anchor | Shear-Tension | Root of Inclined Thread |
| WEDGG01 | Anchor | Shear-Tension | Root of Inclined Thread |
| WEDGG02 | Anchor | Shear-Tension | Root of Inclined Thread |
| WEDGG03 | Anchor | Shear-Tension | Root of Inclined Thread |
| 3MEPX01 | Concrete | Shear Friction | Below Adhered Surface |
| 3MEPX02 | Concrete | Shear Friction | Below Adhered Surface |
| 3MEPX03 | Concrete | Shear Friction | Below Adhered Surface |
| 3M24H01 | Concrete | Shear Friction | Below Adhered Surface |

| 3M24H02 | Concrete | Shear Friction | Below Adhered Surface |
|---------|----------|----------------|----------------------|
| 3MSTS01 | Concrete | Shear Friction | Below Adhered Surface |
| 3MSTS02 | Concrete | Shear Friction | Below Adhered Surface |
| 3MCNS01 | Concrete | Shear Friction | Below Adhered Surface |
| 3MCNS02 | Concrete | Shear Friction | Below Adhered Surface |

All tested methods except the Epoxy Plate method failed when the connector failed by a combination of shear and tension. Welded stud connectors failed by shear through the anchor immediately above the weld pool at the base of the anchor (Figure 6.2).



*Figure 6.2: Typical failure of Welded Stud above the weld pool*

The first HIT-TZ Adhesive Anchor specimen and every Wedge-Bolt Concrete Screw specimen failed below the concrete-steel interface at one of the first roots of the inclined cutting thread (Figure 6.3).

125
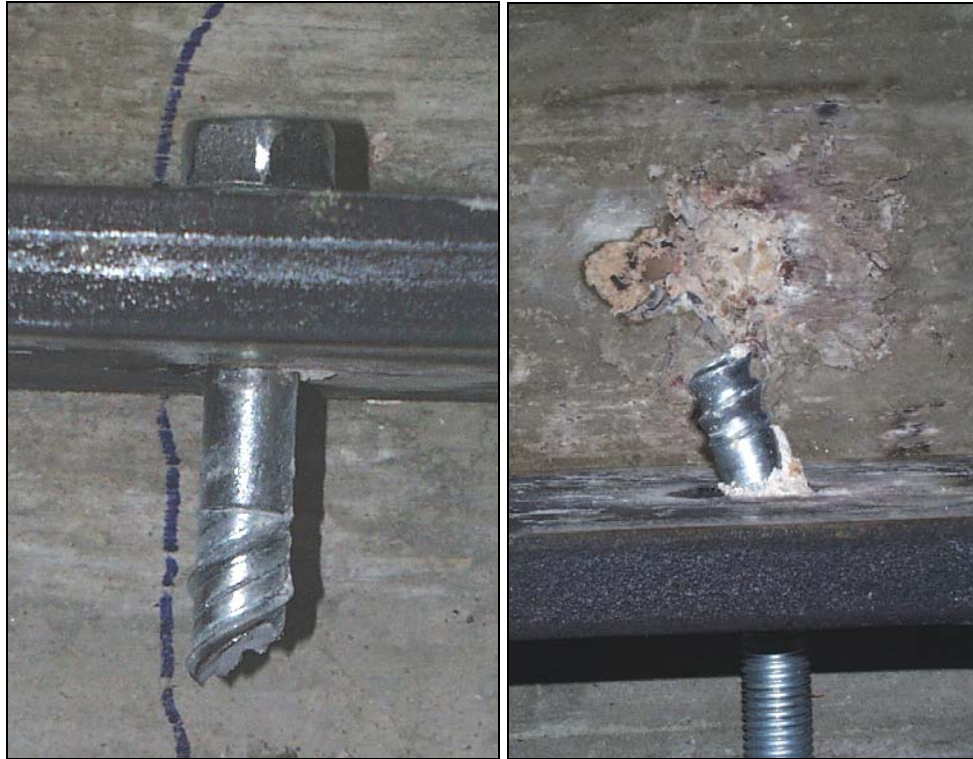
*Figure 6.3: Typical failures at thread root below the shear plane*

The HAS-E Adhesive Anchor tests and the second two HIT-TZ Adhesive Anchor tests were the only specimens discussed here fail in direct shear through the anchor at the concrete-steel interface (Figure 6.4).

*Figure 6.4:  HAS-E Adhesive Anchor failure at the shear plane*

In contrast with the other specimens, the Epoxy Plate method failed in a brittle manner, by shear-friction in the concrete on a plane immediately below and parallel to the adhered surface (Figure 6.5).

*Figure 6.5: Epoxy Plate failure of the concrete below the adhered surface*

## 6.2.2 Load-Slip Curves and Failure Mode for Cast-In-Place Welded Stud (CIPST)

Load-slip curves for the Cast-in-Place Welded Stud (CIPST) are shown in Figure 6.6, and a graph of 0- to 0.3-in. slip range only is shown Figure 6.7. The curves display many of the typical features noted earlier. Noteworthy, however, are the high initial connection stiffness, the impressive ductility, and the 6-kip difference in the ultimate strengths of CIPST01 and CIPST03 tests. Also, Test CIPST01 shows much more ductility than the other two CIPST tests.
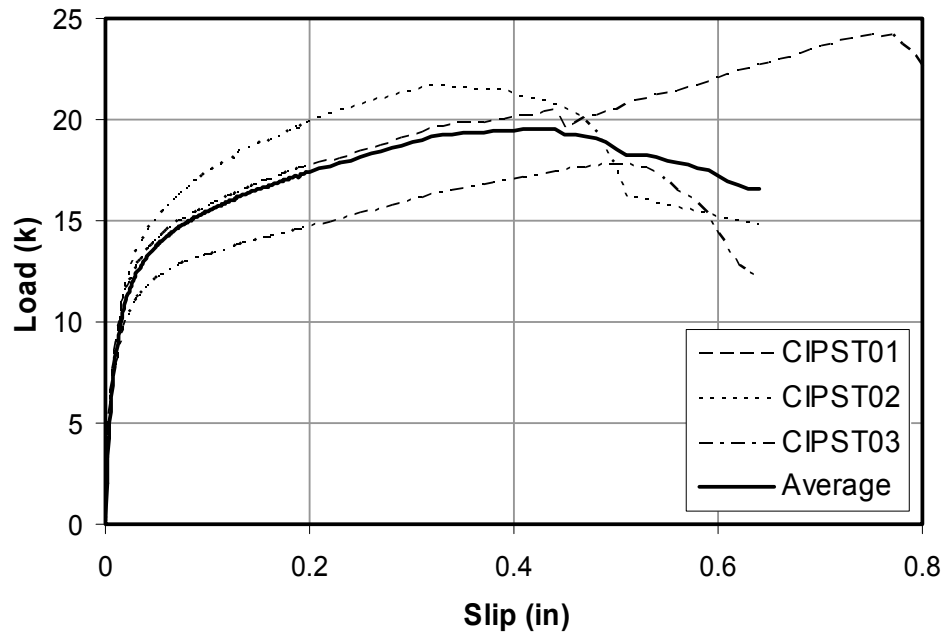
*Figure 6.6: Cast-In-Place Welded Stud, slip 0 to 0.8 in.*
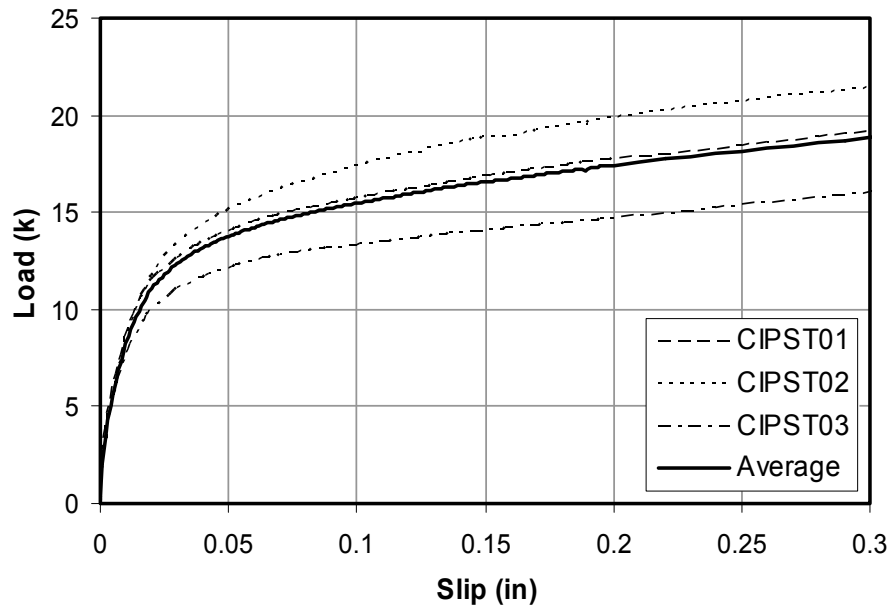


*Figure 6.7:  Cast-In-Place Welded Stud, slip 0 to 0.3 in.*

129

All three CIPST specimens experienced failure of the stud under combinations of shear and tension, combined with localized crushing of the concrete at the base of the stud (Figure 6.8).



***Figure 6.8: Typical failure of Cast-In-Place Welded Stud, particular specimen with air void***

In Figure 6.7, the load-slip curve for Test CIPST03 is shown to substantially lower than those of the other two CIPST tests after the elastic range of the anchor is exceeded (slips exceeding about 0.025 in.). This may be due to an air void (the depressed area in Figure 6.8) at the base of the stud, which coincides with the location of greatest bearing stress on the concrete.

### 6.2.3 Load-Slip Curves and Failure Mode for the Welded Threaded Rod (POSTR)

Load-slip curves for the Welded Threaded Rod (POSTR) are shown in Figure 6.9, and a graph of the 0- to 0.3-in. slip range only is shown in Figure 6.10.

The curves are substantially different from those of the CIPST. The POSTR has initial load without slip (due to the static friction mechanism); static friction is overcome at approximately 5 kips of applied load. Slip then increases from about 0.05 to 0.15 in. without much increase in load. Load is resisted in bearing beginning at a slip of about 0.15 in. The ultimate strength of Test POSTR02 exceeds that of the average CIPST specimen. This is almost true as well for Test POSTR01. The capacity of both POSTR specimens decreases very quickly after ultimate strength is reached.
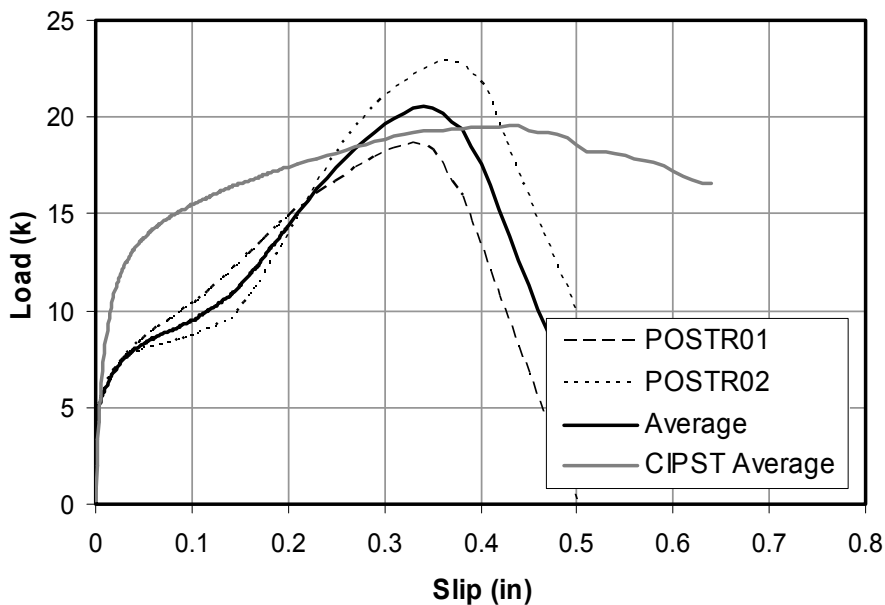


*Figure 6.9: Welded Threaded Rod, slip 0 to 0.8 in.*
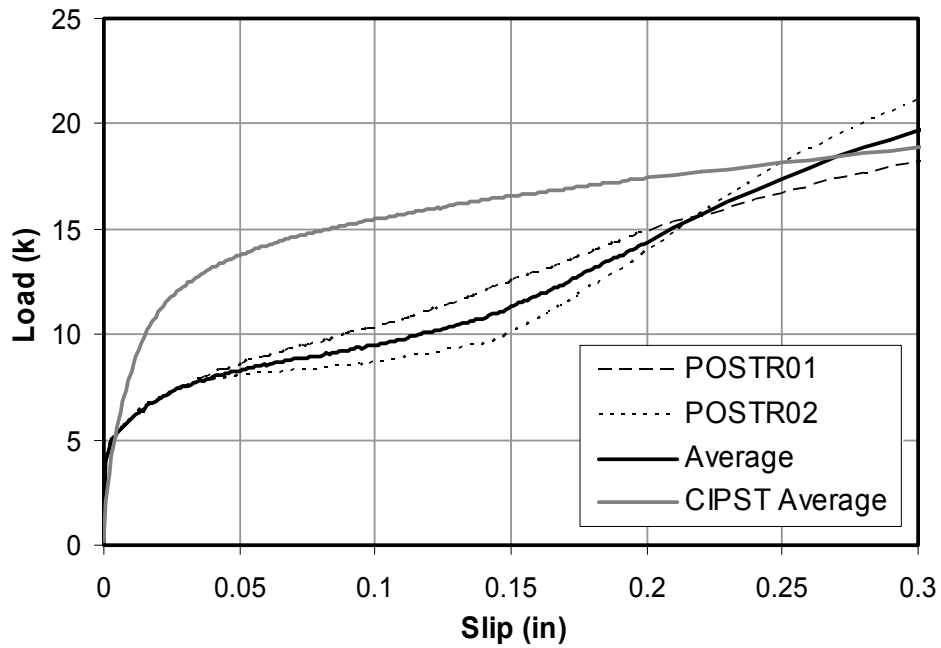
***Figure 6.10: Welded Threaded Rod, slip 0 to 0.3 in.***

The failure of POSTR specimens, shown in Figure 6.11, is marked by a shear failure immediately above the weld pool on the steel test plate. The white material around the threaded rod is sealant, applied to prevent the RS Anchor Gel Adhesive from entering the concrete-steel interface. Use of this sealant is discussed more thoroughly later in this chapter. Also clearly visible is the sizeable gap between the threaded rod and the inside of the hole in the grout.

*Figure 6.11: POSTR01 failure*

## 6.2.4 Load-Slip Curves and Failure Mode for the HAS-E Adhesive Anchor (HASAA)

The load-slip curves for the HAS-E Adhesive Anchor (HASAA) are shown in Figure 6.12, and a graph showing the 0- to 0.3-in. slip range only is shown in Figure 6.13. The HASAA01 and HASAA02 curves have a similar shape to that of the CIPST. Unintentionally, the HASAA03 test had adhesive at the concrete-steel interface due to the overflow of excess HY 150 during installation. This condition caused bonding of the concrete and steel, and the unique load-slip curve of the HASAA03. The HASAA specimens' primary resistance mechanism is static friction, which is overcome and replaced by bearing at about 10 kips of applied load. The secondary bearing mechanism is

comparable in stiffness to the initial stiffness of the CIPST connection. HASAA tests have ultimate strengths exceeding exceed that of the average CIPST, but their ductility is substantially less, particularly in the case of Test HASAA01.
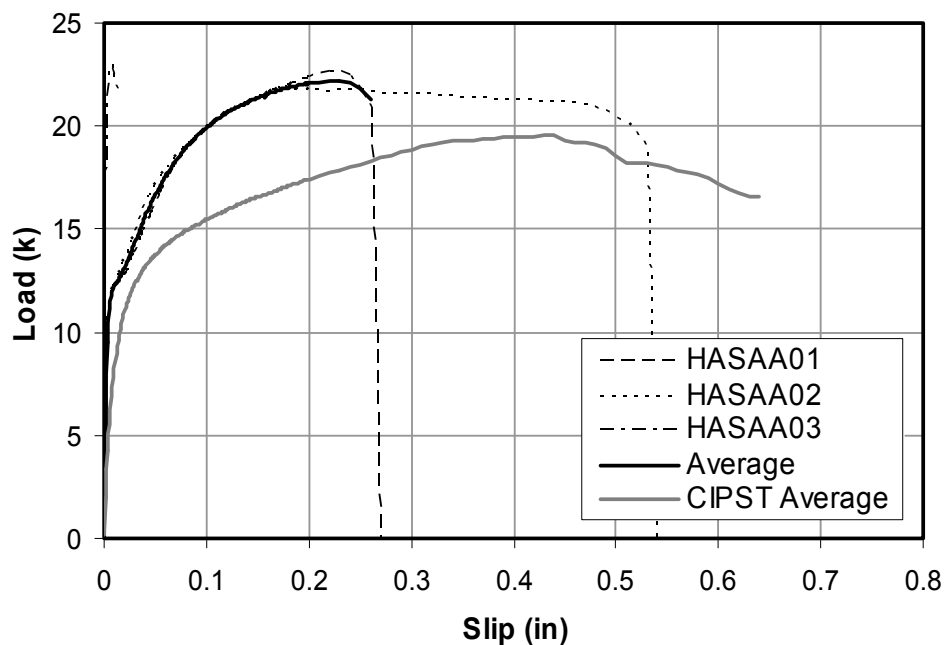


*Figure 6.12: HAS-E Adhesive Anchor, slip 0 to 0.8 in.*
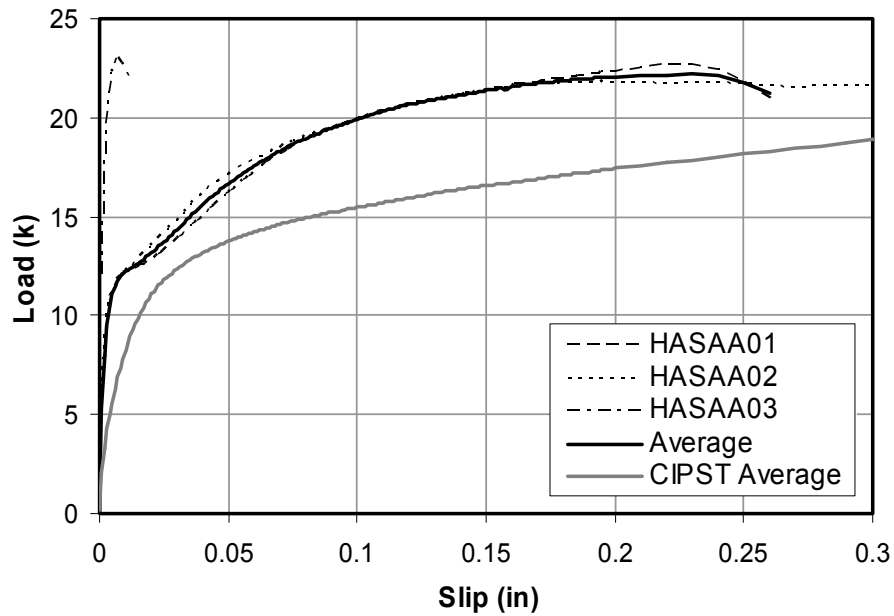
***Figure 6.13: HAS-E Adhesive Anchor, slip 0 to 0.3 in.***

HASAA specimens failed by shear of the threaded rod at the concrete-steel interface. A small localized area of crushed concrete (outlined in blue in Figure 6.14) was noted in front of the rod, near the concrete-steel interface, and is typical of anchors in bearing.

*Figure 6.14: HASAA02 failure*

### 6.2.5 Load-Slip Curves and Failure Modes for the HIT-TZ Adhesive Anchor (HITTZ)

Load-slip curves for the HIT-TZ Adhesive Anchor (HITTZ) are shown in Figure 6.15, and a graph showing the 0- to 0.3-in. slip range only is shown in Figure 6.16. Curves for tests HITTZ01 and HITTZ03 have a shape similar to those of HASAA and CIPST specimens. Unintentionally, the HITTZ02 test had adhesive at the concrete-steel interface due to the overflow of excess HY 150 when the anchor was installed; this problem was seen in the earlier HASAA03 test. The apparent oscillations in the load-slip curve for Test HITTZ02 between slips of 0 and 0.05 in. are caused by the successive formation of cracks in the adhesive at the concrete-steel interface, and the resulting slip from each crack.

It was determined that the inadvertent overflow of HY 150 adhesive was a serious problem because the prevented achievement of the intended load-slip behavior of the connector. The overflow was prevented in subsequent tests by a small ring of sealant at the interface around the hole in the concrete and steel. The ring of sealant acted only as a barrier to contain the HY 150 adhesive within the hole, and did not increase capacity significantly.

The HITTZ specimens maintain the primary static-friction mechanism up to a lower load (about 6 kips) than the HASAA specimens (about 10 kips), and it is unknown why this occurred. The bearing stiffness of Tests HITTZ02 and HITTZ03 was higher than that of the CIPST specimens, and the ultimate strength of all three HITTZ specimens exceeded that of the average CIPST specimen.
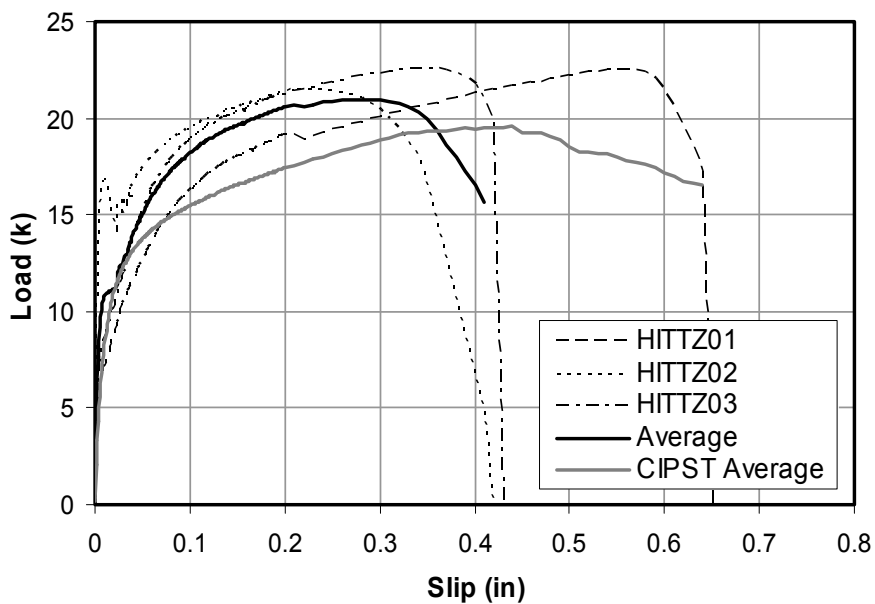


*Figure 6.15: HIT-TZ Adhesive Anchor, slip 0 to 0.8 in.*
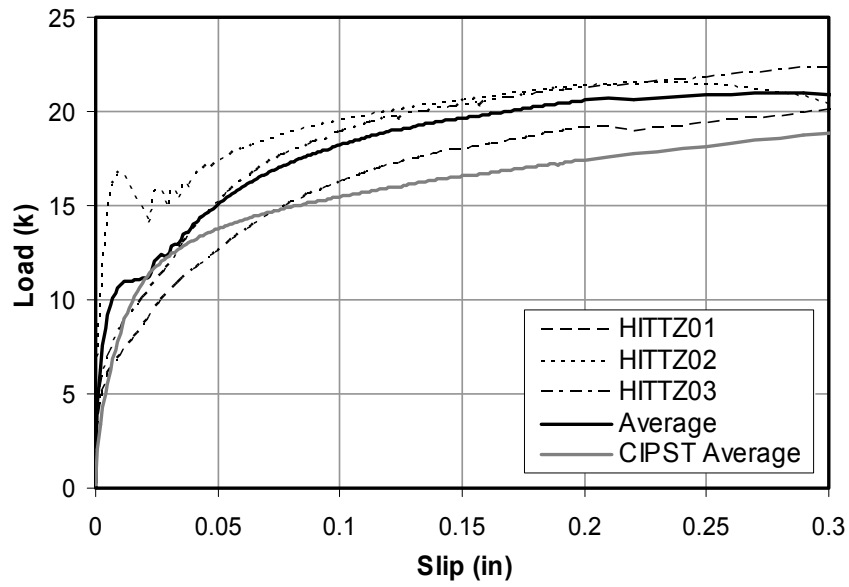
*Figure 6.16: HIT-TZ Adhesive Anchor, slip 0 to 0.3 in.*



*Figure 6.17: HITTZ03 failure with sealant around hole*

Tests HITTZ02 and HITTZ03 failed in shear connector at the concrete-steel interface (Figure 6.17), like the HASAA tests. Test HITTZ01 failed at the

138

root of one of the threads below the shear plane as discussed earlier in this chapter.  The white material in Figure 6.17 is sealant, placed around the hole of the anchor to confine the HY 150 adhesive.

### 6.2.6   Load-Slip Curves and Failure Modes for the HY 150 Plate (HY150)

The load-slip curve for the HY 150 Plate (HY150) is shown in Figure 6.18, and a graph of the 0- to 0.3-in. slip range only is shown in Figure 6.19.  The curve shows very little slip before brittle failure at an ultimate strength of about 5.4 kips.
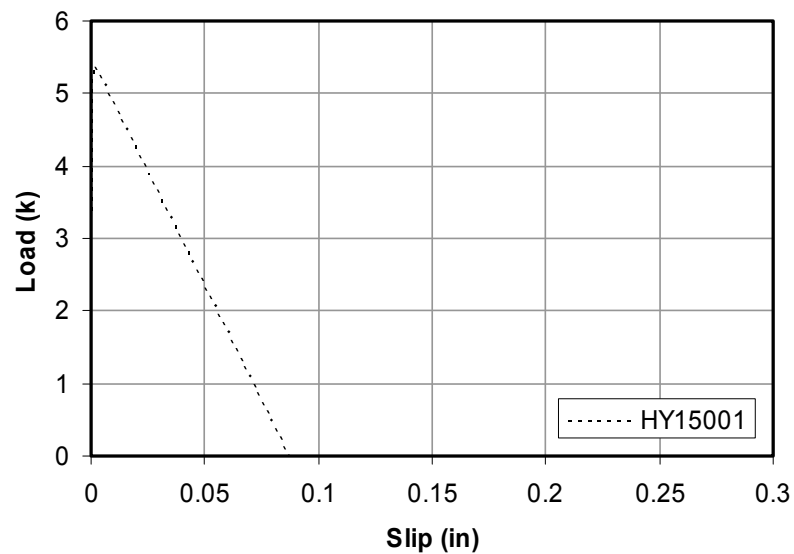


***Figure 6.18: HY 150 Adhesive Plate, slip 0 to 0.3 in.***
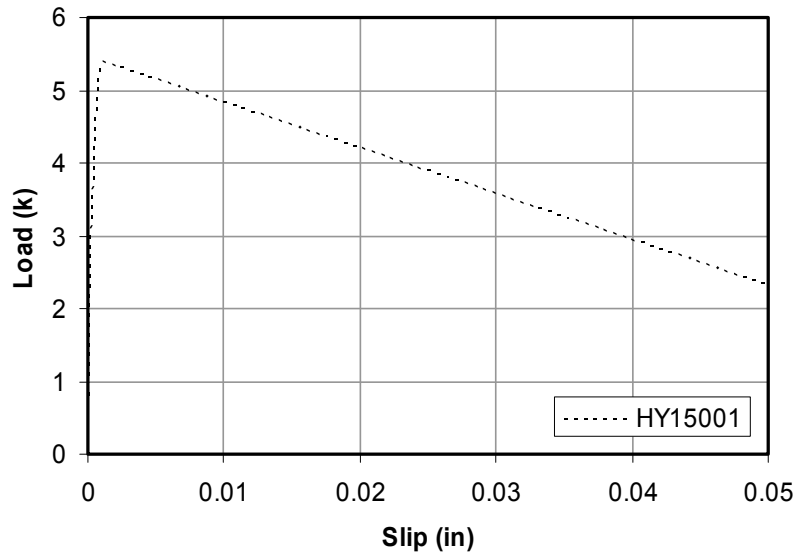
***Figure 6.19: HY 150 Adhesive Plate, slip 0 to 0.05 in.***

The HY 150 specimens failed in the adhesive itself. The concrete-steel interface was not fully covered with HY 150, and the adhesive had not fully cured when the specimen was tested. It was still soft to the touch after the specimen had been tested.

### 6.2.7 Load-Slip Curves and Specimen Failure for the Wedge-Bolt Concrete Screw (WEDGB, WEDGG, WEDGS)

The Wedge-Bolt Concrete Screw tests comprise three related series of tests: on the Wedge-Bolt Concrete Screw (WEDGB); on the Wedge-Bolt Concrete Screw with Sheath (WEDGS); and on the Wedge-Bolt Concrete Screw with RS Anchor Gel (WEDGG). The load-slip results for each test series are discussed here in that order. The failure mode for all except in the WEDGS tests is discussed at the end of this section. Comments particular to the WEDGS tests are presented immediately following the WEDGS load-slip results because much of its discussion is unique.

The load-slip curves for the Wedge-Bolt Concrete Screw (WEDGB) are shown in Figure 6.20, and a graph of the 0- to 0.3-in. slip range only is shown in Figure 6.21. The WEDGB specimens show early slip without load, and begin bearing at about 0.05 in. for Tests WEDGB01 and WEDGB03, and about 0.1 in. for Test WEDGB02. The bearing stiffness is less than that of the CIPST specimens, but the ultimate strengths are substantially higher. All WEDGB tests experienced a large slip (0.6 to 0.7 in.) before a sharp drop in the load-slip curve at failure.
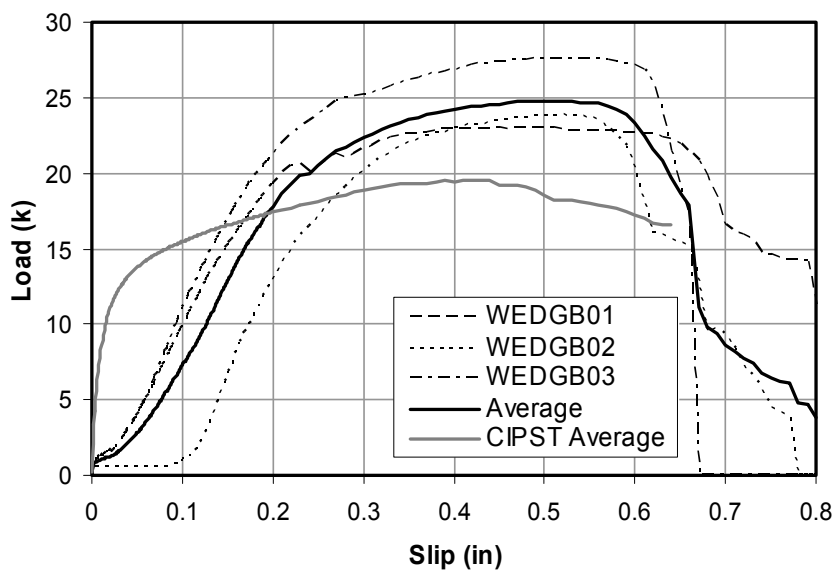


***Figure 6.20: Wedge-Bolt Concrete Screw (WEDGB), slip 0 to 0.8 in.***
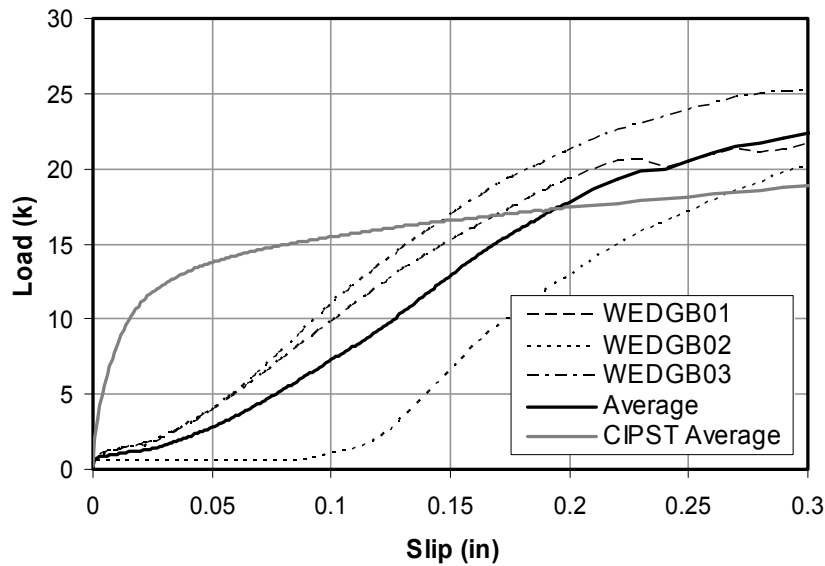
***Figure 6.21: Wedge-Bolt Concrete Screw (WEDGB), slip 0 to 0.3 in.***

In an attempt to reduce the slip without load seen in the WEDGB series, the Wedge-Bolt Concrete Screw with Sheath specimen (WEDGS) was devised. The load-slip curve for that specimen is shown in Figure 6.22, and a graph of the 0- to 0.3-in. slip range only is shown in Figure 6.23. The WEDGS specimens do not display the early slip without load typical of the WEDGB specimens. Instead, they have a constant connection stiffness, significantly less than that of the CIPST. The average ultimate strength of the WEDGS specimens exceeds that of the CIPST specimens, and is comparable to that of the WEDGB specimens. Failure occurs very quickly after ultimate strength is reached, with a very sudden drop in load-carrying capacity.
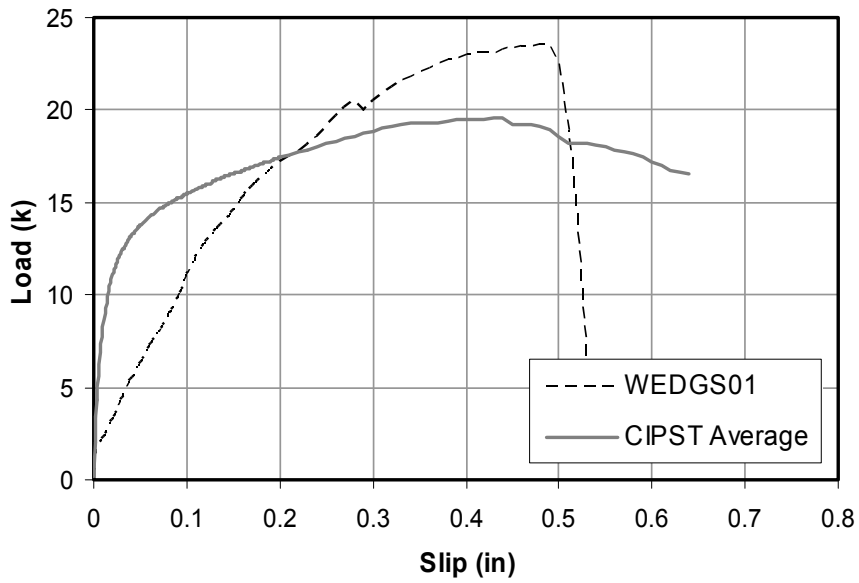
*Figure 6.22: Wedge-Bolt Concrete Screw with Sheath (WEDGS), slip 0 to 0.8 in.*
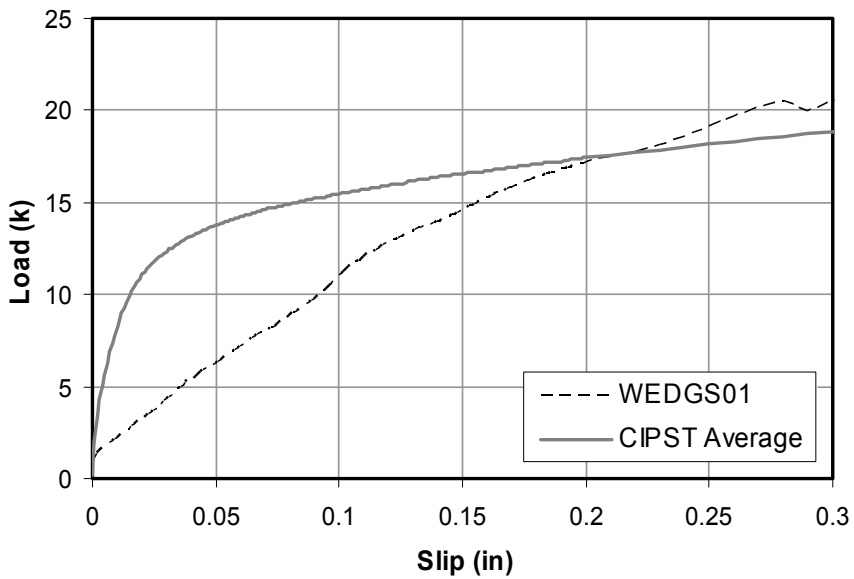


*Figure 6.23: Wedge-Bolt Concrete Screw with Sheath (WEDGS), slip 0 to 0.3 in.*

143

During installation of the WEDGS anchor, one side of the sheath pushed below the bottom surface of the steel plate due to friction with the screw. Figure 6.24 shows an image of this condition at failure.



*Figure 6.24: WEDGS failure with protruding sheath*

Half the protruding sheath became positioned behind (relative to the direction of applied load) the anchor shank, and may have allowed excessive flexural deformation of the screw by allowing the it to bend over the top edge of the protruding sheath as shown in Figure 6.25.
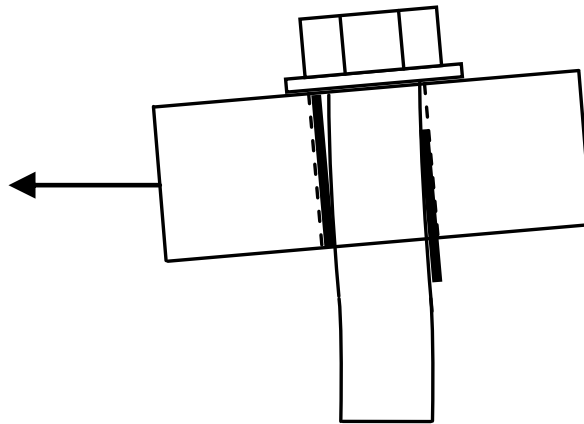
***Figure 6.25: Deformation permitted by protruding sheath in WEDGS test***

Given this problem with the sheath, another way of reducing the gap between the screw and the steel test plate was attempted:  filling the gap with an adhesive, to produce the Wedge-Bolt Concrete Screw with RS Anchor Gel WEDGG) specimens.  Load-slip curves for those specimens are shown in Figure 6.26, and a graph of the 0- to 0.3-in. slip range only is shown in Figure 6.27.  All WEDGG tests show early slip with little load-carrying capacity.  While Test WEDGG01 has a load-slip curve similar to those of the WEDGB series, the other two WEDGG tests differ substantially:  their stiffnesses and ultimate strengths are lower those of Test WEDGG01 test, the WEDGB series, the WEDGS test, and the average CIPST test.
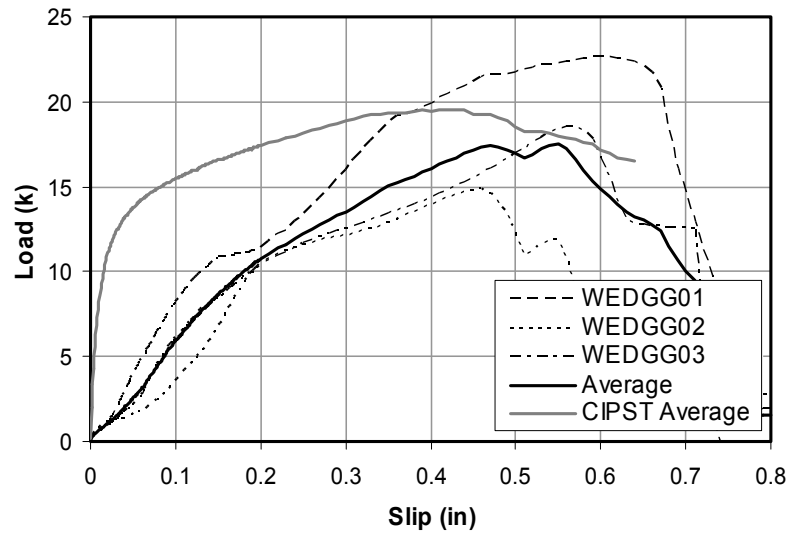
***Figure 6.26: Wedge-Bolt Concrete Screw with RS Anchor Gel (WEDGG), slip 0
to 0.8 in.***
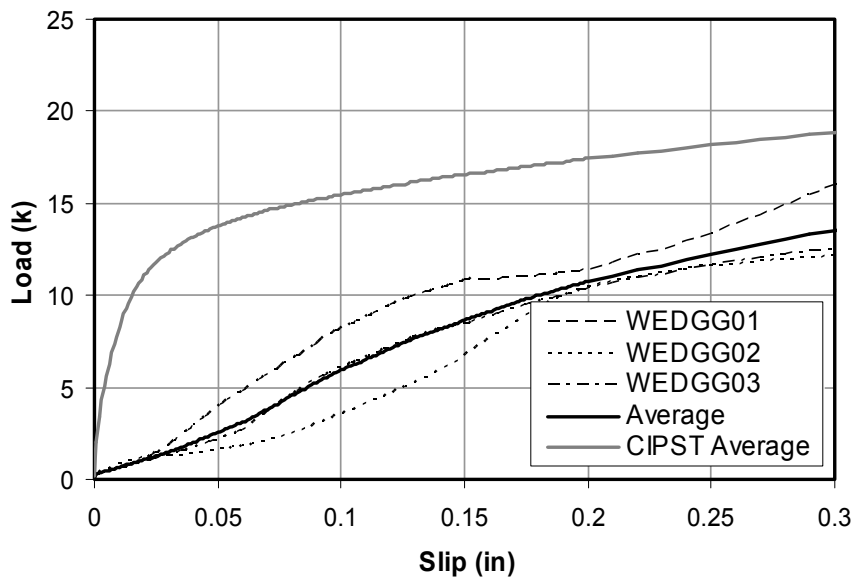
*Figure 6.27: Wedge-Bolt Concrete Screw with RS Anchor Gel (WEDGG), slip 0 to 0.3 in.*

The WEDGG specimens were not successful.  It was not possible to place the adhesive in the narrow gap between the screw shank and the hole in the steel test plate.  Also, because the holes were not drilled deep enough, the hex-washer head of the anchor was not flush with the top of the steel test plate.  This allowed the screw to rotate with respect to the shear plane and permitted increased slip.

All Wedge-Bolt specimens failed by a combination of shear and tension in the screw, at the root of a thread about 1.5 in. below the concrete-steel interface, accompanied by substantial crushing and spalling of concrete.  A typical failure (WEDGB01) is shown in Figure 6.28.

147

*Figure 6.28: WEDGB01 failure with spalled concrete*

The large spalled area is probably a local breakout failure of concrete around the threads nearest the surface of the concrete. Also, the concrete test block cracked through its entire width perpendicular to the direction of applied load in the WEDGB01 and WEDGB03 specimens.

## 6.2.8 Load-Time Curves and Failure Mode for the 3M Epoxy Plate (3MEPX, 3M24H, 3MSTS, 3MCNS)

The 3M Epoxy Plate method included four series of tests: the 3M Epoxy Plate (Heat-Cure); the 3M Epoxy Plate (24-Hour Cure); the 3M Epoxy Plate (Steel Surface); and the 3M Epoxy Plate (Concrete Surface). Ultimate strengths of these specimens exceeded 50 kips, and corresponded to zero measurable. While these ultimate strengths are well above those attained by the average CIPST, the Epoxy Plate method displayed no ductility. Distinctions among the

148

setups used in this test series, and the corresponding results, are given in Table 6.2. Because there was no slip, load-time curves are used instead, and are presented and discussed in the order in which the test series are listed above.

*Table 6.2: 3M Epoxy Plate tests*

| Test | Cure Time (days) | Cure Temperature (F) | Applied Pressure During Curing (psi) | Ultimate Capacity (kip) | Series Average (kip) |
|---|---|---|---|---|---|
| 3MEPX01 | 4 | 130 | 5 | 52.68 | |
| 3MEPX02 | 4 | 130 | 5 | 59.77 | 55.43 |
| 3MEPX03 | 4 | 130 | 5 | 53.84 | |
| 3M24H01 | 1 | 70 | 2 | 57.46 | 58.01 |
| 3M24H02 | 1 | 70 | 2 | 58.55 | |
| 3MSTS01 | 2 | 70 | 2 | 56.84 | 57.11 |
| 3MSTS02 | 2 | 70 | 2 | 57.39 | |
| 3MCNS01 | 2 | 70 | 2 | 61.07 | 61.38 |
| 3MCNS02 | 2 | 70 | 2 | 61.68 | |

In the first test series (3MEPX) specimens were cured at above-room temperature conditions (about 130 F), for 4 days, with 5 psi pressure on the connection. The load-time graph is given in Figure 6.29.
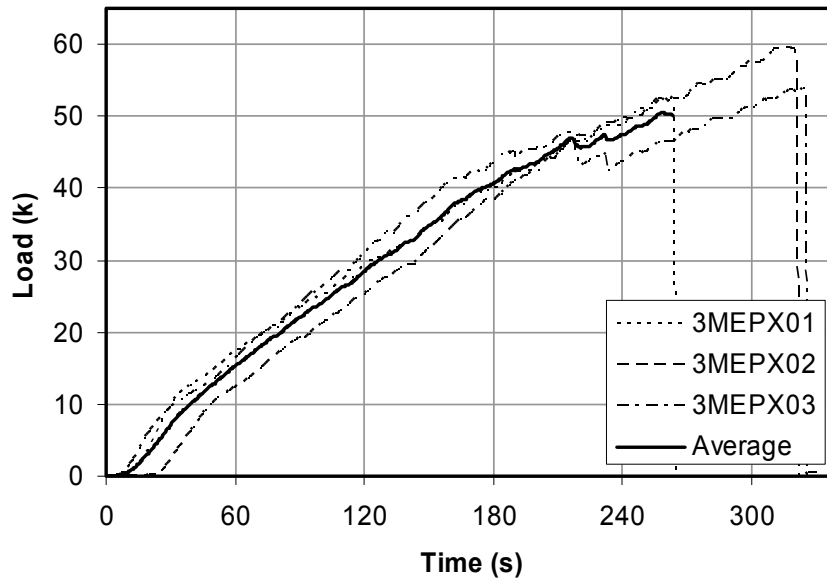
***Figure 6.29: 3M Epoxy Plate (3MEPX), load versus time***

The sudden drops in load-carrying capacity for 3MEPX03 at 215 seconds and 232 seconds are due to the development of cracks in the concrete. The load dropped from 47.8 to 43.1 kips, and from 44.7 to 42.5 kips, respectively, decreases of 10% and 5%.

The next series of tests was the 24-Hour series (3M24H), whose purpose was to determine if the epoxy could develop the capacity observed in the 3MEPX tests with only 24 hours of curing at room temperature, using only 2 psi of pressure on to the connection during the cure time. No sudden drops in load occurred during these tests. Figure 6.30 shows load-time curves for the 3M24H specimens.
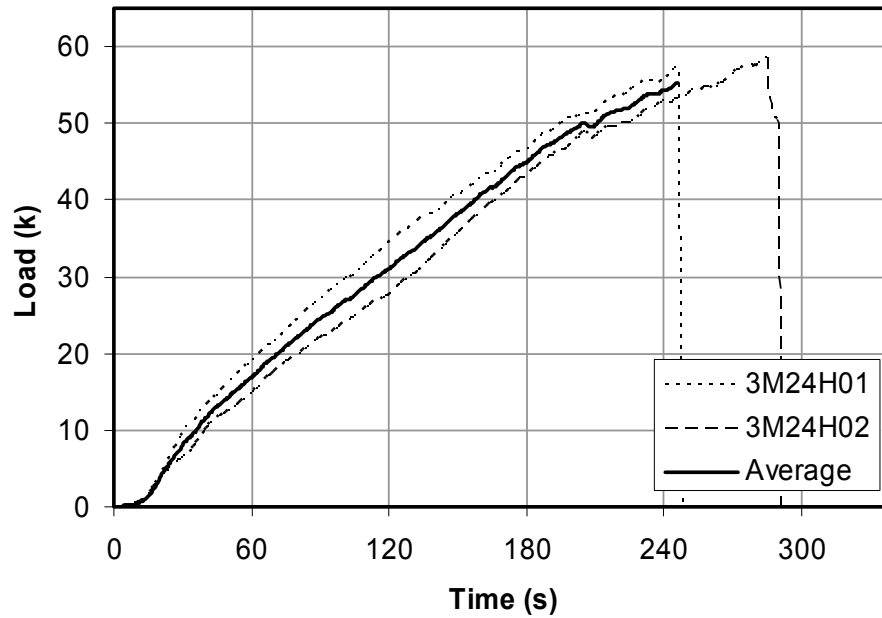
***Figure 6.30: 3M Epoxy Plate (3M24H), load versus time***

The 3MSTS tests were intended to investigate a lower degree of steel surface preparation than had been performed in earlier 3M Epoxy Plate tests. The specimens were cured for two days at room temperature under 2 psi of pressure. Their load versus time graph is shown in Figure 6.31.
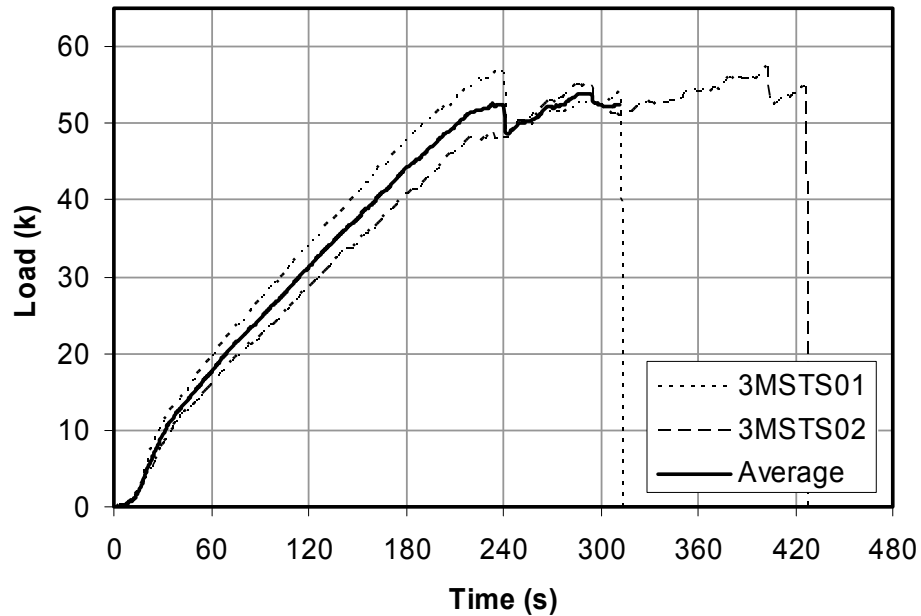
*Figure 6.31: 3M Epoxy Plate (3MSTS), load versus time*

One major drop in load-carrying capacity occurred in Test 3MSTS01.  At 241 seconds, load dropped from 56.7 to 49.0 kips at 241 seconds (a 14% drop), and the specimen later failed at 54.0 kips (95% of the ultimate load).

Specimen 3MSTS02 experienced two major decreases in load, the first less distinctive than the second.  The first drop, from 294 to 314 seconds, was from 55.3 to 50.9 kips (a drop of 8%).  The second drop, at 403 seconds, was a sudden drop from 57.4 to 52.4 kips (a drop of 9%).  The specimen failed at 54.9 kips (96% of the ultimate load).

The 3MCNS tests were intended to investigate the effects of inferior concrete surface preparation.  Specimens were allowed to cure for 2 days at room temperature, with about 2 psi of pressure on the connection.  The 3MCNS tests resulted in the highest ultimate strengths attained by any of the 3M Epoxy Plate tests.  Load-time curves are given in Figure 6.32.

152
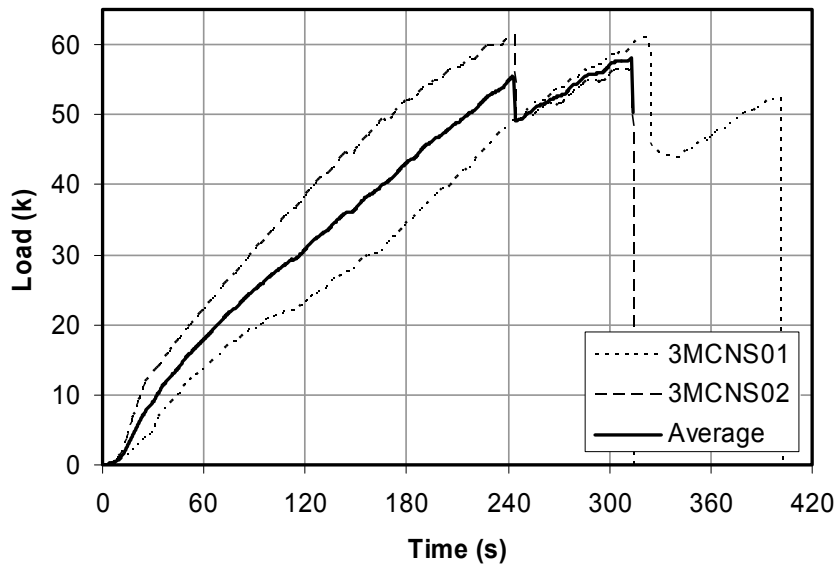
*Figure 6.32: 3M Epoxy Plate (3MCNS), load versus time*

The 3MCNS tests had more extreme drops in load-carrying capacity than Test 3MEPX03. Both 3MCNS specimens had one major drop in load before failure, and in both specimens the load at failure was less than the load at which the earlier drop had occurred.

Specimen 3MCNS01 had slightly less than the ultimate load of 61.1 kips at 323 seconds, when the load dropped to 43.8 kips (a 28% decrease in capacity). The load at failure was 52.5 kips (86% of the ultimate load). Specimen 3MCNS02 reached an ultimate capacity of 61.9 kips, and its capacity began to decrease. At 244 seconds, the load dropped suddenly from 60.8 to 49.0 kips, a decrease of 19%. The load at failure was 56.6 kips (91% of the ultimate load).

The sudden drops in load-carrying capacity in the Epoxy Plate specimens are caused by the formation of cracks in the concrete. The typical failure of an Epoxy Plate specimen is shown in Figure 6.33 with the blue lines indicating cracks in the concrete test block.

153
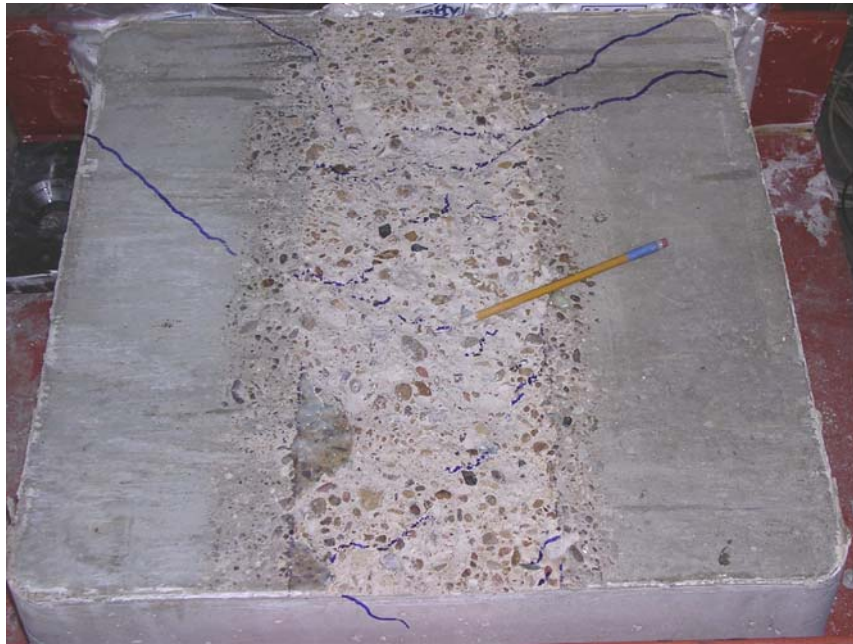
*Figure 6.33: Typical failure of Epoxy Plate specimen (cracks marked in blue)*

The swath in the middle of the test block is the concrete side of the steel-concrete interface after failure. At the top middle of the picture the color of the failure surface changes because the failure surface is flatter and smoother at the front (nearest the applied load) of the test specimen. The surface is flatter and smoother because little concrete was removed there.

# CHAPTER 7

# Estimating Load-Slip Demand on Retrofit Shear Connectors

## 7.1 PRELIMINARY REMARKS

In current AASHTO provisions, shear connectors are presumed to be welded shear studs or shear lugs, and their design is based on ultimate shear strength, without considering slip. In the author's opinion, this design approach is incomplete. As is demonstrated later in this chapter, connector stiffness under load (described in terms of load-slip behavior) is as important as strength for design. Shear connectors can be designed by comparing their load-slip characteristics, with the anticipated load and slip demand on them in retrofit applications. The purpose of this chapter is to suggest some general techniques for estimating load-slip demand on retrofit shear connectors.

As an initial step, one could investigate the slip that occurs at the shear stud strength given in the *AASHTO LRFD Bridge Design Specifications* (1998), using empirical equations proposed by Ollgaard *et al*. (1971) based on their research. The first of their empirical equations, repeated here as Equation 7.1, gives ultimate shear strength in terms of the cross-sectional area of the stud, the specified concrete compressive strength, and the concrete modulus of elasticity:

$$Q_u = 0.5 \cdot A_{sc} \cdot \sqrt{f_c' \cdot E_c} \le A_{sc} \cdot F_u \qquad \textbf{\textit{(Equation 7.1)}}$$

where:

$Q_u$ = ultimate strength of a shear stud (kip)

155

$A_{sc}$ = cross-sectional area of a shear stud (in.$^2$)

$f'_c$ = specified compressive strength of concrete at 28 days (ksi)

$E_c$ = modulus of elasticity of concrete (ksi)

$F_u$ = specified minimum ultimate tensile strength of a shear stud (ksi)

The modulus of elasticity of concrete is defined by Equation 7.2.

$$E_c = 57 \cdot \sqrt{f'_c} \qquad \textbf{\textit{(Equation 7.2)}}$$

where

$E_c$ = modulus of elasticity of concrete (ksi)

$f'_c$ = specified compressive strength of concrete at 28 days (psi)

The second of these, repeated here as Equation 7.3, gives the load-slip relationship in terms of that ultimate shear strength:

$$Q = Q_u \cdot \left(1 - e^{-18\Delta}\right)^{2/5} \qquad \textbf{\textit{(Equation 7.3)}}$$

where:

$\Delta$ = slip of shear stud (in.)

$Q$ = strength of shear stud at slip $\Delta$ (kips)

$Q_u$ = ultimate strength of shear stud (kips), obtained from Equation 7.1.

If Equation 7.3 is rearranged and solved for the slip $\Delta$ in terms of ($Q/Q_u$), Equation 7.4 is obtained. The variables retain the above definitions.

$$\Delta = -\frac{\ln\left[1 - \left(\dfrac{Q}{Q_u}\right)^{5/2}\right]}{18} \qquad \textbf{\textit{(Equation 7.4)}}$$

In Figure 7.1 are shown values of slip $\Delta$ corresponding to different values of $(Q/Q_u)$ as calculated from Equation 7.3, and also the mean observed values from the direct shear tests of cast-in-place welded shear studs conducted in this study. Figure 7.2 shows the same information, presented in the more familiar form with displacements on the horizontal axis.
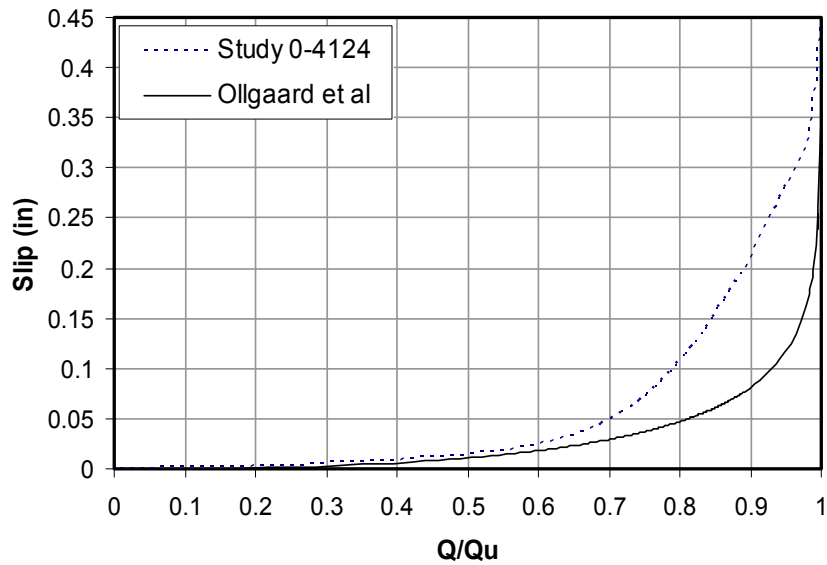


***Figure 7.1: Slip Δ in terms of (Q/Q_u) (Equation 7.4)***
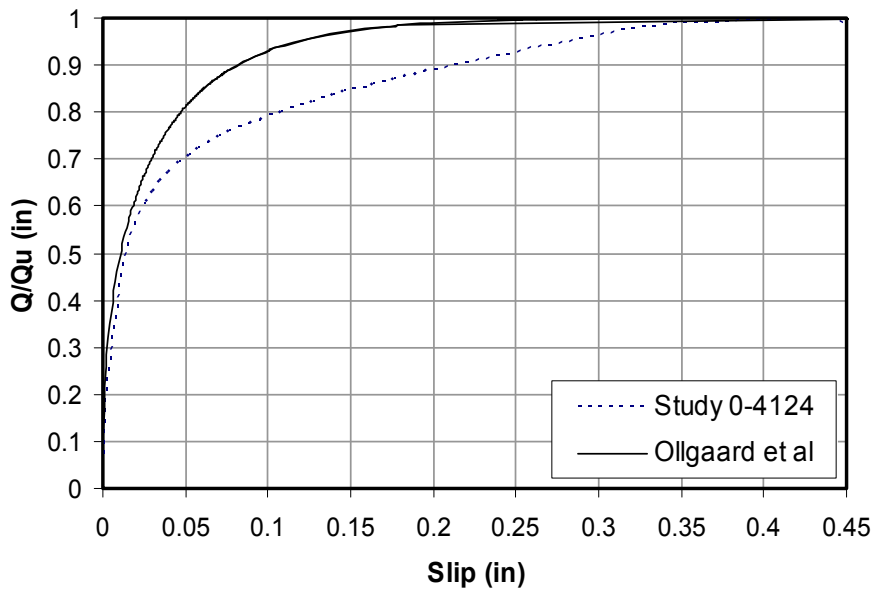
*Figure 7.2: (Q/Q_u) in terms of slip Δ (Equation 7.3)*

Examination of Figure 7.2 shows that the predictions of Equation 7.3 are inconsistent with the load-slip data obtained in the tests of this study, and also potentially inconsistent with current AASHTO design methods:

o     According to Equation 7.3, a cast-in-place welded shear stud attains approximately 95% of its ultimate strength at a slip of 0.1 in., and 99% of its ultimate strength at a slip of 0.2 in. This predicted behavior is far stiffer than that actually observed in this study.

o     According to Equation 7.3, the shear stud requires a slip of 0.2 in. to reach its 99% of its ultimate strength. This implies that the slip of shear connectors must be considered in composite design. In addition, because bridge components are essentially designed for fatigue, shear connectors

should be designed for service-level load-slip demand, and not simply ultimate strength.

To have a consistent approach to connector design, overall bridge response (deflection, stress, or stress range) should be related to the load-slip demand on the shear connectors, so that serviceability limits on the bridge can be related to corresponding load-slip demands on the shear connectors.  This can be accomplished through existing mechanics-based equations, existing empirical equations, or finite-element analyses.  In the remainder of this chapter, the first two approaches are discussed briefly, and the last approach is explored in more detail.

## 7.2    OVERALL BRIDGE RESPONSE VERSUS LOAD-SLIP DEMANDS ON SHEAR CONNECTORS

### 7.2.1    Existing Analytical Equations

Using the principles of engineering mechanics, direct and indirect relationships can be derived between overall bridge response to applied load and the load-slip demand on the shear connectors.

In the direct solution, a complete relationship is derived between the overall bridge response and the load-slip demand on shear connectors.  This approach is attractive because it is complete, but its development is difficult and the final form of the solution is lengthy.

In the indirect solution, a relationship exists between the applied load and the load-slip demand on the shear connector, and an additional relationship relates the applied load to the overall bridge response.  This requires an intermediate step, and the relationship between the applied load and the overall bridge response is still not compact.  The association between the applied load and the load-slip

demand on the shear is easily performed using basic mechanics. Further information on this subject may be found in Schaap (2004).

### 7.2.2 Existing Empirical Equations

Through extensive experimentation, empirical relationships between applied load and overall member response could be developed based on the variables in the construction of a composite member. The process would be similar to that performed by Ollgaard *et al.* (1971), but on a larger scale of testing. The author is not currently aware of any empirical equations that relate overall bridge response to load-slip demand on the shear connector.

### 7.2.3 Finite-Element Analysis

In addition to the methods discussed above, a finite-element analysis can be performed on the composite cross-section, with the concrete and steel components connected by nonlinear springs whose load-slip behavior is based on experimental results. This approach can provide excellent predictions of the relationship between overall bridge behavior and local load-slip demand on connectors, provided that the components (particularly the connectors) are correctly modeled.

While it can in principle be applied for any level of applied load, it is probably most useful for design if it is used for the specific case in which overall bridge behavior is limited by an allowable load, or by an allowable deflection. To compute the load-slip demands on a shear connector in a bridge subject to an allowable deflection limit, the following procedure is used with the finite-element model:

o      Select a limiting service deflection for the overall bridge.

o      Using the finite-element model, find the applied load necessary to cause that limiting service deflection. If the connector load-slip behavior is non-linear, iteration may be required.

o      At that load level, find the corresponding load-slip demands on individual shear connectors.

For purposes of this study, the above procedure was performed on the idealized prototype bridge.

o      A finite-element model of the bridge was prepared using the using the commercial finite-element analysis program ANSYS. A 50-ft, simply supported span was modeled assuming linear elastic material behavior for the steel girders and the concrete deck, because stresses in those materials were assumed to be quite low at service-level loads. The deck was modeled using plane-stress elements with uniform thickness equal to the width of the deck (74 in.). A schematic of the finite-element model cross-section is shown in Figure 7.3.
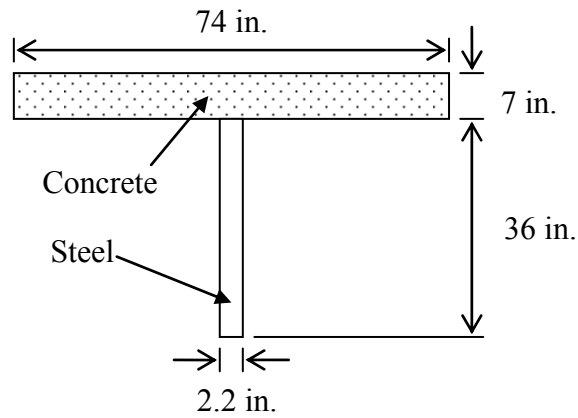
***Figure 7.3: Finite-element model cross-section***

The steel girder was modeled using plane-stress elements, and was assigned the uniform thickness necessary to give a moment of inertia equal to that of the measured cross-section. A 1-in. square mesh was generated for both components. The interface was modeled with two sets of collocated nodes. Along the interface, at longitudinal spacings of 1 ft, deck nodes were connected with the girder node one element-dimension away by a nonlinear spring oriented parallel to the interface, and whose nonlinear load-slip relationship was based on mean load-slip data for the cast-in-place welded studs. Each set of collocated deck and girder nodes was constrained to have the same vertical deflection. Figure 7.4 shows the details of the concrete-steel interface with the concrete and steel components separated at the interface for clarity.

162

concrete element (typ.)

1 in.

1 in.

nonlinear
spring
(12-in. sp.)

collocated
nodes (typ.),
same vertical
deflection

1 in.

1 in.

steel element (typ.)

element node (typ.)
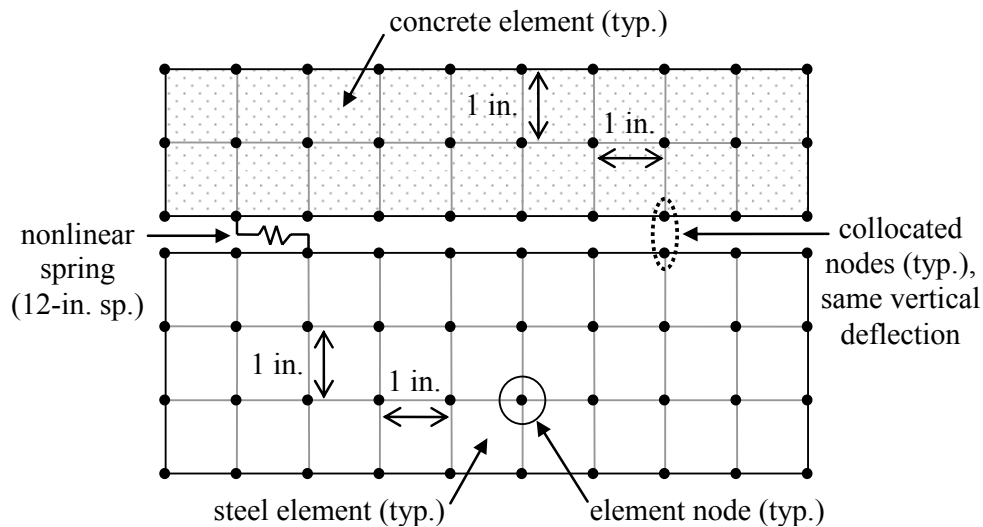
*Figure 7.4: Interface detail of finite-element model*

o    A sample limiting service-level deflection of the span divided by 360 was
     assumed.  While to a certain extent arbitrary, this limiting deflection is
     typical for many bridges, and can reasonably be used here to demonstrate
     the procedure.  Using the finite-element model, it was determined that this
     deflection (1.67 in.) would be produced by a uniformly distributed load of
     4.1 psi on the deck.  The resulting maximum slip occurred at the end of
     the member, and was 0.125 in.

o    Based on this result, one would assess the suitability of proposed retrofit
     connectors by comparing their resistance with that of the reference
     connector (Cast-In-Place Welded Stud) at a slip of 0.125 in.

For this study, however, the limiting slip value of 0.125 in. was not used directly.
After completing the procedure described above, it was realized that the finite
element model was over-constrained.  Each set of collocated deck and girder

163

nodes was constrained to have the same vertical deflection, rather than the same deflection normal to the interface. In the finite-element model, such springs were represented numerically by diagonal stiffness matrices. When the model deflected under vertical load, and the interface rotated away from the horizontal, the springs rotated as well (Figure 7.5).
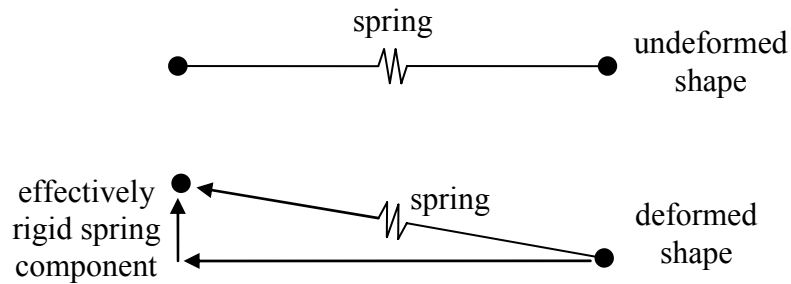


*Figure 7.5: Over-constraint of the finite-element model*

Because the vertical displacements of collocated points were constrained to be identical, the diagonal component of the spring stiffness corresponding to vertical displacements was effectively forced to be infinite.
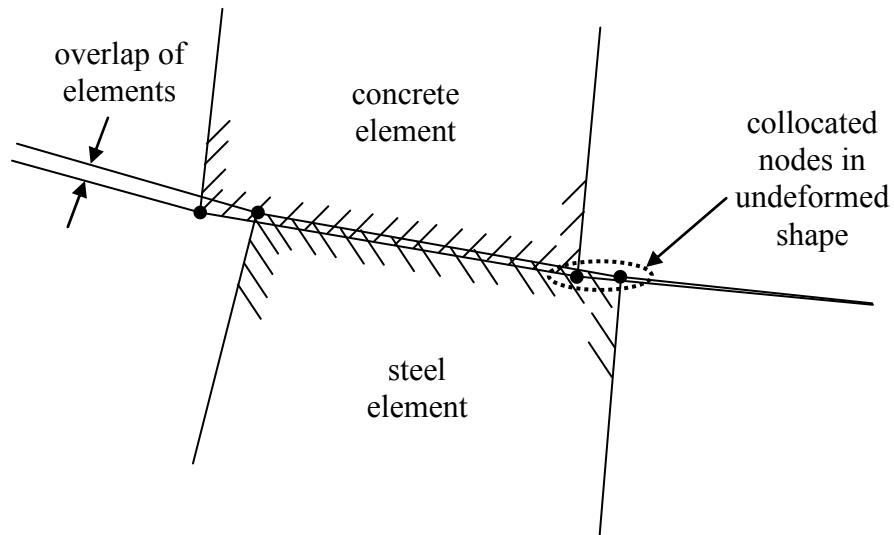


*Figure 7.6: Overlap of interface elements due to over-constraint in finite element model*

164

In this sense, the idealized spring was slightly stiffer than the real one. This increased the stiffness of the idealized load-slip behavior, made the predicted slip slightly low for any level of applied load on the girder, and made the idealized girder stiffer under load than the real one.

Based on the possibility of over-constraint, the suggested slip limit is probably less certain than the value of 0.125 obtained here. Based in part on results for analytical formulas (Schaap 2004), connector load-slip performance was compared at slips of 0.1 and 0.2 in. Ultimate strengths were compared as well. These comparisons are presented in Chapter 8.

The load-slip results obtained here using finite-element analysis, while generally realistic, are regarded only as an indicator of the slip limit. Results would be expected to vary based on the limiting load or deflection, state, the connector spacing, and the connector load-slip behavior. Nevertheless, the results compare reasonably with those from existing analytical equations (Schaap 2004), and in the author's opinion represent a promising and rational design approach for shear connectors.

# CHAPTER 8

# Discussion of Observed versus Required Load-Slip Performance for Retrofit Shear Connectors

## 8.1 PRELIMINARY REMARKS

In this chapter, using results from the direct-shear, single-connector tests described here, applied loads for each retrofit connector are compared, at slips of 0.1 and 0.2 in., with the mean applied loads for Cast-In-Place Welded Stud. Based on those comparisons, comparatively well-performing shear connectors are identified, and are recommended for retrofitting applications.

From the viewpoint of this study alone, this discussion could end there, because the observed results for all connectors were obtained using a single test method. Because the results of this study, and any associated design recommendations, will be used in an AASHTO design context based on the work of Ollgaard *et al.* (1971), they will inevitably be compared with that work. It is therefore useful to begin that comparison here. Major points of this comparison are given in this chapter; additional details are given in Appendices B and C.

## 8.2 PERFORMANCE OF POST-INSTALLED SHEAR-TRANSFER METHODS COMPARED TO THAT OF CAST-IN-PLACE WELDED STUDS

### 8.2.1 Average Load-Slip Behavior and Capacities versus CIPST

In Table 8.1 are shown the average applied loads from tests on each shear-connector method at slips of 0.1 in. and 0.2 in., and also the ultimate shear strength. In Table 8.2 is shown the ultimate strength of each post-installed method as a percentage of that of the Cast-In-Place Welded Stud.

166

*Table 8.1:  Average strength of shear-transfer methods at slips of 0.1 in., 0.2 in.,
and at ultimate strength*

| Test Series | Strength at 0.1 in. (kip) | Strength at 0.2 in. (kip) | Average Slip at Ultimate Strength (in.) | Average Ultimate Strength (kip) |
|---|---|---|---|---|
| CIPST | 15.48 | 17.43 | 0.532 | 21.25 |
| POSTR | 9.49* | 14.40* | 0.351 | 20.84* |
| HASAA | 19.92 | 22.08 | 0.212 | 22.52 |
| HITTZ | 18.22 | 20.58 | 0.379 | 22.21 |
| HY150 | - | - | 0.005 | 5.40* |
| WEDGB | 7.28* | 17.81 | 0.506 | 24.84 |
| WEDGG | 5.93* | 10.74* | 0.543 | 18.68* |
| WEDGS | 11.03* | 17.14* | 0.484 | 23.60 |
| 3MEPX | - | - | 0 | 55.43 |
| 3M24H | - | - | 0 | 58.01 |
| 3MSTS | - | - | 0 | 57.11 |
| 3MCNS | - | - | 0 | 61.38 |

Those values followed by an asterisk are less than the corresponding
CIPST values.  Remaining results of the post-installed methods are discussed in
Schaap (2004).

*Table 8.2: Percentage of CIPST strength attained by post-installed shear-transfer methods at slips of 0.1 in., 0.2 in., and at ultimate strength*

| Test Series | Strength at 0.1 in. (%) | Strength at 0.2 in. (%) | Average Slip at Ultimate Strength (%) | Average Ultimate Strength (%) |
|---|---|---|---|---|
| CIPST | 100 | 100 | 100 | 100 |
| POSTR | 61* | 83* | 66 | 98* |
| HASAA | 129 | 127 | 40 | 106 |
| HITTZ | 118 | 118 | 71 | 105 |
| HY150 | 0 | 0 | 0.9 | 25* |
| WEDGB | 47* | 102 | 95 | 117 |
| WEDGG | 38* | 62* | 102 | 88* |
| WEDGS | 71* | 98* | 91 | 111 |
| 3MEPX | - | - | 0 | 261 |
| 3M24H | - | - | 0 | 273 |
| 3MSTS | - | - | 0 | 269 |
| 3MCNS | - | - | 0 | 289 |
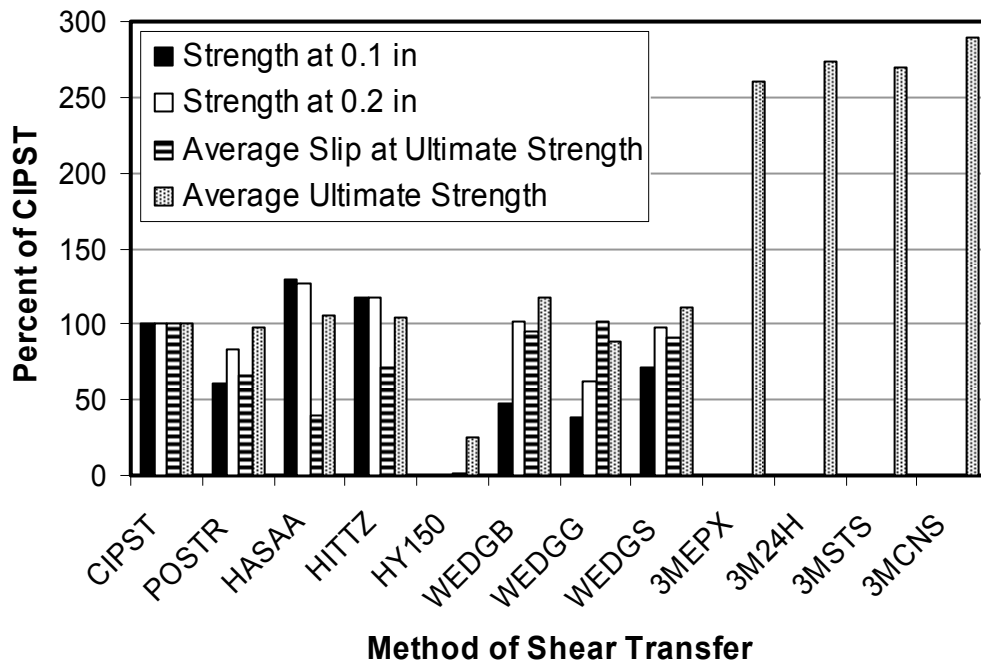
**Figure 8.1: Percentage of CIPST strength attained by post-installed methods to transfer shear at slips of 0.1 in., 0.2 in., and at ultimate strength**

In the following pages, graphs are presented comparing the average load-slip curves for each of various post-installed connection methods, with the average load-slip curve for the Cast-In-Place Welded Stud. All post-installed methods except the HY 150 Plate and 3M Epoxy Plate are presented. The HY 150 Plate does not have sufficient load-slip data to compare with the Cast-In-Place Welded Stud, and in the 3M Epoxy Plate series, slip was not electronically monitored because the slip was too small to be measured.

In examining the comparison graphs, note that average load-slip curves can be created only up to the lowest failure slip in the series. Also, because the ultimate strengths of the individual tests do not occur at a simultaneous slip, the

average graph of their behavior has an ultimate strength less than the average of the ultimate strengths from the individual tests.

In Figure 8.2, this comparison is presented for the Welded Threaded Rod (POSTR) and the Cast-in-Place Welded Stud (CIPST). It is evident that the POSTR is less strong than the CIPST at the key slip values of 0.1 and 0.2 in, and has about the same ultimate strength.
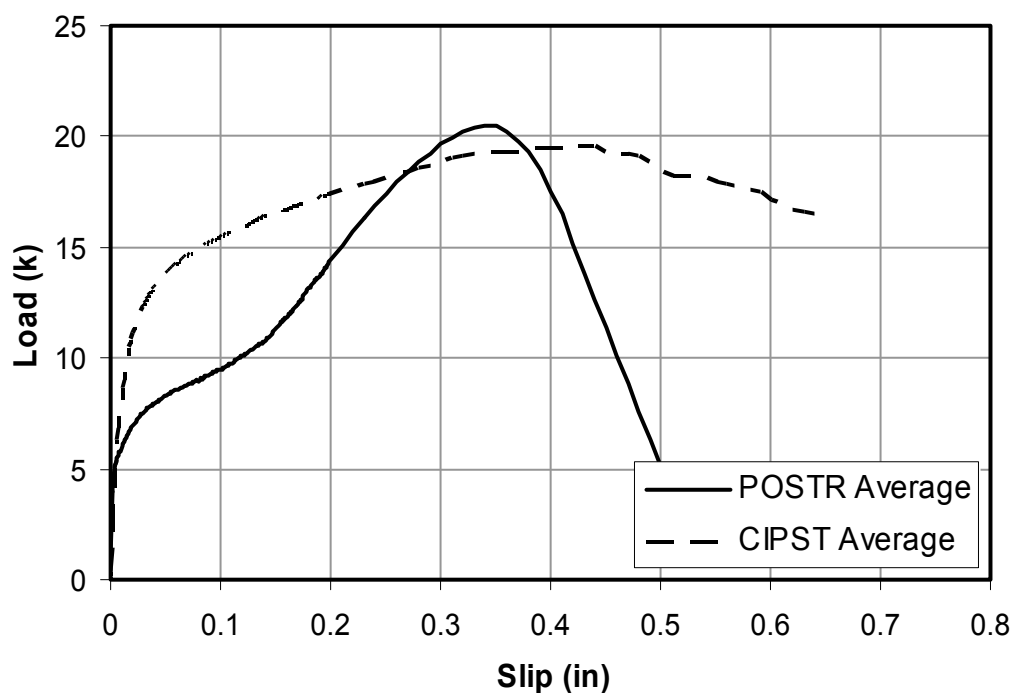


*Figure 8.2: Average load-slip behavior of the Welded Threaded Rod and the Cast-In-Place Welded Stud*

The comparison of the HAS-E Adhesive Anchor (HASAA) and the Cast-In-Place Welded Stud (CIPST) is shown in Figure 8.3. The HASAA is stronger than the CIPST at slips of 0.1 and 0.2 in., and at ultimate strength.

170
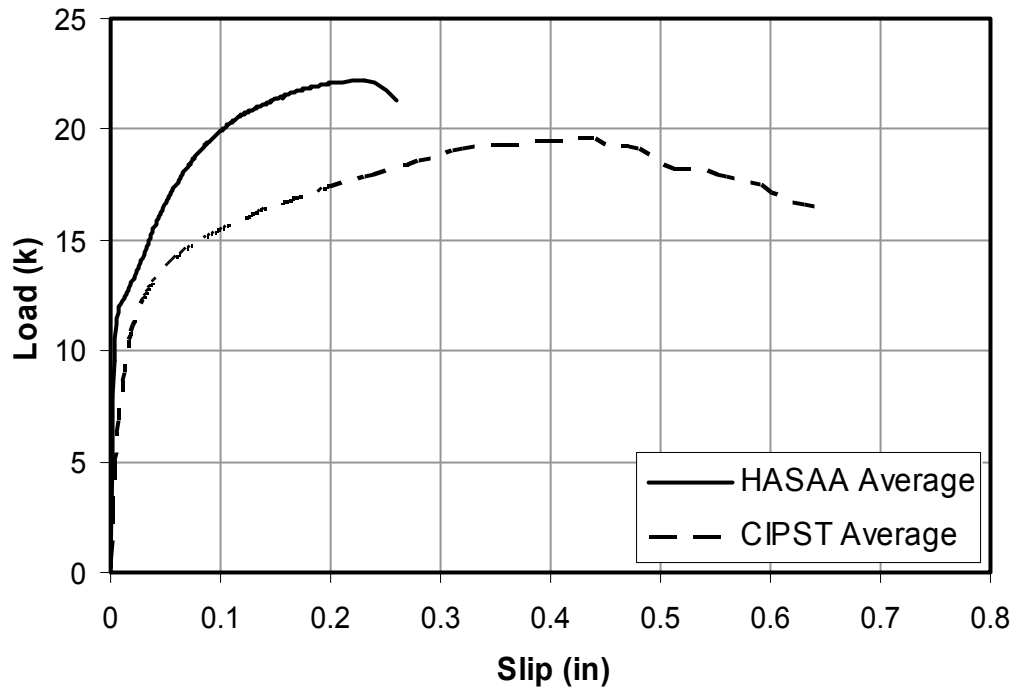
***Figure 8.3: Average load-slip behavior of the HAS-E Adhesive Anchor and the***
***Cast-In-Place Welded Stud***

In Figure 8.4, the comparison of the HIT-TZ Adhesive Anchor (HITTZ) and the Cast-in-Place Welded Stud (CIPST) is presented. The strength of the HITTZ at 0.1 and 0.2 in. is more than that of the CIPST. The ultimate strength of the HASAA is a little more than the ultimate strength of the CIPST.

171
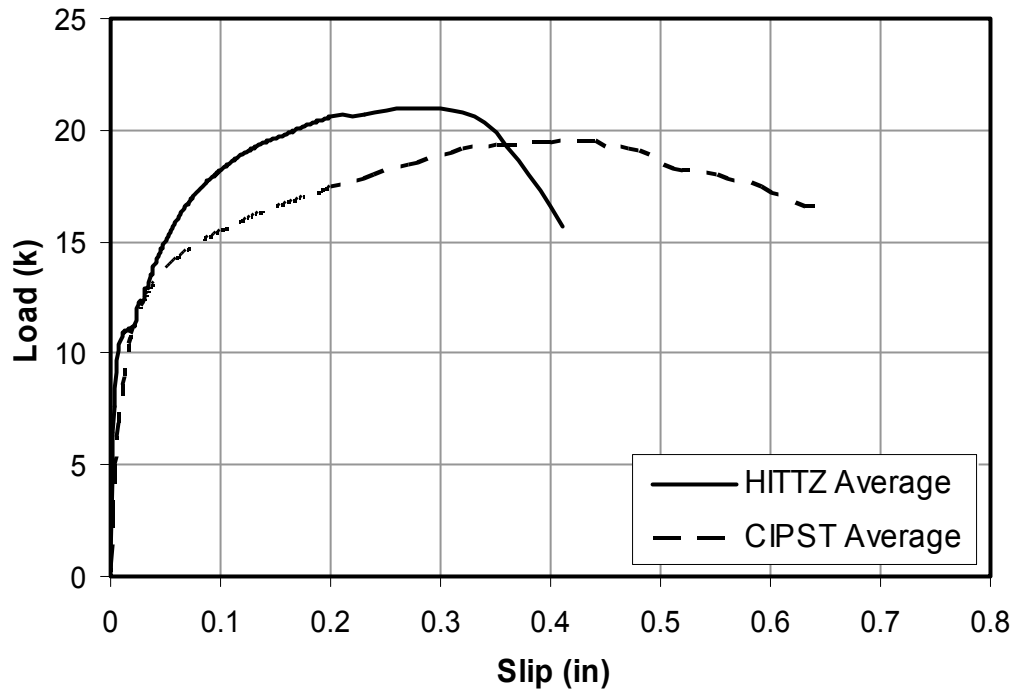
***Figure 8.4: Average load-slip behavior of the HIT-TZ Adhesive Anchor and the Cast-In-Place Welded Stud***

The comparison of the Wedge-Bolt Concrete Screw (WEDGB) and the Cast-in-Place Welded Stud (CIPST) is presented in Figure 8.5. The WEDGB is less strong than the CIPST at a slip of 0.1 in., but the two methods are nearly equal at a slip of 0.2 in. The ultimate strength of the WEDGB is higher than that of the CIPST.
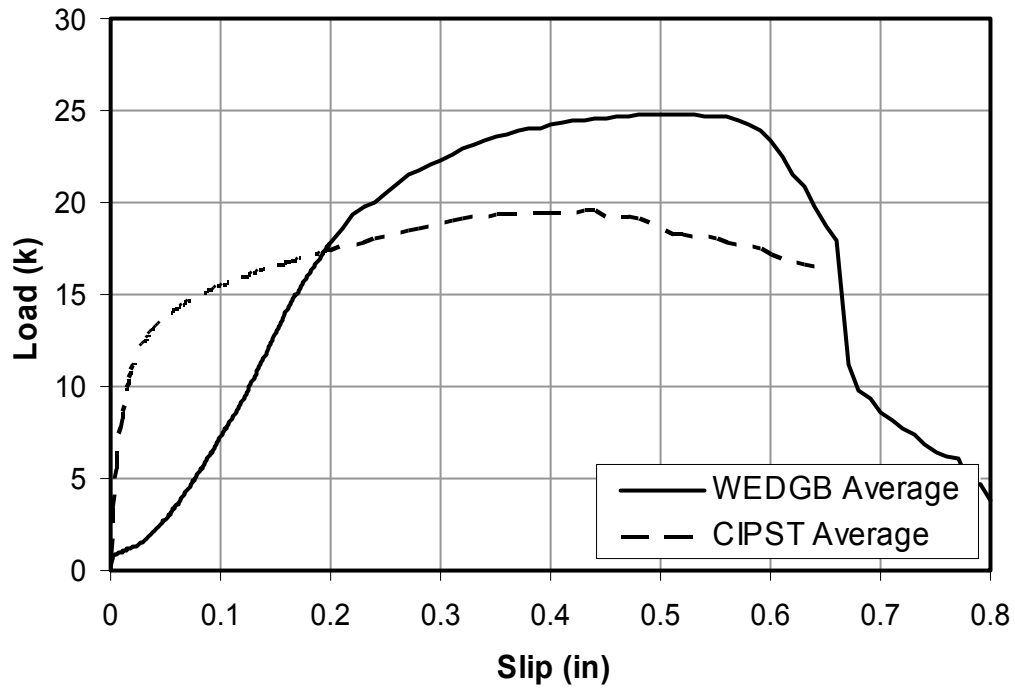
***Figure 8.5: Average load-slip behavior of the Wedge-Bolt Concrete Screw and the Cast-In-Place Welded Stud***

In Figure 8.6, the comparison of the Welded Wedge-Bolt Concrete Screw with Sheath (WEDGS) and the Cast-in-Place Welded Stud (CIPST) is presented. The WEDGS test has lower strength than the CIPST at 0.1 in., and again the two methods have nearly the same strength at 0.2 in. The ultimate strength of the WEDGS exceeds that of the CIPST.
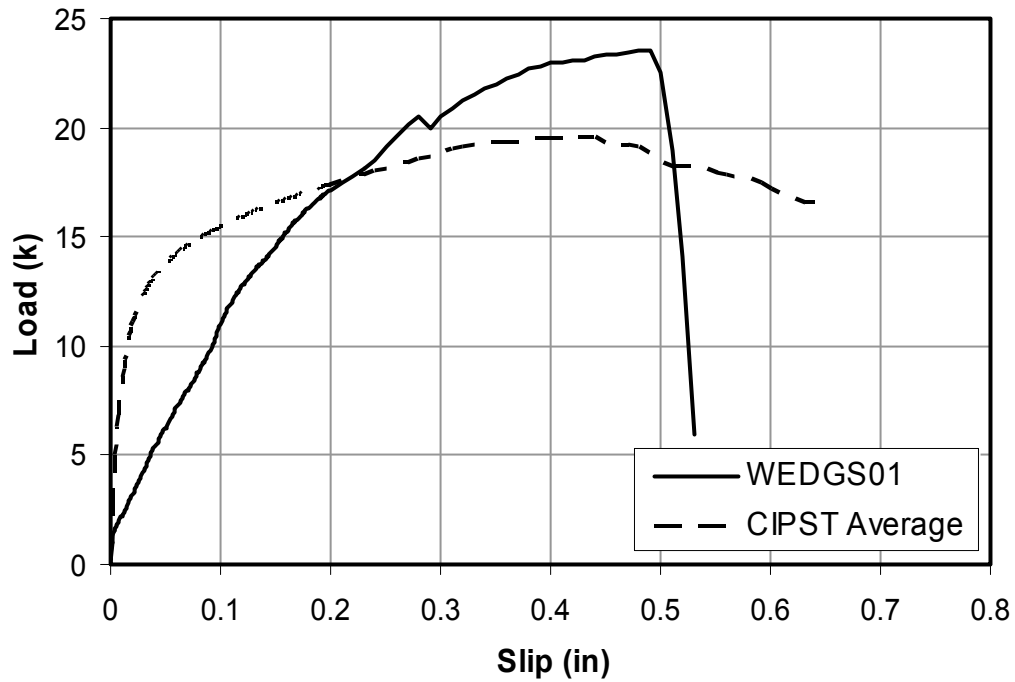
***Figure 8.6: Average load-slip behavior of the Wedge-Bolt Concrete Screw with Sheath and the Cast-In-Place Welded Stud***

The Wedge-Bolt Concrete Screw with RS Anchor Gel (WEDGG) and the Cast-In-Place Welded Stud (CIPST) are compared in Figure 8.7. The graph clearly shows that the strengths of the WEDGG at slips of 0.1 in. and 0.2 in. are much less than those of the CIPST. The ultimate strength of the WEDGG is also less than the ultimate strength of the CIPST.
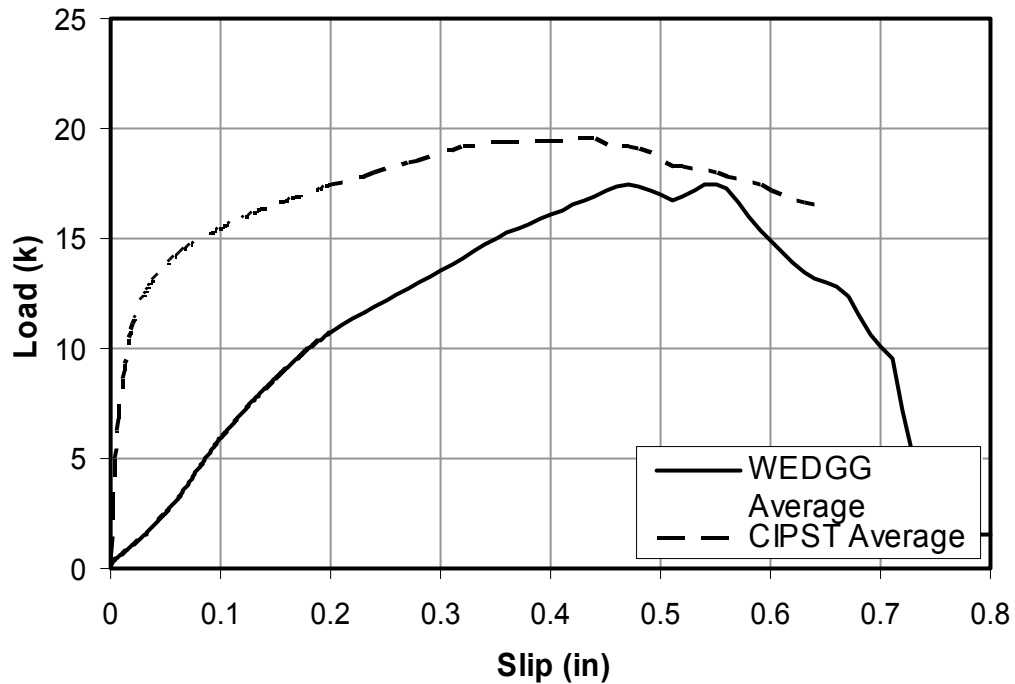
***Figure 8.7: Average load-slip behavior of the Wedge-Bolt Concrete Screw with RS Anchor Gel and the Cast-In-Place Welded Stud***

Although not directly compared with the Cast-In-Place Welded Stud in a graph, the 3M Epoxy Plate method had no measurable slips, and ultimate strengths of the 3MEPX, 3M24H, 3MSTS, and 3MCNS were 2 to 3 times higher than that of the CIPST.

### 8.2.2   Preliminary Recommendations based on Comparisons with CIPST

Based on this preliminary information, the following connection methods compare favorably with the Cast-In-Place Welded Stud, and should be investigated further:

o        HAS-E Adhesive Anchor (HASAA)

o       Wedge-Bolt Concrete Screw with Sheath (WEDGS)

o       3M Epoxy Plate (3MEPX, 3M24H, 3MSTS, 3MCNS)

## 8.3    COMPARISON OF THE LOAD-SLIP RESULTS OF THIS STUDY WITH THOSE OF OLLGAARD ET AL. (1971), FOR THE CAST-IN-PLACE WELDED STUD

Because the information presented in the preceding section involves the results of a single set of direct-shear tests, it is complete in itself. As noted previously, however, because the direct-shear setup used in this study was different from the push-out setup of Ollgaard *et al.* (1971), whose work has been used as the basis for current AASHTO design provisions, it was deemed useful to compare the results obtained here with those of that earlier study. That comparison is conducted in terms of ultimate strengths, and observed load-slip relationships, for cast-in-place welded studs (CIPST), the only anchor tested in both studies.

The intent of this comparison is to determine whether the results of this study for CIPST specimens are statistically comparable with those of Ollgaard *et al.* If so, then results obtained for the other anchors can meaningfully be compared with the results obtained by Ollgaard *et al.* for welded studs, substantiating the preliminary recommendations made above.

### 8.3.1    Comparison of Ultimate Strengths of this Study with those of Ollgaard et al. (1971), for the Cast-In-Place Welded Stud

This section contains the results of a statistical comparison of the ultimate strengths of the Cast-In-Place Welded Stud of this study and of that earlier study. The comparison is expressed in terms of the ratios of observed capacities to those

predicted by Equation 8.3.  Results are summarized in Table 8.3 and Table 8.4, and additional details are given in Appendix C.

***Table 8.3: Statistical comparison of ultimate strengths of welded shear studs in this study with those Ollgaard et al. (1971)  (all specimens)***

| Tests | $Q_{observed}/Q_{predicted}$ | | |
| --- | --- | --- | --- |
| | Mean | Standard Deviation | Coefficient of Variation |
| Ollgaard *et al.* (1971), all specimens | 0.923 | 0.070 | 0.076 |
| Study 0-4124 | 0.878 | 0.135 | 0.154 |

The ratio of the mean of ($Q_{observed}/Q_{predicted}$) in this study to that from Ollgaard et al. (1971) is 0.95 when the statistical analysis is based on all of the results of the research performed by Ollgaard *et al.* (1971).  When the statistical comparison is confined to "relevant specimens" the results remain similar (Table 8.4). "Relevant specimens," as described in this section, refer to test specimens reported by Ollgaard *et al.* (1971) as "lower compressive strength" specimens. Those specimens had been cast in concrete of 2500 to 3500 psi strength, similar to the strength of concrete used in this study.   Those tests included 9 relevant specimens in three series.  All used 3/4-in. diameter studs, and were push-out tests with four studs per slab (each side), and used normal-weight concrete.

***Table 8.4: Statistical comparison of ultimate strengths of welded shear studs in this study with relevant specimens from Ollgaard et al. (1971)***

| Tests | $Q_{observed}/Q_{predicted}$ | | |
| | Mean | Standard Deviation | Coefficient of Variation |
| --- | --- | --- | --- |
| Ollgaard *et al.* (1971), relevant specimens | 0.910 | 0.065 | 0.071 |
| Study 0-4124 | 0.878 | 0.135 | 0.154 |

When the statistical analysis is based on the relevant specimens from the research performed by Ollgaard *et al.* (1971), the ratio of the mean of ($Q_{observed}/Q_{predicted}$) in this study to that from Ollgaard *et al.* (1971) is 0.96. From the first analysis (all specimens) to the second analysis (relevant specimens) of Ollgaard *et al.* (1971), the standard deviation and coefficient of variation change only 7%. The small changes in the statistical results indicate that there is little statistical difference between the results for all studs tested by Ollgaard *et al.* (1971), and the results for concrete strengths like that used in this study. Regardless of which group of studs is compared, the ratio ($Q_{observed}/Q_{predicted}$) for the anchors of this study is within 5% of the corresponding ratio for the anchors tested by Ollgaard *et al.* (1971), and therefore can be considered statistically close to the ultimate strength predicted by Equation 8.5.

Another possible concern regarding the results of this study is that its coefficient of variation for ($Q_{observed} Q_{predicted}$) is more than twice that of Ollgaard *et al.* (1971). This occurs for two reasons:

o   This study performed tests on only 3 cast-in-place welded stud specimens while Ollgaard *et al.* (1971) tested 48 specimens (16 series of 3 specimens each).  Sample standard deviation is calculated by Equation 8.1,

$$SD = \sqrt{\frac{\sum (\bar{x} - x_i)^2}{(n-1)}}$$

(*Equation 8.1*)

where

  SD = standard deviation of test results

  $\bar{x}$ = mean of test results

  $x_i$ = single test result

  n = number of tests

Fewer test specimens result in a higher standard deviation, because of the term $\dfrac{1}{\sqrt{(n-1)}}$ in the equation for coefficient of variation.  Because fewer tests were conducted in this study, one would expect a greater coefficient of variation for results of this study compared to those of Ollgaard *et al.* (1971).

o   Additionally, the tests performed in this study had only 1 connector in each specimen while the research conducted by Ollgaard *et al.* (1971) had 8 (2 slabs with 4 connectors per slab).  The statistical dispersion of ultimate strength obtained from single-connector tests is expected to be substantially higher than that obtained as the average of 8 connectors.  This would also cause a greater coefficient of variation for results of this study compared to those of Ollgaard *et al.* (1971).

For these reasons the results of this study are deemed statistically comparable with those of Ollgaard *et al.* (1971), even though its coefficient of variation is greater.

## 8.3.2 Comparison of Load-Slip Behavior of this Study with that of Ollgaard et al. (1971), for the Cast-In-Place Welded Stud

This section contains a comparison of the load-slip behavior for this study and those obtained by Ollgaard *et al.* (1971). Initial load-slip response (stiffness) and ultimate strength are discussed. Possible explanations for differences between the initial load-slip responses of the two studies are proposed here. Possible reasons for the slight differences in observed ultimate strengths between the two studies are discussed in the previous section.

According to Ollgaard *et al.* (1971), the load-slip curve for a cast-in-place welded stud depends only the compressive strength of the concrete and the cross-sectional area of the shear stud. Their proposed load-slip relationship is given below by Equations 8.2 and 8.3.

$$Q = Q_u \cdot \left(1 - e^{-18\Delta}\right)^{2/5} \qquad \textit{(Equation 8.2)}$$

where

$$Q_u = 1.106 \cdot A_s \cdot f_c'^{0.3} \cdot E_c^{0.44} \qquad \textit{(Equation 8.3)}$$

where

$Q_u$ = ultimate strength of a shear stud (kips)

$\Delta$ = slip of a shear stud (in.)

$Q$ = capacity of a shear stud at the slip $\Delta$ (kips)

$A_s$ = cross-sectional area of a shear stud (in.$^2$)

$f_c'$ = specified compressive strength of concrete at 28 days (ksi)

$E_c$ = modulus of elasticity of concrete (ksi)

$F_{ut}$ = specified minimum ultimate tensile strength of a shear stud (ksi)

The modulus of elasticity of concrete is defined by Equation 8.4.

$$E_c = 57 \cdot \sqrt{f_c'}$$
*(Equation 8.4)*

where

$E_c$ = modulus of elasticity of concrete (ksi)

$f_c'$ = specified compressive strength of concrete at 28 days (psi)

For design purposes, their proposed equation for ultimate capacity was simplified to Equation 8.5.

$$Q_u = 0.5 \cdot A_s \cdot \sqrt{f_c' \cdot E_c} \le A_s \cdot F_{ut}$$
*(Equation 8.5)*

In Figure 8.8 are shown the load-slip curves obtained in this study for Cast-In-Place Welded Studs, and the average of those curves. Those studs had a diameter of 3/4 in., a tested ultimate tensile strength of 66.2 ksi, and were embedded in concrete with a tested compressive strength of 3200 psi. Shown in that same figure is a graph of Equation 8.2 (using Equation 8.3 to determine ultimate strength) for the same stud diameter and material strengths.
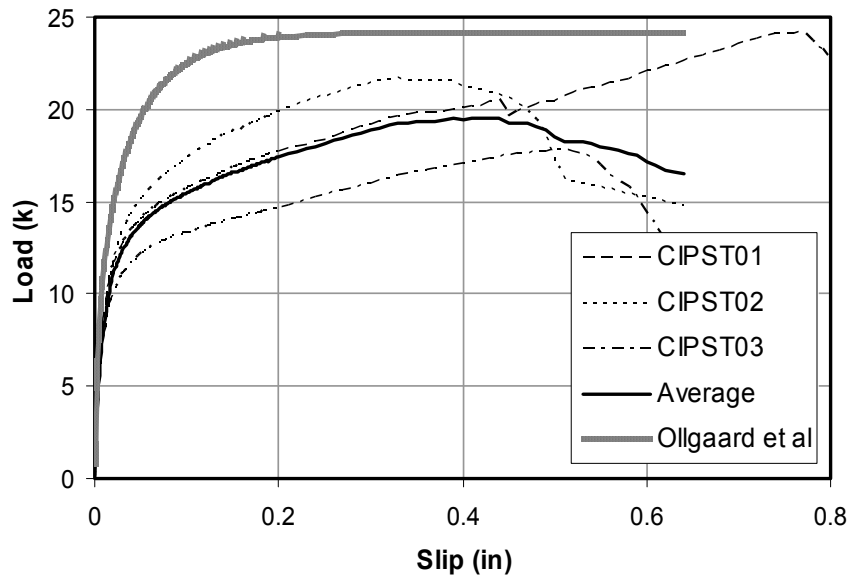
*Figure 8.8: Comparison of Equations 8.1 and 8.2 for Cast-In-Place Welded Stud (slip 0 to 0.8 in.)*

The load-slip results of this study differ from the empirical predictive equations of Ollgaard *et al.* (1971) in three important respects:

o    First, the initial slopes (stiffness) of the load-slip curves of this study are much lower than that predicted by Ollgaard *et al.* (1971).

o    Second, after the initial elastic range, the applied loads at which the observed load-slip curves begin to deviate significantly from that initial elastic behavior (begin to "bend over"), are much less than the predicted value of that load.  For example, referring to Figure 8.8, the observed load-slip curve begins to deviate significantly from linear elastic behavior at a load of about 12 kips, far less than the predicted load of about 20 kips.

182

o   Third, the observed ultimate strengths from this study are consistently and significantly lower than those predicted by Equation 8.3 of Ollgaard *et al.* (1971), and also consistently and significantly lower than those predicted by the simplified Equation 8.5 derived from that work. For example, referring to Figure 8.7, the average of the maximum values of the three load-slip curves (not equal to the maximum of the "Average" curve) is about 21 kips, considerably below the prediction of Equation 8.2 (24.2 kips) and the somewhat below the more conservative prediction of Equation 8.4 (22.4 kips). The conservatism of Equation 8.5 as compared to Equation 8.3 is shown in Figure 8.9, in which both predictive equations are graphed simultaneously versus values of the specified compressive strength of concrete at 28 days ($f'_c$).
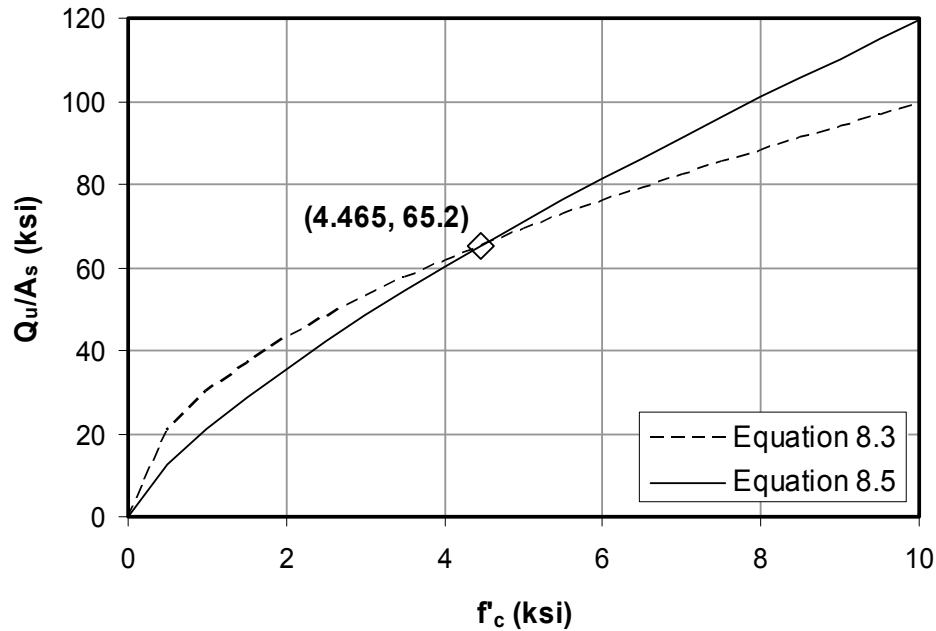
*Figure 8.9: Comparison of Equation 8.3 and Equation 8.5*

As shown Figure 8.9, when $f'_c$ is less than 4465 psi, Equation 8.5 (design version) predicts lower capacities than Equation 8.3 (exact version). When $f'_c$ is greater than 4465 psi, the opposite is true. This second region is of little importance, however, because it is irrelevant for $Q_u/A_s$ greater than $F_{ut}$. For the most common stud material, the specified minimum tensile strength $F_{ut}$ is 60 ksi, and the portion of the simplified design curve to the right of the intersection point does not govern. For our tested ultimate strength of 65.2 ksi, the two equations give practically identical values. For all reasonable values of ultimate tensile strength, the two equations yield very similar results.

***Table 8.5: Comparison of observed to predicted (Equation 8.5) ultimate***
***strengths of welded shear studs in Ollgaard et al. (1971)***

| Tests | $Q_{observed}/Q_{predicted}$ | | |
| --- | --- | --- | --- |
| | Mean | Standard Deviation | Coefficient of Variation |
| Ollgaard *et al.* (1971), all specimens | 0.960 | 0.081 | 0.084 |
| Study 0-4124 | 0.950 | 0.119 | 0.126 |

When Equation 8.5 is used for the same statistical comparison of Table 8.3, the results of Table 8.5 are obtained. The tested capacities of this study are nearly 99% of those of Ollgaard *et al.* (1971) based on Equation 8.5. The coefficient of variation of this study is greater than that of Ollgaard *et al.* (1971), by about the same amount and for the same reasons.

The first two differences between the load-slip behavior of this study and that of Ollgaard *et al.* (1971) (lower initial stiffness and lower load for inelastic behavior) are now discussed in more detail. Those differences are emphasized in Figure 8.10, which presents the same information from Figure 8.8, in the slip range between 0.1 and 0.3 in. In the author's opinion, both are caused by differences between the test setup used in this study, and that used by Ollgaard *et al.* (1971).
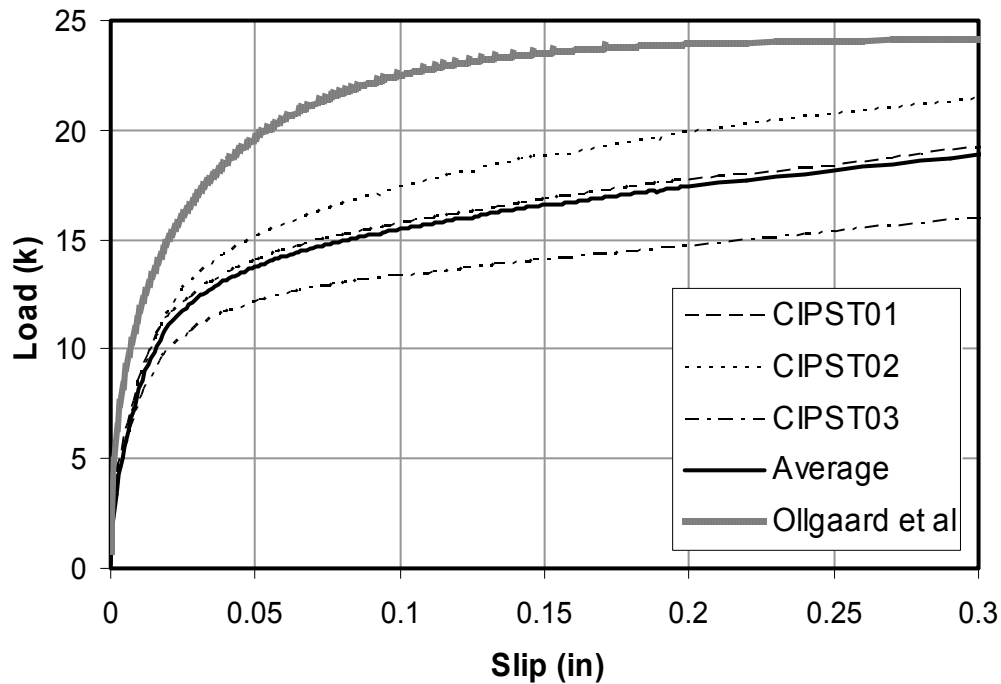
***Figure 8.10: Comparison of load-slip curves for Cast-In-Place Welded Stud
versus Equations 8.1 and 8.2, slip 0 to 0.3 in.***

The initial stiffness of the load-slip response is the elastic stiffness of the
anchor-concrete connection. The push-out test setup of Ollgaard *et al.* (1971) is
stiffer than the single-connector, direct-shear test setup of this study, for two
reasons:

o the push-out setup has a flange stiffened by a web, while the direct-shear
setup has no web; and

o the push-out setup's multiple anchors keep the flange close to the
concrete, preventing rotation more than the single-anchor, direct-shear
setup.

These are illustrated schematically in Figure 8.11. The shear stud in the Ollgaard *et al.* (1971) push-out tests deformed in double curvature, while the shear stud in this study was permitted to deform in single curvature.



**(a)**          **(b)**
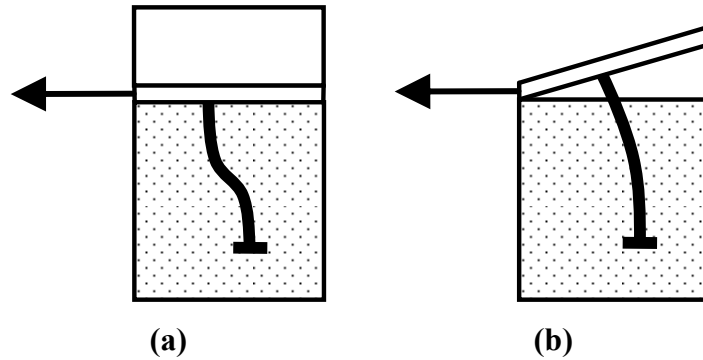
*Figure 8.11: (a) Push-out test forces double curvature of anchor; (b) direct shear test allows single curvature of anchor*

The third difference between the results of this study and those of Ollgaard *et al.* (1971) relationship is the discrepancy in the ultimate strength (the maximum value of the predicted load-slip curve). According to the AASHTO LRFD equation for the ultimate capacity of a shear connector (Equation 8.5), the ultimate strength of the 3/4-in. diameter shear stud in 3200-psi concrete is 22.44 kips, and the value from the more complex equation of Ollgaard *et al.* (1971) would be 24.22 kips. In Table 8.6, the ultimate strengths for each test, and their average, are compared with the capacities predicted by Equation 8.3 and its simplified version, Equation 8.5.

*Table 8.6: Observed versus predicted ultimate shear strengths for Cast-In-Place Welded Stud tests, Equation 8.3, and Equation 8.5*

| Test | Observed Ultimate Strength (kip) | Predicted Strength, Equation 8.3 (kip) | Observed/ Predicted Strength, Equation 8.3 | Predicted Strength, Equation 8.3 (kip) | Observed/ Predicted Strength, Equation 8.5 |
|---|---|---|---|---|---|
| CIPST01 | 24.26 | 24.22 | 1.00 | 22.44 | 1.08 |
| CIPST02 | 21.69 | 24.22 | 0.90 | 22.44 | 0.97 |
| CIPST03 | 17.81 | 24.22 | 0.73 | 22.44 | 0.79 |
| Average of Ultimate Strengths | 21.25 | 24.22 | 0.88 | 22.44 | 0.95 |
| Ultimate Strength of the Graph of the Average | 19.57 | 24.22 | 0.81 | 22.44 | 0.87 |
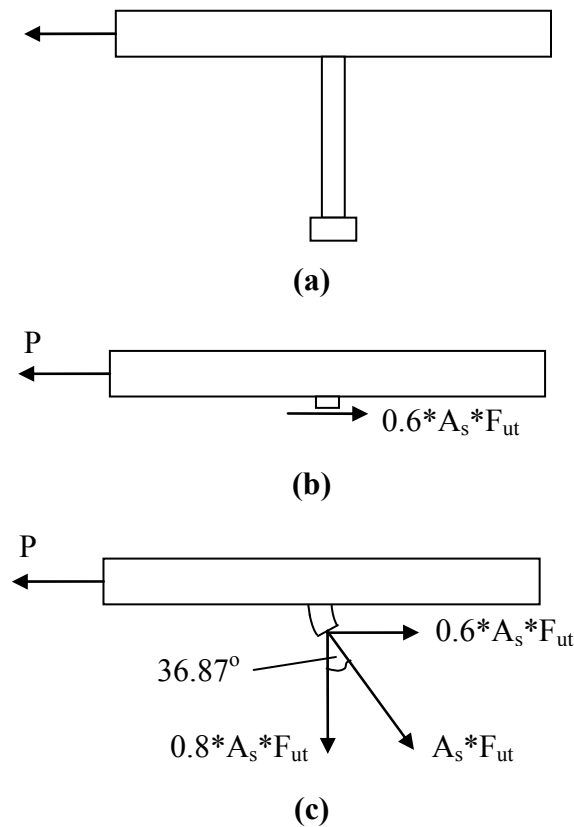
*Figure 8.12: Possible deformed shapes of a shear connector at failure: (a) undeformed shape; (b) failure in pure shear; (c) failure in combined shear and tension at 36.87 degrees*

In the pure-shear case, the shear on the connector reaches the observed capacity of 0.6 $A_s$ $f_{ut}$ in pure shear. In the combined shear-tension case, if the connector deforms to an angle of 36.87 degrees ($Sin^{-1}$ 0.6), and the anchor has an inclined tensile force of $A_s$ $f_{ut}$ , it has a horizontal component (resisting shear) of 0.6 $A_s$ $f_{ut}$ , and a vertical component (clamping force) of 0.8 $A_s$ $f_{ut}$ . Both mechanisms satisfy statics and stress-strain relationships, and can therefore be classified as acceptable lower-bound solutions giving safe (low) predictions of shear capacity. In other words, the capacity of a shear would be expected to be 0.6 $A_s$ $f_{ut}$ regardless of the rotational stiffness of the welded end of the stud.

Table 8.5 clearly shows that the ultimate strengths of Ollgaard *et al.* (1971) lie considerably below the predicted values of Equation 8.3. Because the author's tested strengths are statistically similar to those of the earlier study, they lie similarly below that predicted values.

In applying the above lower-bound approach to connectors other than shear studs, it is important to note the significant differences between these two types of shear connectors. Because shear studs are welded, the critical shear occurs at the top of the weld, some distance away from the concrete-steel interface, where the shear is less than the applied shear due to horizontal bearing forces from the concrete on weld (Meinheit and Anderson 2002). In recognition of this, ACI 318-05 (repeated here as Equation 8.6) computes the shear capacity of a welded stud as:

$$V_s = A_s \cdot F_{ut} \qquad \textit{(Equation 8.6)}$$

while for other types of shear connectors, it is 0.6 $A_s$ $f_{ut}$.

### 8.3.3 Conclusions regarding Comparison of Results from this Study with those of Ollgaard et al.

Based on this comparison with the observed values and predictive equations of Ollgaard *et al.* (1971), it is concluded that the strengths of cast-in-place welded studs of this study are statistically comparable with those of that previous study (and hence valid), and that while the stiffnesses of this study are considerably lower than those of that previous study, the difference is explained by the greater rotational flexibility of the welded end of the stud in the test setup of this study.

Because the results are statistically comparable for cast-in-place welded studs, comparisons in this thesis that use those studs as a baseline reference are

valid, and so are conclusions regarding the performance of different retrofit shear connectors vis-à-vis that of cast-in-place welded studs.


## 8.4 INITIAL OBSERVATIONS AND DISCUSSION REGARDING RESULTS OF THE LOAD-SLIP TESTS

This section includes initial observations and discussions of the results of the load-slip tests. Physical reasons for differences between a post-installed method and the Cast-In-Place Welded Stud are given, and the variations on primary methods are compared.

Table 8.1 and Table 8.2 permit several observations meriting further discussion:

o    At a slip of 0.1 in., only two of the post-installed connection methods (HASAA and HITTZ) had strengths greater than or equal to that of the CIPST. This is probably because only those connection methods involved anchors that were "confined" (surrounded by steel at the level of the base plate, and by concrete within their embedded length) in the same way as the Cast-In-Place Welded Stud.

o    At a slip of 0.2 in., the HASAA and HITTZ connection methods continued to perform at least as well as the CIPST. They were joined by the WEDGB and WEDGS connection methods. Even though the latter are initially more flexible due to the gap between the anchor and the surrounding concrete, at slips of 0.2 in. this gap has closed, and the anchors have gone into bearing.

191

o The ultimate strengths of nearly all anchors were as high as that of the CIPST. This is because some connectors were made of higher-strength steel than that used in the welded studs.

o Slip at ultimate strength increases with decreasing connector confinement (see above) for post-installed methods. For example, as shown in Table 8.7, slips at ultimate strength are small for the HAS-E Adhesive Anchor (HASAA) because it was fully encased in adhesive. The Wedge-Bolt Concrete Screw with RS Anchor Gel (WEDGG) was not well confined because there was a gap between the anchor and the steel, and the anchor was installed incompletely.

*Table 8.7: Average slip at ultimate strength for post-installed connectors, divided by slip at ultimate for CIPST*

| Test Series | Average Slip at Ultimate Strength, Compared to Slip of CIPST (%) |
|---|---|
| HASAA | 40 |
| POSTR | 66 |
| HITTZ | 71 |
| WEDGS | 91 |
| WEDGB | 95 |
| WEDGG | 102 |

This table is logical, because a more confined connector cannot deform as much as a less confined one. As the deformation increases and the connector rotates or bends relative to the concrete-steel interface, load is applied to the connector increasingly in the form of tension. Deformation before failure under a tensile force is greater than that under shear force, because the tensile deformation involves inelastic deformation of the anchor over a large longitudinal gage length, while the shear failure involves inelastic deformation only of the steel near the failure plane. As a result, connectors that are less confined exhibit greater slip at ultimate strength.

The ductility of the metal used in the connector is also significant. Several post-installed anchors tested here are made of higher-strength, less-ductile steel than that of the CIPST (Table 8.8).

*Table 8.8: Ultimate tensile strengths of anchors*

| Test Series | Ultimate Tensile Strength of Anchor (ksi) |
|---|---|
| CIPST | 66.2 |
| POSTR | 61 |
| HASAA | 72.5 |
| HITTZ | 87 |
| WEDGB | 58 |

o     No post-installed method was as ductile as the CIPST (Table 8.9). While ductility has not been explicitly identified in this thesis as a desirable connection characteristic, it is generally useful as an index of a connection

193

method's ability to continue to resist load while deforming inelastically. In this thesis, ductility is defined as the maximum slip divided by the slip at yield. For purposes of this thesis, slip at yield was identified approximately as the middle of the transition from linear elastic behavior to inelastic behavior. While other more precise methods, such as a percentage of offset, could have been used for determining this, such additional precision was not deemed warranted for purposes of this comparison.

As shown in Table 8.9, the primary connection methods can be placed in three rough categories with respect to ductility. The highly confined connectors (HASAA and HITTZ) approach the CIPST in ductility, because they have relatively low slips at yield due to their high confinement and hence high initial stiffness. A less highly confined connector (POSTR) has intermediate ductility, because its slip at yield is higher. Connection methods with little or no ductility are either very flexible, and hence have high slips at yield (WEDGB); or they fail in a brittle manner (3MEPX).

*Table 8.9: Computed average ductility of primary methods*

| Test Series | Slip at Yield (in.) | Slip at Failure (in.) | Computed Ductility |
|---|---|---|---|
| CIPST | 0.023 | 0.768 | 33.4 |
| HASAA | 0.016 | 0.398 | 24.9 |
| HITTZ | 0.022 | 0.474 | 21.5 |
| POSTR | 0.026 | 0.400 | 15.4 |
| WEDGB | 0.217 | 0.746 | 3.4 |
| 3MEPX | 0 | 0 | 0 |

o    The POSTR connection was very flexible; as shown in Figure 8.2, the load remains well below that of the CIPST until slips reach 0.15 in. This flexibility was due to the gap between the threaded rod and the surrounding grout, and the rotational flexibility of the washer, nut and threaded rod at the point where they bear against the grout.

o    Although not graphically compared to the CIPST in this chapter, the HY150 method only had about 1/4 of the ultimate strength of the CIPST.

o    It is the author's opinion that although the HASAA (Figure 8.3) and the HITTZ (Figure 8.4) anchors seem similar, the HASAA performs better because it is a more confined connection. The HITTZ, by design, transfers axial load (to develop static friction) to the concrete by "wedging" the cured adhesive against the surrounding concrete. When static friction is overcome, the wedged pieces of adhesive allow for a slightly more flexible connector response in bearing.

o    For the Wedge-Bolt Concrete Screw tests (WEDGB, WEDGG, and WEDGS), the following observations are valid:

-    As shown in Figure 8.5 and Figure 8.6, the WEDGB and WEDGS tests had ultimate strengths greater than the CIPST at slip values (0.45 to 0.5 in.) nearly equal to the slip occurring at the ultimate strength of the CIPST.

-    The WEDGG method shown in Figure 8.7 was more flexible than the WEDGB (Figure 8.5) and WEDGS (Figure 8.6) methods because the WEDGG method had less strength at slips of 0.1 and 0.2 in.  The WEDGG also attained 8 and 6 kips less ultimate strength than the WEDGB and WEDGS methods, respectively. Because the screw in the WEDGG series was not properly installed, the hex-washer head was not flush with the top of the steel test plate, and this allowed the screw to be more flexible.  The WEDGG had substantially more slip at a lower ultimate strength than either the WEDGB or the WEDGS.

-    If Figure 8.6 and Figure 8.5 are compared, the WEDGS method was clearly effective in improving on the early stiffness of the WEDGB.  The WEDGS attained 24% higher strength than the WEDGB at a slip of 0.1 in., and the strength of each method was nearly identical to that of the CIPST at a slip of 0.2 in.

o    For the 3M Epoxy Plate tests, the following observations are valid:

- The 3M Epoxy Plate tests (3MEPX, 3M24H, 3MSTS, 3MCNS) all had very high ultimate strengths; the ultimate strengths were 2 to 3 times more than that of the CIPST.

- The 3M Epoxy Plate tests were completely non-ductile; there was no measurable slip before failure.

- For a substantial percentage of the cure time, the 3MEPX specimens were cured under higher temperatures, and this condition seems to have slightly lowered their ultimate strengths.

- The 3M24H test results indicate that the adhesive has sufficiently cured in 24 hours.

- The 3MSTS test results indicate that the steel plate may only need to be wiped clean once in its surface preparation, but another repetition is recommended to be confident in the surface condition.

- The 3MCNS test results indicate, opposite to the expectations of the author, that the concrete surface should be worn away to a small degree in the concrete surface preparation. It had been thought that it was best to remove paste from between the aggregate to a high degree in order to allow the adhesive to bond with a greater surface area of the exposed aggregate, but it appears that aggregate that is more embedded in the cement matrix may be the reason the 3MCNS specimens had higher ultimate strengths.

197

**8.5    ADDITIONAL DISCUSSION OF THE POST-INSTALLED METHODS, TEST RESULTS, AND CONSTRUCTABILITY**

This section includes additional discussion on the structural performance of the post-installed shear connection methods, with particular emphasis on how that performance was affected by the required construction procedures, and on general constructability issues.

**8.5.1    Welded Threaded Rod (POSTR)**

The POSTR required a complicated construction procedure, and the installation resulted in a flexible connection (Figure 8.2). The Five Star RS Anchor Gel was too viscous to place successfully in the gap between the threaded rod and the grout, and a less-viscous adhesive could not have been used in the required overhead application. The gap allowed the POSTR to bend and slip a substantial distance before bearing was initiated. As a result, the Welded Threaded Rod had significant slip without much load resistance.

**8.5.2    HAS-E Adhesive Anchor (HASAA)**

Test HASAA03 was not included in calculations of mean load-slip performance because its behavior was adversely affected by unintentional adhesive bonding of the concrete and steel.

The secondary shear-transfer mechanism of bearing in the HASAA produced stiffness greater than that of the CIPST. This was due to a combination of two mechanisms. The first mechanism is the effect of the 3/4-in. diameter anchor bearing on the HY 150 adhesive. The HY 150 has a compressive strength of 10.42 ksi while the concrete had a compressive strength of approximately 3250 psi. The compressive strength of the substrate surrounding the anchor exponentially affects the stiffness of the connection according to Equations 8.1 and 8.2. The second mechanism affecting the bearing response of the HASAA is

198

the adhesive acting jointly with the threaded rod. This combined rod-adhesive connector has an effective diameter of 13/16 in. An increased anchor diameter improves the bearing behavior of the connection. These mechanisms affect the load-slip response of the HIT-TZ Adhesive Anchor as well.

### 8.5.3 HIT-TZ Adhesive Anchor (HITTZ)

The first two tests had a significant amount of adhesive between the concrete and steel. This was unintentional, and it appears that the adhesive bond was only effective in the HITTZ02 test. The values from the HITTZ02 test were still used in average calculations because the plate de-bonded from the concrete well before a slip of 0.1 in., and the load-slip curve then followed a path similar to the other two tests. The problem of the adhesive at the interface was avoided in the HITTZ03 specimen by applying a ring of caulk between the steel and concrete around the hole.

### 8.5.4 HY150 Adhesive Plate (HY150)

The Hilti HY 150 was a poor adhesive to act alone as a shear connector because of its gritty consistency, and it was improperly installed. The adhesive did not fully cover the concrete-steel interface, and it had not completely cured at the time of testing. These were valuable lessons learned and employed when installing the 3M Epoxy Plate specimens.

### 8.5.5 Wedge-Bolt Concrete Screw (WEDGB, WEDGG, WEDGS)

In Section 8.4, basic observed behavior of the Wedge-Bolt Concrete Screw is discussed. In this section, factors contributing to that performance are examined further.

Wedge-Bolt Concrete Screw specimens exhibited low capacities at slips of 0.1 and 0.2 in., due to the gaps between the anchors and the hole in the steel test

plate. Efforts were made in the WEDGG test series to fill the gap with Five-Star RS Anchor Gel, and in the WEDGS test, to fill the gap with a steel sheath made from electrical metal conduit (EMT).

In the WEDGG test, efforts to fill the gap were unsuccessful. The Five Star RS Anchor Gel was difficult to place in the gap between the screw shank and the hole in the steel. Further problems were experienced because the holes for the WEDGG specimens were not drilled deep enough, and the bottom of the hex-washer head was not flush with the top of the steel test plate. The result was low capacity at low slip levels. The steel test plate rotated and slid relative to the anchor shank because the hex-washer head did not restrain the rotational movement of the steel test plate (Figure 8.13).
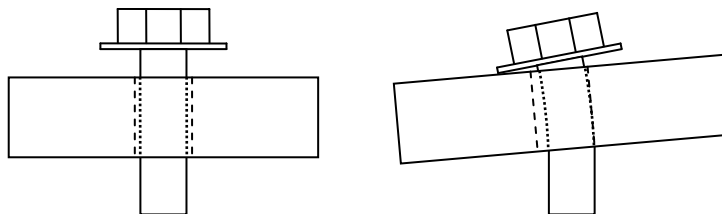


*Figure 8.13: Rotation of the Wedge-Bolt Concrete Screw if the hex-washer head is not flush with the steel test plate*

In the WEDGS test, the effort to fill the gap was promising. The sheath reduced the early slip into bearing seen in the WEDGB series, and may even be possible to install more effectively in future tests, hopefully with even better results. The improved installation is described in Chapter 5.

The ideal way of filing the gap between the plate and the concrete strew in general would be to change the form of the screw itself. Instead of using an upset thread (greater in diameter than the unthreaded shank), it would be much better to use a one-piece screw in which the 1-in. length of shank below the hex-washer head were almost the same diameter as the hole in the steel. This would essentially eliminate the gap between the shank and the bearing plate, and also

essentially eliminate the slip required to mobilize the bearing resistance of the anchor.  Such a modified concrete screw is shown in Figure 8.14.
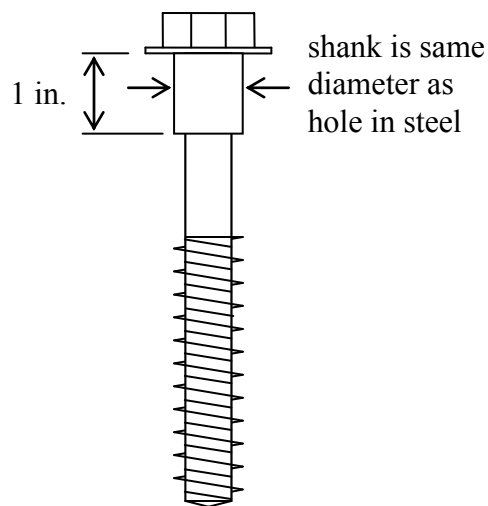


*Figure 8.14: Ideal design of Powers Wedge-Bolt*

The possibility of such a Wedge-Bolt modification was investigated with Powers Fasteners, who indicated that a large-volume order would be required for the variation on the anchor design to be feasible.  This option may be possible in the future if this method is used on a large scale for bridge retrofitting.

The Powers Wedge-Bolt Concrete Screw was an attractive solution from its conception as a possible shear connector, for many reasons:  it is easy to install, even in overhead applications; it does not require welding; it does not require access closing the bridge to traffic to permit access to the top of the deck; the resulting connection is stiff once it goes into bearing.  Its lone drawback of this method is its loose fit in the hole in the steel flange, which can lead to large initial slips before the bearing mechanism begins to act.  The gap between the anchor shank and the hole in the steel may be dealt with as discussed earlier in the section.

### 8.5.6  3M Epoxy Plate (3MEPX, 3M24H, 3MSTS, 3MCNS)

The Epoxy Plate is a very different shear connection from the other post-installed methods, in that it does not use a metallic anchor.  Because the connection is effected with a stiff adhesive, essentially no slip occurs prior to failure.  Because the epoxy adhesive has a much higher interface shear capacity than the concrete to which it is attached, the capacity of this connection can be predicted using shear-friction provisions of Section 11.7.5 or ACI 318-02, reproduced here as Equation 8.7.

$$V_n = 0.2 \cdot f_c' \cdot A_c \leq 800\, psi \cdot A_c \qquad \textbf{\textit{(Equation 8.7)}}$$

where

$V_n$ = nominal shear-friction capacity of normal-weight concrete (lb)

$f'_c$ = specified compressive strength of concrete at 28 days (psi)

$A_c$ = area of concrete section resisting shear transfer (in.$^2$)

The area that failed in shear friction measured 6 x 22 in., giving a value of 90 kips for the first part of this equation and 106 kips for the second part, and a governing nominal capacity of 90 kips.   The observed mean ultimate strength of the Epoxy Plate tests was 58 kips, or 64% of the predicted nominal value.

*Figure 8.15: Concrete remaining adhered to steel plate after failure*

The discrepancy between the test results and the predicted nominal capacity may have been due to the following:

o    The most likely explanation for the reduced capacity compared with classical interface shear-transfer models was the presence of local tensile forces at the interface.  As is discussed below, these are a consequence of the out-of-plane flexibility of the plate and moment at the concrete-steel interface, and these would not be present in an otherwise identical interface between concrete and concrete.

o    To a small extent, a surface effect may contribute to the observed capacity being less than the predicted nominal capacity.  The surface effect was the loss of adhesion between some of the aggregate and the adhesive bonded to the steel test plate.  This condition was not prevalent in the failure surfaces of the specimens, and it was not likely as important to the failure of the specimens as the previous cause of discrepancy.

To determine if local tensile forces could be a cause of the premature failure of the Epoxy Plate specimens, a simple finite-element model was conceived and implemented in the commercial finite-element program ANSYS. That model is now discussed in detail.

The portion of the test setup that contributes to the applied forces and the restraint of the test specimen are modeled based the components shown in Figure 8.16.
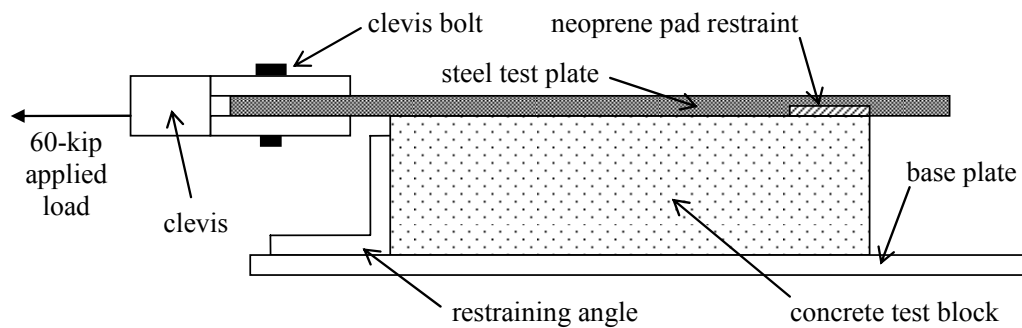


*Figure 8.16: Portion of test setup considered in FEM of Epoxy Plate method*

Figure 8.16 shows the clevis that applies the load in the direct shear test and the clevis bolt that transfers the applied load to the steel test plate. Movement of the concrete test block in the direction of the applied load is prevented by the restraining angle at its front; vertical movement is prevented by the base plate at the bottom of the specimen and a neoprene pad restraint at the top of the specimen. In that figure, only the neoprene pad is shown for simplicity; the steel restraint system holding it in place is not shown. The resulting finite-element model of the Epoxy Plate specimen is shown in Figure 8.17.

204
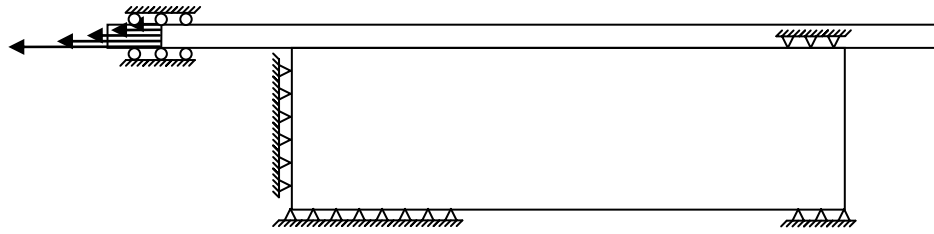
***Figure 8.17: Finite-element model of the Epoxy Plate method***

The clevis was assumed to prevent vertical movement of the first several inches of the steel test plate, and roller supports were used to simulate this condition. The remaining support conditions were treated as pinned, represented the restraining angle at the front of the block, the base plate beneath the block, and the neoprene pad restraint on the top rear of the block. The placement of the pinned supports iteratively determined as follows:

o       Pinned supports were placed at all points of bearing in the three locations mentioned above.

o       The analysis was run, and any location where a tensile reaction existed, the pin support there was removed, because tensile reactions did not exist in the actual setup. This step was repeated until only compression reactions remained at the pinned supports.

The mesh size generated was 0.1-in. square for the steel test plate as shown in Figure 8.18, and the same was used for the concrete test block. The collocated interface nodes of the steel test plate and concrete test block were merged to simulate the attachment of the two components by rigid epoxy. The material models of the steel and concrete were both linear-elastic.

205
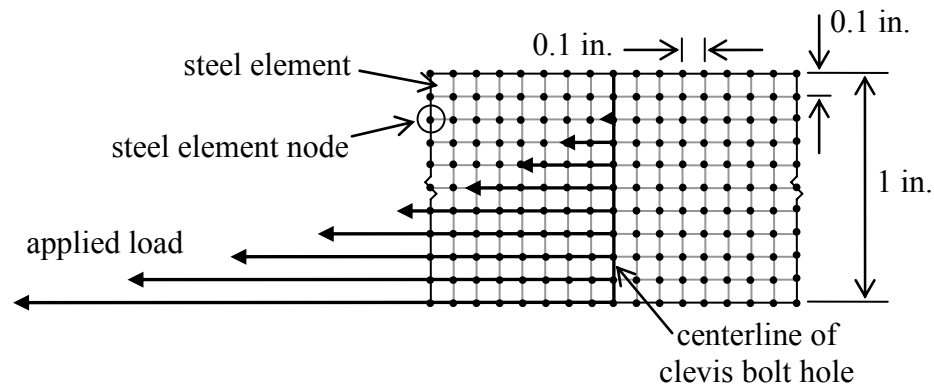
*Figure 8.18: Close-up of FEM of steel test plate with applied load*

The clevis was designed to transfer the applied load in the plane of the bottom surface of the steel test plate. This could not occur in the real test, however, because that would imply an infinite tensile stress at the bottom surface of the plate. As shown in Figure 8.18, the distribution of applied tension in the plate was therefore assumed to be parabolic, with maximum value at the node on the bottom surface of the steel test plate and zero load applied at the node on the top surface. A parabolic distribution of concentrated loads with a 60-kip resultant was applied to the element nodes at the centerline of the of the clevis bolt hole location in the test setup. For example, the largest three applied loads (from the bottom of the steel test plate, upward) were 15.58 kips, 12.62 kips, and 9.97 kips. The concentrated loads were applied as shown in Figure 8.18.

The resulting deformation of the concrete and steel components of the test setup is shown in Figure 8.19. The local bending of the plate is clearly evident.

206
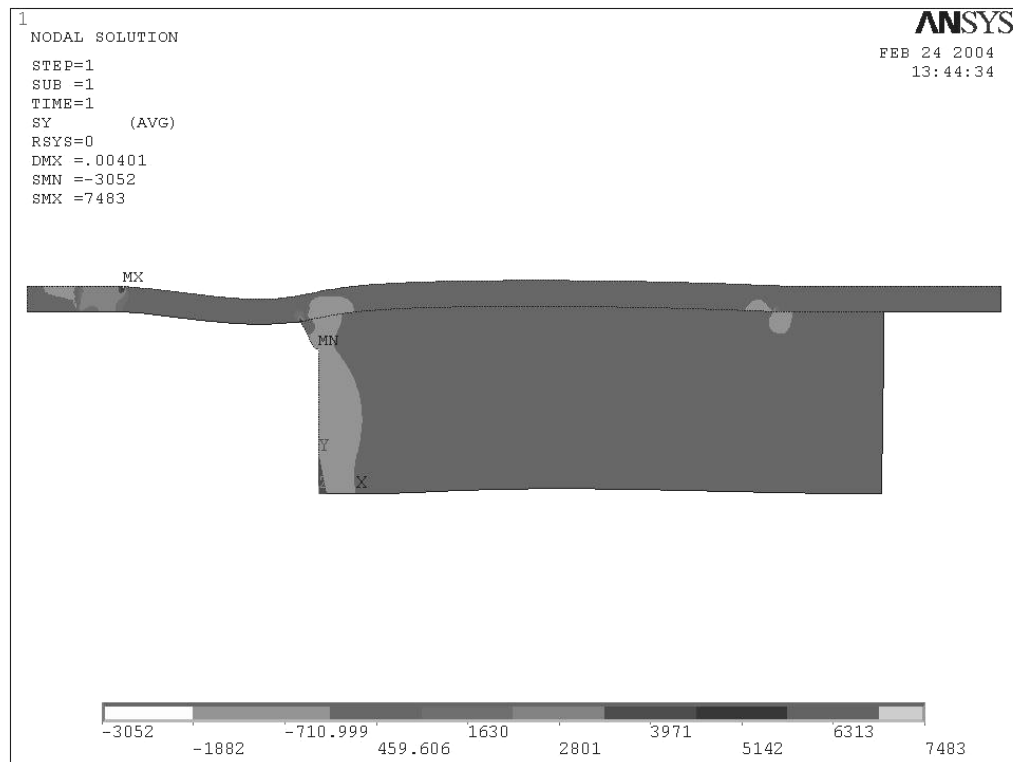
*Figure 8.19: Displaced shape and out-of-plane stresses in the Epoxy Plate test specimen*

This moment is caused by the eccentricity, e, of the applied load, P, relative to the concrete-steel interface as shown in Figure 8.20.



*Figure 8.20: Eccentricity of load in the steel test plate*

While moment also exists in the concrete test block, the block is much stiffer, its consequent deformations are much less. The moment in the concrete block is caused by the eccentricity, e, of the reaction with the restraint angle at the

front of the block, P, relative to the concrete-steel interface as shown in Figure 8.21.
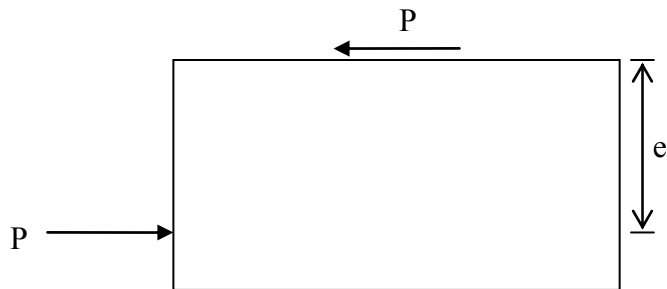


***Figure 8.21: Eccentricity of load in the concrete test block***

The deformations in the concrete contribute to the extraneous forces experienced at the concrete-steel interface, but they are not as prevalent as the deformations in the steel. Neither of these moments would be present in a real composite member.

Based on the numerical results of ANSYS for the 60-kip applied load, the concrete-steel interface experienced the shear stress distribution shown in Figure 8.22 and the out-of-plane stress distribution shown in Figure 8.23. The latter is particularly important. Examination of these two figures shows that the loaded end of the concrete-steel interface experiences very high combined shear and tensile stresses. It is believed that these are responsible for the failure of the Epoxy Plate specimens at loads lower than those corresponding to the nominal shear-friction capacity. They are probably also responsible for the change in the appearance of the failure surface along the direction of applied load.
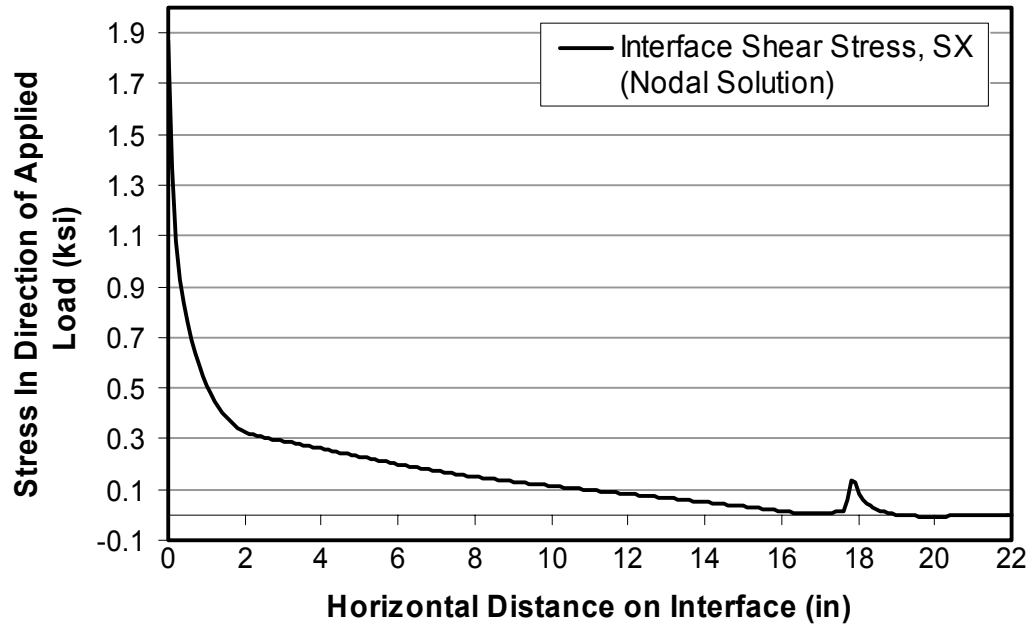
*Figure 8.22: Shear stress on concrete at the concrete-steel interface of Epoxy Plate FEM, 60-kip applied load*
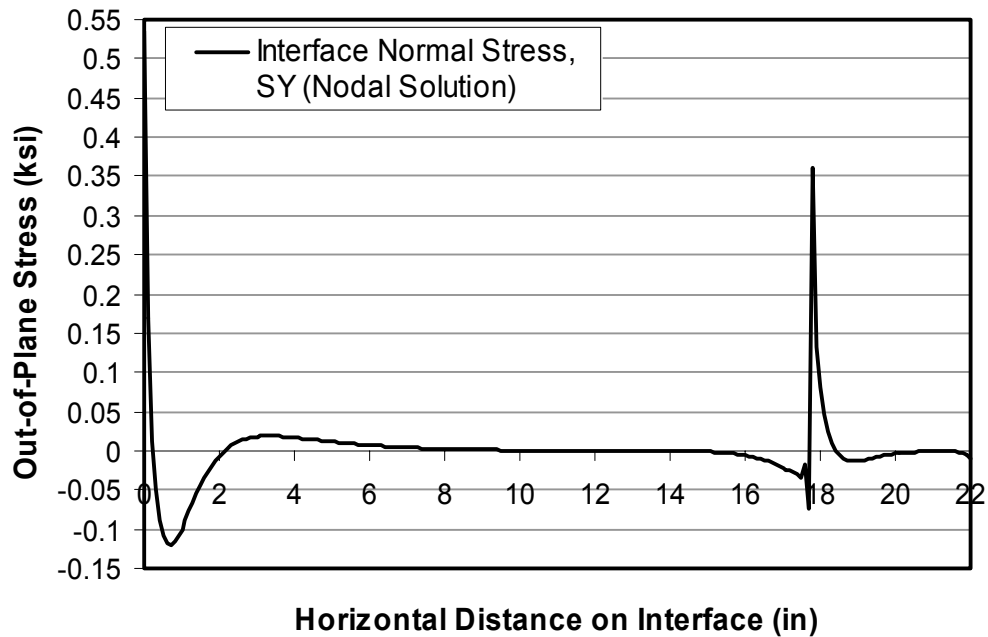
*Figure 8.23: Out-of-Plane stress at the concrete-steel interface of Epoxy Plate FEM, 60-kip applied load*

Evident in Figure 8.22 and Figure 8.23 is that the concrete-steel interface experienced high shear stresses and out-of-plane tensile stresses in two locations along the length of the specimen. Each of these locations will be discussed relative to horizontal shear and out-of-plane stress.

The first location occurs at 0 in. (left edge of the concrete test block), where the shear stress was 1.87 ksi, and the second location occurs at 17.8 in., where the shear stress was 0.14 ksi. The shear stress was expected to be very high nearest to the applied load (first location), and the second location of high shear was due to the restraint caused by the pin supports representing the neoprene pad restraint. The maximum shear stress on the concrete as calculated by Equation 8.7 is 0.64 ksi. Therefore, the shear stresses in the concrete in the first 0.7 in. of

the concrete block, where shear stresses exceed 0.64 ksi, are sufficient to cause a shear-friction failure of the concrete.

The out-of-plane stress at 0 in. was 0.54 ksi (first location) and 0.36 ksi at 17.8 in. (second location). The high tensile stresses at the first location are due to the bending of the steel test plate, and the second location is again the result of the concrete being vertically restrained beneath the neoprene pad. The steel test plate tends to lift, but is attached to the restrained concrete test block; this condition creates tension at the concrete-steel interface. The maximum direct tensile strength of concrete as calculated by Equation 8.8 is 0.23 ksi.

$$f_t' = 4 \cdot \sqrt{f_c'}$$        *(Equation 8.8)*

Therefore, the tensile stresses in the first 0.1 in. of the concrete block surface and at 17.8 in. in the finite element model were sufficient to cause local tensile failures of the concrete.

In the actual tests, many of the failed specimens cracked severely (Figure 8.24 and Figure 8.25). Their cracking patterns are consistent with compression at the portion of the concrete-steel interface nearest the load, and tension near the other end. Vertical restraint of the corners of the concrete block clearly contributes to the development of flexural cracking.

*Figure 8.24: Cracking pattern typical of an Epoxy Plate specimen showing the end of the concrete test block away from the applied load*

***Figure 8.25: Cracking pattern typical of an Epoxy Plate specimen showing the
side of the concrete test block (loading direction to the left)***

In the area of the failed concrete in Figure 8.25, the slightly darker surface
on the left half of the failure surface is a smoother failure surface than the right
half.  This is because the compression on the left side forced the concrete to shear
along a smoother failure surface.  The right side, in contrast, has large chunks of
concrete missing because that concrete was pulled away from the block through
tension at failure.

The ultimate strength of the Epoxy Plate specimen would likely increase if
the moment in shear connection were eliminated in the test setup because tension
in the concrete would be reduced.  Also, a stiffened steel test plate would decrease
the bending of the plate and the development of extraneous tensile stresses.

213

The Epoxy Plate method performed the best of all the investigated methods if one considers only the load-slip curve. It has more than twice the shear capacity of a cast-in-place shear stud, and zero slip prior to failure. The Epoxy Plate is possibly one of the more expensive shear connection methods, however. Also, its failure is sudden and brittle when the adhered surface of the concrete fails in shear. Because of this, its design requires a high factor of safety. The construction sequence for this method is sensitive to the surface preparation of both the concrete and steel, and requires significant preparation setup and material. In addition, traditional reservations regarding the use of adhesives in structural applications would have to be overcome.

# CHAPTER 9

# Summary, Conclusions, and Recommendations

## 9.1 SUMMARY

The purpose of this study is to identify at least one post-installed shear connector method that is structurally adequate, constructible, and cost-effective for use in retrofitting bridges for increased capacity due to composite action. In this thesis, structural performance of post-installed connectors is judged on initial stiffness, ultimate capacity, ductility, and failure mode. Many different ways of connecting concrete and steel are investigated, and the most promising methods are tested using direct-shear tests on single connectors. Connectors behaving relatively well are intended to be tested further in full-sized bridges and in pilot field studies. Design guidelines are intended to be produced.

The part of the study addressed by this thesis includes the following steps:

o   A wide range of possible connectors was studied, and the most promising were selected for testing.

o   A test setup was developed for direct-shear tests of single connectors.

o   Using that setup, tests were conducted on 13 primary types of shear connectors and several variants of these primary types.

o   Test results were compared with those of Ollgaard *et al.* (1971), which serve as the basis for current AASHTO design of shear connectors.

o   Test results were compared with design and analysis models.

o   Procedures were explored for estimating load-slip demand on bridges in service.

o      Load-slip performance of different retrofit connection methods was compared with that of the Cast-In-Place Welded Stud, over the range of probable slip demands.

o      Based on those comparisons, relatively promising connection methods were identified for further testing.

## 9.2 CONCLUSIONS

### 9.2.1 Conclusions with respect to Methods of Post-Installed Shear Connection

1. At this stage of the study, several retrofit connection methods appear to be structurally sound, cost-effective, and constructible: the HAS-E Adhesive Anchor (HASAA); the Wedge-Bolt Concrete Screw with Sheath (WEDGS); and the 3M Epoxy Plate (3MEPX). All three methods performed as well or better than the Cast-In-Place Welded Stud in direct-shear tests of single connectors under static loading.

### 9.2.2 Conclusions with respect to the Design of Post-Installed Shear Connectors

1. Current AASHTO procedures for the design of shear connectors under serviceability limits are incomplete. Rather than simply comparing ultimate load with ultimate capacity, they should compare load-slip demand with load-slip capacity, and slip demand with slip capacity at ultimate strength.

2. For design purposes, the coefficient of static friction between in-place concrete and weathered steel should be taken as 0.4.

### 9.2.3 Conclusions with respect to the Testing of Shear Connectors

1. The direct shear test used in this study is in principle better than the push-out test, because it introduces lower extraneous tensions in connectors.

2. Single-connector shear tests are in principle better than multiple-connector tests, because they permit closer study of the behavior of individual connectors.

3. The direct-shear setup used in this study was not ideal, because its out-of-plane flexibility introduced local tensions normal to the steel-concrete interface. These influenced the test results somewhat.

## 9.3 RECOMMENDATIONS

### 9.3.1 Recommendations with respect to Methods of Post-Installed Shear Connection

1. The HAS-E Adhesive Anchor (HASAA), the Wedge-Bolt Concrete Screw with Sheath (WEDGS), and the 3M Epoxy Plate (3MEPX) methods performed are recommended for further testing.

### 9.3.2 Recommendations with respect to the Design of Post-Installed Shear Connectors

1. Current AASHTO design procedures for shear connectors should be augmented so that they compare load-slip demand with load-slip capacity, and slip demand with slip capacity at ultimate strength.

### 9.3.3 Recommendations with respect to the Testing of Shear Connectors

1. The direct-shear, single-connector test setup described in this thesis should be stiffened with a plate running parallel to the direction of the

217

applied load, and simulating the web that would be present in a wide-flange section.

2. Individual shear connectors should be tested under fatigue loading.

3. Groups of shear connectors should be tested under static and fatigue loading.

4. Large-scale tests should be performed on the best shear connectors.

# Appendix A
## Tests to Determine the Coefficient of Static Friction

| Concrete Block Weight: | 22.06 | lb |
|---|---|---|
| | 10.01 | kg |

Test Date: 7/28/2003
Bridge Location: Honeysuckle Lane, San Antonio, Texas

| Beam 1 | Left End | | | Middle | | | Right End | | |
|---|---|---|---|---|---|---|---|---|---|
| | Test 1 | Test 2 | Test 3 | Test 1 | Test 2 | Test 3 | Test 1 | Test 2 | Test 3 |
| Load (kg) | 7.25 | 6.5 | 6.75 | 6.75 | 6.25 | 7.33 | 7.4 | 7.3 | 7 |
| Fs (kg) | 6.726 | 5.976 | 6.226 | 6.226 | 5.726 | 6.806 | 6.876 | 6.776 | 6.476 |
| Angle (degrees) | 3 | 3 | 3 | 3 | 3 | 3 | 3 | 3 | 3 |
| Coef. of Friction | 0.673 | 0.598 | 0.623 | 0.623 | 0.573 | 0.681 | 0.688 | 0.678 | 0.648 |

| Beam 2 | Left End | | | Middle | | |
|---|---|---|---|---|---|---|
| | Test 1 | Test 2 | Test 3 | Test 1 | Test 2 | Test 3 |
| Load (kg) | 6.75 | 8.25 | 7 | 7.25 | 7 | 7 |
| Fs (kg) | 6.226 | 7.726 | 6.476 | 6.726 | 6.476 | 6.476 |
| Angle (degrees) | 3 | 3 | 3 | 3 | 3 | 3 |
| Coef. of Friction | 0.623 | 0.773 | 0.648 | 0.673 | 0.648 | 0.648 |

| Beam 3 | Left End | | | Middle | | |
|---|---|---|---|---|---|---|
| | Test 1 | Test 2 | Test 3 | Test 1 | Test 2 | Test 3 |
| Load (kg) | 7.25 | 5.75 | 6.25 | 5.67 | 6.75 | 7 |
| Fs (kg) | 6.552 | 5.052 | 5.552 | 4.972 | 6.052 | 6.302 |
| Angle (degrees) | 4 | 4 | 4 | 4 | 4 | 4 |
| Coef. of Friction | 0.656 | 0.506 | 0.556 | 0.498 | 0.606 | 0.631 |

| Beam 4 | Left End | | |
|---|---|---|---|
| | Test 1 | Test 2 | Test 3 |
| Load (kg) | 6 | 7 | 6.25 |
| Fs (kg) | 5.651 | 6.651 | 5.901 |
| Angle (degrees) | 2 | 2 | 2 |
| Coef. of Friction | 0.565 | 0.665 | 0.590 |

| | |
|---|---|
| Mean = | 0.628 |
| Min = | 0.498 |
| Max = | 0.773 |
| St. Dev. = | 0.061 |
| COV = | 0.097 |
| Precision = | 0.037 |

219

# Appendix B
# Q/Qu versus Delta

- This analysis uses the ultimate strength of the average of the three 0-4124 tests.
- The strength Q is taken from the average graph of the three tests.

| Qu = | 19.57 | kip |
|------|-------|-----|

| Study 0-4124 | | Ollgaard *et al.* (1971) | |
|--------------|---|--------------------------|---|
| Delta (in.) | Q | Q/Qu | Delta (in.) |
| 9E-06 | 0.17493 | 0.00894 | 0.00000 |
| 0.0001 | 0.34458 | 0.01761 | 0.00000 |
| 0.001 | 2.03050 | 0.10376 | 0.00019 |
| 0.002 | 3.35645 | 0.17151 | 0.00068 |
| 0.003 | 4.29319 | 0.21938 | 0.00127 |
| 0.004 | 5.03862 | 0.25747 | 0.00190 |
| 0.005 | 5.56410 | 0.28432 | 0.00245 |
| 0.006 | 6.27893 | 0.32084 | 0.00334 |
| 0.007 | 6.86360 | 0.35072 | 0.00420 |
| 0.008 | 7.31467 | 0.37377 | 0.00496 |
| 0.009 | 7.75816 | 0.39643 | 0.00579 |
| 0.01 | 8.23844 | 0.42097 | 0.00679 |
| 0.011 | 8.62008 | 0.44047 | 0.00766 |
| 0.012 | 8.99767 | 0.45977 | 0.00859 |
| 0.013 | 9.31291 | 0.47588 | 0.00944 |
| 0.014 | 9.59674 | 0.49038 | 0.01024 |
| 0.015 | 9.89186 | 0.50546 | 0.01114 |
| 0.016 | 10.15631 | 0.51897 | 0.01198 |
| 0.017 | 10.43819 | 0.53338 | 0.01294 |
| 0.018 | 10.65411 | 0.54441 | 0.01371 |
| 0.019 | 10.85355 | 0.55460 | 0.01445 |
| 0.02 | 11.09428 | 0.56690 | 0.01539 |
| 0.021 | 11.24425 | 0.57457 | 0.01600 |
| 0.022 | 11.39093 | 0.58206 | 0.01661 |
| 0.023 | 11.51930 | 0.58862 | 0.01717 |

| | | | |
|---|---|---|---|
| 0.024 | 11.66789 | 0.59621 | 0.01783 |
| 0.025 | 11.78650 | 0.60227 | 0.01837 |
| 0.026 | 11.90652 | 0.60841 | 0.01893 |
| 0.027 | 12.02316 | 0.61437 | 0.01949 |
| 0.028 | 12.13865 | 0.62027 | 0.02005 |
| 0.029 | 12.25728 | 0.62633 | 0.02065 |
| 0.03 | 12.36152 | 0.63166 | 0.02119 |
| 0.031 | 12.45689 | 0.63653 | 0.02169 |
| 0.032 | 12.53694 | 0.64062 | 0.02212 |
| 0.033 | 12.62514 | 0.64513 | 0.02260 |
| 0.034 | 12.70161 | 0.64903 | 0.02303 |
| 0.035 | 12.79464 | 0.65379 | 0.02356 |
| 0.036 | 12.88370 | 0.65834 | 0.02407 |
| 0.037 | 12.96868 | 0.66268 | 0.02458 |
| 0.038 | 13.02935 | 0.66578 | 0.02494 |
| 0.039 | 13.10169 | 0.66948 | 0.02538 |
| 0.04 | 13.16648 | 0.67279 | 0.02578 |
| 0.041 | 13.23934 | 0.67651 | 0.02624 |
| 0.042 | 13.30482 | 0.67986 | 0.02666 |
| 0.043 | 13.36435 | 0.68290 | 0.02704 |
| 0.044 | 13.42278 | 0.68589 | 0.02743 |
| 0.045 | 13.48255 | 0.68894 | 0.02782 |
| 0.046 | 13.54733 | 0.69225 | 0.02826 |
| 0.047 | 13.60265 | 0.69508 | 0.02864 |
| 0.048 | 13.65643 | 0.69782 | 0.02901 |
| 0.049 | 13.70770 | 0.70044 | 0.02937 |
| 0.05 | 13.75526 | 0.70287 | 0.02971 |
| 0.051 | 13.81018 | 0.70568 | 0.03010 |
| 0.052 | 13.86120 | 0.70829 | 0.03047 |
| 0.053 | 13.89991 | 0.71027 | 0.03076 |
| 0.054 | 13.95766 | 0.71322 | 0.03119 |
| 0.055 | 14.00668 | 0.71572 | 0.03156 |
| 0.056 | 14.05902 | 0.71840 | 0.03196 |
| 0.057 | 14.10266 | 0.72063 | 0.03229 |
| 0.058 | 14.14620 | 0.72285 | 0.03263 |
| 0.059 | 14.18841 | 0.72501 | 0.03297 |
| 0.06 | 14.21778 | 0.72651 | 0.03320 |
| 0.061 | 14.26412 | 0.72888 | 0.03357 |

| | | | |
|---|---|---|---|
| 0.062 | 14.30511 | 0.73097 | 0.03391 |
| 0.063 | 14.34570 | 0.73305 | 0.03424 |
| 0.064 | 14.38056 | 0.73483 | 0.03453 |
| 0.065 | 14.42629 | 0.73716 | 0.03491 |
| 0.066 | 14.46590 | 0.73919 | 0.03525 |
| 0.067 | 14.50178 | 0.74102 | 0.03555 |
| 0.068 | 14.53197 | 0.74256 | 0.03581 |
| 0.069 | 14.58443 | 0.74524 | 0.03627 |
| 0.07 | 14.62689 | 0.74741 | 0.03665 |
| 0.071 | 14.66040 | 0.74913 | 0.03694 |
| 0.072 | 14.68692 | 0.75048 | 0.03718 |
| 0.073 | 14.71880 | 0.75211 | 0.03747 |
| 0.074 | 14.74985 | 0.75370 | 0.03775 |
| 0.075 | 14.76973 | 0.75471 | 0.03794 |
| 0.076 | 14.80003 | 0.75626 | 0.03822 |
| 0.077 | 14.84039 | 0.75832 | 0.03859 |
| 0.078 | 14.87565 | 0.76013 | 0.03893 |
| 0.079 | 14.90545 | 0.76165 | 0.03921 |
| 0.08 | 14.93315 | 0.76306 | 0.03948 |
| 0.081 | 14.96387 | 0.76463 | 0.03977 |
| 0.082 | 14.98950 | 0.76594 | 0.04002 |
| 0.083 | 15.01190 | 0.76709 | 0.04024 |
| 0.084 | 15.04464 | 0.76876 | 0.04057 |
| 0.085 | 15.07756 | 0.77044 | 0.04089 |
| 0.086 | 15.11290 | 0.77225 | 0.04125 |
| 0.087 | 15.13982 | 0.77362 | 0.04152 |
| 0.088 | 15.17092 | 0.77521 | 0.04184 |
| 0.089 | 15.19328 | 0.77636 | 0.04207 |
| 0.09 | 15.21371 | 0.77740 | 0.04228 |
| 0.091 | 15.23828 | 0.77866 | 0.04254 |
| 0.092 | 15.26097 | 0.77981 | 0.04278 |
| 0.093 | 15.25486 | 0.77950 | 0.04272 |
| 0.094 | 15.30151 | 0.78189 | 0.04321 |
| 0.095 | 15.34343 | 0.78403 | 0.04366 |
| 0.096 | 15.38135 | 0.78597 | 0.04407 |
| 0.097 | 15.40506 | 0.78718 | 0.04433 |
| 0.098 | 15.42991 | 0.78845 | 0.04461 |
| 0.099 | 15.45376 | 0.78967 | 0.04487 |

| | | | |
|---|---|---|---|
| 0.1 | 15.47646 | 0.79083 | 0.04513 |
| 0.101 | 15.49645 | 0.79185 | 0.04535 |
| 0.102 | 15.52137 | 0.79312 | 0.04564 |
| 0.103 | 15.54203 | 0.79418 | 0.04587 |
| 0.104 | 15.55840 | 0.79501 | 0.04606 |
| 0.105 | 15.58134 | 0.79619 | 0.04633 |
| 0.106 | 15.61035 | 0.79767 | 0.04666 |
| 0.107 | 15.63144 | 0.79874 | 0.04691 |
| 0.108 | 15.66130 | 0.80027 | 0.04727 |
| 0.109 | 15.68303 | 0.80138 | 0.04752 |
| 0.11 | 15.70967 | 0.80274 | 0.04785 |
| 0.111 | 15.73338 | 0.80395 | 0.04813 |
| 0.112 | 15.75605 | 0.80511 | 0.04841 |
| 0.113 | 15.77908 | 0.80629 | 0.04869 |
| 0.114 | 15.79211 | 0.80696 | 0.04885 |
| 0.115 | 15.82573 | 0.80867 | 0.04927 |
| 0.116 | 15.85064 | 0.80995 | 0.04959 |
| 0.117 | 15.87287 | 0.81108 | 0.04987 |
| 0.118 | 15.89497 | 0.81221 | 0.05015 |
| 0.119 | 15.92457 | 0.81372 | 0.05053 |
| 0.12 | 15.94648 | 0.81484 | 0.05082 |
| 0.121 | 15.96624 | 0.81585 | 0.05107 |
| 0.122 | 15.98782 | 0.81696 | 0.05136 |
| 0.123 | 16.00508 | 0.81784 | 0.05159 |
| 0.124 | 15.99958 | 0.81756 | 0.05151 |
| 0.125 | 16.00297 | 0.81773 | 0.05156 |
| 0.126 | 16.03391 | 0.81931 | 0.05197 |
| 0.127 | 16.09531 | 0.82245 | 0.05280 |
| 0.128 | 16.13220 | 0.82433 | 0.05331 |
| 0.129 | 16.16127 | 0.82582 | 0.05372 |
| 0.13 | 16.18414 | 0.82699 | 0.05404 |
| 0.131 | 16.20322 | 0.82796 | 0.05431 |
| 0.132 | 16.22375 | 0.82901 | 0.05460 |
| 0.133 | 16.24482 | 0.83009 | 0.05490 |
| 0.134 | 16.26560 | 0.83115 | 0.05521 |
| 0.135 | 16.28713 | 0.83225 | 0.05552 |
| 0.136 | 16.30571 | 0.83320 | 0.05579 |
| 0.137 | 16.32256 | 0.83406 | 0.05604 |

| | | | |
|---|---|---|---|
| 0.138 | 16.34222 | 0.83506 | 0.05633 |
| 0.139 | 16.36026 | 0.83599 | 0.05660 |
| 0.14 | 16.38587 | 0.83730 | 0.05699 |
| 0.141 | 16.40786 | 0.83842 | 0.05733 |
| 0.142 | 16.43468 | 0.83979 | 0.05774 |
| 0.143 | 16.45232 | 0.84069 | 0.05801 |
| 0.144 | 16.47061 | 0.84163 | 0.05830 |
| 0.145 | 16.48600 | 0.84241 | 0.05854 |
| 0.146 | 16.50788 | 0.84353 | 0.05888 |
| 0.147 | 16.52618 | 0.84446 | 0.05917 |
| 0.148 | 16.54207 | 0.84528 | 0.05943 |
| 0.149 | 16.56212 | 0.84630 | 0.05975 |
| 0.15 | 16.57595 | 0.84701 | 0.05998 |
| 0.151 | 16.58534 | 0.84749 | 0.06013 |
| 0.152 | 16.60140 | 0.84831 | 0.06039 |
| 0.153 | 16.61126 | 0.84881 | 0.06056 |
| 0.154 | 16.62281 | 0.84940 | 0.06075 |
| 0.155 | 16.63635 | 0.85009 | 0.06097 |
| 0.156 | 16.64959 | 0.85077 | 0.06119 |
| 0.157 | 16.66282 | 0.85145 | 0.06142 |
| 0.158 | 16.67988 | 0.85232 | 0.06170 |
| 0.159 | 16.69308 | 0.85299 | 0.06193 |
| 0.16 | 16.71298 | 0.85401 | 0.06227 |
| 0.161 | 16.73772 | 0.85527 | 0.06270 |
| 0.162 | 16.75452 | 0.85613 | 0.06299 |
| 0.163 | 16.77654 | 0.85726 | 0.06338 |
| 0.164 | 16.80000 | 0.85846 | 0.06379 |
| 0.165 | 16.82179 | 0.85957 | 0.06418 |
| 0.166 | 16.84067 | 0.86054 | 0.06452 |
| 0.167 | 16.86070 | 0.86156 | 0.06488 |
| 0.168 | 16.87645 | 0.86236 | 0.06517 |
| 0.169 | 16.88800 | 0.86295 | 0.06539 |
| 0.17 | 16.91330 | 0.86425 | 0.06586 |
| 0.171 | 16.92969 | 0.86508 | 0.06616 |
| 0.172 | 16.94801 | 0.86602 | 0.06651 |
| 0.173 | 16.97097 | 0.86719 | 0.06694 |
| 0.174 | 16.98782 | 0.86805 | 0.06727 |
| 0.175 | 17.00548 | 0.86896 | 0.06761 |

| | | | |
|---|---|---|---|
| 0.176 | 17.02170 | 0.86979 | 0.06793 |
| 0.177 | 17.03596 | 0.87051 | 0.06821 |
| 0.178 | 17.05710 | 0.87159 | 0.06862 |
| 0.179 | 17.07451 | 0.87248 | 0.06897 |
| 0.18 | 17.08340 | 0.87294 | 0.06915 |
| 0.181 | 17.11033 | 0.87431 | 0.06969 |
| 0.182 | 17.12741 | 0.87519 | 0.07004 |
| 0.183 | 17.14496 | 0.87608 | 0.07040 |
| 0.184 | 17.16514 | 0.87712 | 0.07082 |
| 0.185 | 17.18637 | 0.87820 | 0.07127 |
| 0.186 | 17.20702 | 0.87926 | 0.07170 |
| 0.187 | 17.21935 | 0.87988 | 0.07197 |
| 0.188 | 17.22431 | 0.88014 | 0.07207 |
| 0.189 | 17.16669 | 0.87719 | 0.07085 |
| 0.19 | 17.22998 | 0.88043 | 0.07220 |
| 0.191 | 17.27186 | 0.88257 | 0.07310 |
| 0.192 | 17.30048 | 0.88403 | 0.07374 |
| 0.193 | 17.31695 | 0.88487 | 0.07410 |
| 0.194 | 17.33182 | 0.88563 | 0.07444 |
| 0.195 | 17.35405 | 0.88677 | 0.07494 |
| 0.196 | 17.37013 | 0.88759 | 0.07531 |
| 0.197 | 17.39072 | 0.88864 | 0.07579 |
| 0.198 | 17.40516 | 0.88938 | 0.07613 |
| 0.199 | 17.41807 | 0.89004 | 0.07643 |
| 0.2 | 17.43184 | 0.89074 | 0.07676 |
| 0.21 | 17.57763 | 0.89819 | 0.08036 |
| 0.22 | 17.72582 | 0.90576 | 0.08432 |
| 0.23 | 17.86105 | 0.91267 | 0.08825 |
| 0.24 | 18.00318 | 0.91994 | 0.09276 |
| 0.25 | 18.15772 | 0.92783 | 0.09819 |
| 0.26 | 18.30668 | 0.93545 | 0.10406 |
| 0.27 | 18.43772 | 0.94214 | 0.10986 |
| 0.28 | 18.57974 | 0.94940 | 0.11699 |
| 0.29 | 18.72280 | 0.95671 | 0.12535 |
| 0.3 | 18.86555 | 0.96400 | 0.13529 |
| 0.31 | 19.00712 | 0.97124 | 0.14745 |
| 0.32 | 19.14448 | 0.97826 | 0.16270 |
| 0.33 | 19.22592 | 0.98242 | 0.17432 |

| | | | |
|---|---|---|---|
| 0.34 | 19.25699 | 0.98401 | 0.17951 |
| 0.35 | 19.31961 | 0.98721 | 0.19178 |
| 0.36 | 19.32631 | 0.98755 | 0.19327 |
| 0.37 | 19.34579 | 0.98854 | 0.19786 |
| 0.38 | 19.42607 | 0.99265 | 0.22232 |
| 0.39 | 19.48918 | 0.99587 | 0.25424 |
| 0.4 | 19.46340 | 0.99455 | 0.23891 |
| 0.41 | 19.49552 | 0.99619 | 0.25876 |
| 0.42 | 19.50031 | 0.99644 | 0.26245 |
| 0.43 | 19.55666 | 0.99932 | 0.35419 |
| 0.44 | 19.56907 | 0.99995 | 0.50217 |
| 0.45 | 19.24974 | 0.98364 | 0.17826 |
| 0.46 | 19.24358 | 0.98332 | 0.17721 |
| 0.47 | 19.20834 | 0.98152 | 0.17159 |
| 0.48 | 19.10521 | 0.97625 | 0.15788 |
| 0.49 | 18.89577 | 0.96555 | 0.13766 |
| 0.5 | 18.54160 | 0.94745 | 0.11497 |
| 0.51 | 18.23658 | 0.93186 | 0.10121 |
| 0.52 | 18.22788 | 0.93142 | 0.10087 |
| 0.53 | 18.20385 | 0.93019 | 0.09994 |
| 0.54 | 18.13148 | 0.92649 | 0.09723 |
| 0.55 | 17.99408 | 0.91947 | 0.09246 |
| 0.56 | 17.84028 | 0.91161 | 0.08763 |
| 0.57 | 17.75151 | 0.90708 | 0.08504 |
| 0.58 | 17.63288 | 0.90102 | 0.08179 |
| 0.59 | 17.47661 | 0.89303 | 0.07783 |
| 0.6 | 17.18805 | 0.87829 | 0.07130 |
| 0.61 | 16.98211 | 0.86776 | 0.06716 |
| 0.62 | 16.72393 | 0.85457 | 0.06246 |
| 0.63 | 16.60800 | 0.84865 | 0.06050 |
| 0.64 | 16.55633 | 0.84601 | 0.05966 |

# Appendix C
## Ollgaard *et al.* (1971) Pushout Results versus Study 0-4124 CIPST Results

Ollgaard et al. (1971) Pushout Results and Average Concrete Properties, All Tests Included

As*Fut =     31.323  kip

| Test Series | fprc (ksi) | w (pcf) | Ec (ksi) | d (in.) | As (in^2) | Spec. 1 (kip) | Spec. 2 (kip) | Spec. 3 (kip) | Avg. (kip) | Eq. 8.3 (exact) Predicted (kip) | Act/Pred | Eq. 8.5 (design) Predicted (kip) | Act/Pred |
|---|---|---|---|---|---|---|---|---|---|---|---|---|---|
| A | 5.08 | 148.1 | 4239.15 | 0.750 | 0.442 | 29.3 | 32.5 | 30.6 | 30.8 | 31.386 | 0.981 | 31.323 | 0.983 |
| LA | 3.64 | 147.6 | 3570.21 | 0.750 | 0.442 | 24.5 | 26.5 | 24.7 | 25.2 | 26.332 | 0.958 | 25.181 | 1.002 |
| SA | 4.01 | 147.4 | 3739.66 | 0.750 | 0.442 | 19.5 | 20.8 | 19.9 | 20.1 | 27.667 | 0.725 | 27.050 | 0.742 |
| B | 4.78 | 140.5 | 3799.64 | 0.750 | 0.442 | 27.5 | 25.4 | 25.4 | 26.1 | 29.369 | 0.889 | 29.769 | 0.877 |
| LB | 2.67 | 138.6 | 2782.37 | 0.750 | 0.442 | 18.3 | 18.1 | 17.3 | 17.9 | 21.501 | 0.833 | 19.039 | 0.940 |
| SB | 4.03 | 142.6 | 3567.35 | 0.625 | 0.307 | 18.2 | 16.9 | 18.8 | 18.0 | 18.846 | 0.953 | 18.393 | 0.977 |
| 2B | 4.78 | 140.5 | 3799.64 | 0.750 | 0.442 | 26.1 | 25.5 | 25.0 | 25.5 | 29.369 | 0.869 | 29.769 | 0.858 |
| C- | 4.69 | 89.1 | 1900.71 | 0.750 | 0.442 | 19.9 | 21.3 | 21.0 | 20.7 | 21.530 | 0.963 | 20.856 | 0.994 |
| C | 4.28 | 108.2 | 2429.83 | 0.750 | 0.442 | 21.6 | 21.5 | 22.2 | 21.8 | 23.338 | 0.933 | 22.526 | 0.966 |
| D- | 4.72 | 99.2 | 2240.02 | 0.750 | 0.442 | 24.1 | 23.0 | 22.7 | 23.3 | 23.188 | 1.003 | 22.713 | 1.024 |
| D | 4.92 | 113.4 | 2795.22 | 0.750 | 0.442 | 21.6 | 23.3 | 24.4 | 23.1 | 25.881 | 0.893 | 25.904 | 0.892 |
| E- | 3.60 | 97.7 | 1912.08 | 0.750 | 0.442 | 19.6 | 19.2 | 17.8 | 18.9 | 19.940 | 0.946 | 18.327 | 1.029 |
| E | 4.30 | 111.1 | 2534.07 | 0.750 | 0.442 | 23.1 | 22.5 | 21.6 | 22.4 | 23.806 | 0.941 | 23.058 | 0.971 |
| LE | 3.22 | 111.4 | 2201.76 | 0.750 | 0.442 | 18.7 | 19.5 | 19.7 | 19.3 | 20.518 | 0.941 | 18.599 | 1.038 |
| SE | 4.00 | 112.3 | 2483.78 | 0.625 | 0.307 | 15.7 | 15.7 | 17.0 | 16.1 | 16.035 | 1.006 | 15.290 | 1.055 |
| 2E | 4.40 | 111.1 | 2563.37 | 0.750 | 0.442 | 21.2 | 23.1 | 22.7 | 22.3 | 24.092 | 0.927 | 23.459 | 0.952 |
| Mean = | | | | | | | | | | | 0.9226 | | 0.9563 |
| St. Dev. = | | | | | | | | | | | 0.0703 | | 0.0808 |
| COV = | | | | | | | | | | | 0.0762 | | 0.0845 |

Study 0-4124 Direct Shear Test Results of CIPST

As*Fut =     29.2463  kip

| Test Specimen | fprc (ksi) | w(calc) (pcf) | Ec (ksi) | d (in.) | As (in^2) | Ultimate (kip) | Eq. 8.3 (exact) | | Eq. 8.5 (design) | |
|---|---|---|---|---|---|---|---|---|---|---|
| | | | | | | | Predicted (kip) | Act/Pred | Predicted (kip) | Act/Pred |
| CIPST01 | 3.2 | 150 | 3224.41 | 0.750 | 0.442 | 24.3 | 24.223 | 1.003 | 22.438 | 1.083 |
| CIPST02 | 3.2 | 150 | 3224.41 | 0.750 | 0.442 | 21.7 | 24.223 | 0.896 | 22.438 | 0.967 |
| CIPST03 | 3.2 | 150 | 3224.41 | 0.750 | 0.442 | 17.8 | 24.223 | 0.735 | 22.438 | 0.793 |
| Average | 3.2 | 150 | 3224.41 | 0.750 | 0.442 | 21.3 | 24.223 | 0.878 | 22.438 | 0.948 |
| Mean = | | | | | | | | 0.8779 | | 0.9478 |
| St. Dev. = | | | | | | | | 0.1351 | | 0.1191 |
| COV = | | | | | | | | 0.1538 | | 0.1256 |

Ollgaard *et al.* (1971) Pushout Results and Average Concrete Properties,
"Lower Compressive Strength" Tests (3/4-in. studs, normal-weight concrete, 4-stud tests)

| Test Specimen | fprc (ksi) | w (pcf) | Ec (ksi) | d (in.) | As (in^2) | Ultimate (kip) | Eq. 8.3 (exact) Predicted (kip) | Act/Pred |
|---|---|---|---|---|---|---|---|---|
| LA | 3.64 | 147.6 | 3570.21 | 0.750 | 0.442 | 24.5 | 26.332 | 0.930 |
| | 3.64 | 147.6 | 3570.21 | 0.750 | 0.442 | 26.5 | 26.332 | 1.006 |
| | 3.64 | 147.6 | 3570.21 | 0.750 | 0.442 | 24.7 | 26.332 | 0.938 |
| LB | 2.67 | 138.6 | 2782.37 | 0.750 | 0.442 | 18.3 | 21.501 | 0.851 |
| | 2.67 | 138.6 | 2782.37 | 0.750 | 0.442 | 18.1 | 21.501 | 0.842 |
| | 2.67 | 138.6 | 2782.37 | 0.750 | 0.442 | 17.3 | 21.501 | 0.805 |
| LE | 3.22 | 111.4 | 2201.76 | 0.750 | 0.442 | 18.7 | 20.518 | 0.911 |
| | 3.22 | 111.4 | 2201.76 | 0.750 | 0.442 | 19.5 | 20.518 | 0.950 |
| | 3.22 | 111.4 | 2201.76 | 0.750 | 0.442 | 19.7 | 20.518 | 0.960 |
| Mean = | | | | | | | | 0.9105 |
| St. Dev. = | | | | | | | | 0.0651 |
| COV = | | | | | | | | 0.0715 |

# Appendix D
# ANSYS Analysis of Epoxy Plate Specimen

FEM Nodal Solution (from interface steel stresses)

| modular ratio (steel to concrete) |
|---|
| n = 0.11 |

| Node Number | X Coordinate | Y Coordinate | SX (steel) (psi) | SX (concrete) (ksi) | SY (steel) (psi) | SY (concrete) (ksi) |
|---|---|---|---|---|---|---|
| 97 | 0 | 7 | 16814 | 1.86949 | 4821.3 | 0.53606 |
| 98 | 0.1 | 7 | 12323 | 1.37015 | 1521.6 | 0.16918 |
| 99 | 0.2 | 7 | 9701 | 1.07862 | 103.53 | 0.01151 |
| 100 | 0.3 | 7 | 8344.2 | 0.92776 | -434.77 | -0.04834 |
| 101 | 0.4 | 7 | 7495.4 | 0.83339 | -787.97 | -0.08761 |
| 102 | 0.5 | 7 | 6813.8 | 0.75760 | -970.61 | -0.10792 |
| 103 | 0.6 | 7 | 6241.8 | 0.69400 | -1060.3 | -0.11789 |
| 104 | 0.7 | 7 | 5743 | 0.63854 | -1078.4 | -0.11990 |
| 105 | 0.8 | 7 | 5303.5 | 0.58968 | -1047.6 | -0.11648 |
| 106 | 0.9 | 7 | 4915.5 | 0.54654 | -983.06 | -0.10930 |
| 107 | 1 | 7 | 4574.4 | 0.50861 | -897.2 | -0.09976 |
| 108 | 1.1 | 7 | 4276.7 | 0.47551 | -799.48 | -0.08889 |
| 109 | 1.2 | 7 | 4018.7 | 0.44682 | -696.99 | -0.07750 |
| 110 | 1.3 | 7 | 3796.9 | 0.42216 | -594.81 | -0.06613 |
| 111 | 1.4 | 7 | 3607.5 | 0.40111 | -496.47 | -0.05520 |
| 112 | 1.5 | 7 | 3446.8 | 0.38324 | -404.24 | -0.04495 |
| 113 | 1.6 | 7 | 3311.1 | 0.36815 | -319.45 | -0.03552 |
| 114 | 1.7 | 7 | 3197 | 0.35546 | -242.78 | -0.02699 |
| 115 | 1.8 | 7 | 3101.2 | 0.34481 | -174.39 | -0.01939 |
| 116 | 1.9 | 7 | 3020.8 | 0.33587 | -114.13 | -0.01269 |
| 117 | 2 | 7 | 2953.2 | 0.32836 | -61.619 | -0.00685 |
| 118 | 2.1 | 7 | 2896.2 | 0.32202 | -16.337 | -0.00182 |
| 119 | 2.2 | 7 | 2847.6 | 0.31661 | 22.301 | 0.00248 |
| 120 | 2.3 | 7 | 2805.8 | 0.31197 | 54.913 | 0.00611 |
| 121 | 2.4 | 7 | 2769.3 | 0.30791 | 82.118 | 0.00913 |
| 122 | 2.5 | 7 | 2736.8 | 0.30430 | 104.51 | 0.01162 |
| 123 | 2.6 | 7 | 2707.5 | 0.30104 | 122.66 | 0.01364 |
| 124 | 2.7 | 7 | 2680.3 | 0.29801 | 137.1 | 0.01524 |
| 125 | 2.8 | 7 | 2654.7 | 0.29517 | 148.29 | 0.01649 |
| 126 | 2.9 | 7 | 2630.1 | 0.29243 | 156.69 | 0.01742 |
| 127 | 3 | 7 | 2606 | 0.28975 | 162.68 | 0.01809 |
| 128 | 3.1 | 7 | 2582.1 | 0.28709 | 166.62 | 0.01853 |
| 129 | 3.2 | 7 | 2558.2 | 0.28444 | 168.81 | 0.01877 |
| 130 | 3.3 | 7 | 2534.1 | 0.28176 | 169.54 | 0.01885 |
| 131 | 3.4 | 7 | 2509.7 | 0.27904 | 169.03 | 0.01879 |
| 132 | 3.5 | 7 | 2484.8 | 0.27628 | 167.5 | 0.01862 |

| 133 | 3.6 | 7 | 2459.5 | 0.27346 | 165.14 | 0.01836 |
|-----|-----|---|--------|---------|--------|---------|
| 134 | 3.7 | 7 | 2433.7 | 0.27059 | 162.1 | 0.01802 |
| 135 | 3.8 | 7 | 2407.5 | 0.26768 | 158.52 | 0.01763 |
| 136 | 3.9 | 7 | 2380.7 | 0.26470 | 154.51 | 0.01718 |
| 137 | 4 | 7 | 2353.6 | 0.26169 | 150.17 | 0.01670 |
| 138 | 4.1 | 7 | 2326.1 | 0.25863 | 145.6 | 0.01619 |
| 139 | 4.2 | 7 | 2298.2 | 0.25553 | 140.86 | 0.01566 |
| 140 | 4.3 | 7 | 2270.1 | 0.25240 | 136.01 | 0.01512 |
| 141 | 4.4 | 7 | 2241.7 | 0.24925 | 131.1 | 0.01458 |
| 142 | 4.5 | 7 | 2213.2 | 0.24608 | 126.18 | 0.01403 |
| 143 | 4.6 | 7 | 2184.6 | 0.24290 | 121.28 | 0.01348 |
| 144 | 4.7 | 7 | 2156 | 0.23972 | 116.43 | 0.01295 |
| 145 | 4.8 | 7 | 2127.3 | 0.23653 | 111.65 | 0.01241 |
| 146 | 4.9 | 7 | 2098.7 | 0.23335 | 106.97 | 0.01189 |
| 147 | 5 | 7 | 2070.2 | 0.23018 | 102.38 | 0.01138 |
| 148 | 5.1 | 7 | 2041.8 | 0.22702 | 97.921 | 0.01089 |
| 149 | 5.2 | 7 | 2013.6 | 0.22389 | 93.583 | 0.01041 |
| 150 | 5.3 | 7 | 1985.6 | 0.22077 | 89.378 | 0.00994 |
| 151 | 5.4 | 7 | 1957.8 | 0.21768 | 85.308 | 0.00949 |
| 152 | 5.5 | 7 | 1930.3 | 0.21462 | 81.377 | 0.00905 |
| 153 | 5.6 | 7 | 1903 | 0.21159 | 77.585 | 0.00863 |
| 154 | 5.7 | 7 | 1876.1 | 0.20860 | 73.933 | 0.00822 |
| 155 | 5.8 | 7 | 1849.5 | 0.20564 | 70.42 | 0.00783 |
| 156 | 5.9 | 7 | 1823.2 | 0.20272 | 67.044 | 0.00745 |
| 157 | 6 | 7 | 1797.3 | 0.19984 | 63.802 | 0.00709 |
| 158 | 6.1 | 7 | 1771.7 | 0.19699 | 60.692 | 0.00675 |
| 159 | 6.2 | 7 | 1746.5 | 0.19419 | 57.712 | 0.00642 |
| 160 | 6.3 | 7 | 1721.7 | 0.19143 | 54.857 | 0.00610 |
| 161 | 6.4 | 7 | 1697.2 | 0.18871 | 52.123 | 0.00580 |
| 162 | 6.5 | 7 | 1673.1 | 0.18603 | 49.508 | 0.00550 |
| 163 | 6.6 | 7 | 1649.4 | 0.18339 | 47.008 | 0.00523 |
| 164 | 6.7 | 7 | 1626 | 0.18079 | 44.618 | 0.00496 |
| 165 | 6.8 | 7 | 1603.1 | 0.17824 | 42.335 | 0.00471 |
| 166 | 6.9 | 7 | 1580.4 | 0.17572 | 40.155 | 0.00446 |
| 167 | 7 | 7 | 1558.2 | 0.17325 | 38.075 | 0.00423 |
| 168 | 7.1 | 7 | 1536.3 | 0.17082 | 36.09 | 0.00401 |
| 169 | 7.2 | 7 | 1514.8 | 0.16843 | 34.197 | 0.00380 |
| 170 | 7.3 | 7 | 1493.6 | 0.16607 | 32.393 | 0.00360 |
| 171 | 7.4 | 7 | 1472.7 | 0.16374 | 30.673 | 0.00341 |
| 172 | 7.5 | 7 | 1452.2 | 0.16146 | 29.036 | 0.00323 |
| 173 | 7.6 | 7 | 1432 | 0.15922 | 27.476 | 0.00305 |
| 174 | 7.7 | 7 | 1412.1 | 0.15701 | 25.993 | 0.00289 |
| 175 | 7.8 | 7 | 1392.5 | 0.15483 | 24.581 | 0.00273 |
| 176 | 7.9 | 7 | 1373.2 | 0.15268 | 23.239 | 0.00258 |
| 177 | 8 | 7 | 1354.2 | 0.15057 | 21.963 | 0.00244 |
| 178 | 8.1 | 7 | 1335.5 | 0.14849 | 20.752 | 0.00231 |
| 179 | 8.2 | 7 | 1317.1 | 0.14644 | 19.601 | 0.00218 |
| 180 | 8.3 | 7 | 1298.9 | 0.14442 | 18.509 | 0.00206 |

| 181 | 8.4 | 7 | 1281 | 0.14243 | 17.474 | 0.00194 |
| 182 | 8.5 | 7 | 1263.3 | 0.14046 | 16.492 | 0.00183 |
| 183 | 8.6 | 7 | 1245.8 | 0.13852 | 15.562 | 0.00173 |
| 184 | 8.7 | 7 | 1228.6 | 0.13660 | 14.681 | 0.00163 |
| 185 | 8.8 | 7 | 1211.6 | 0.13471 | 13.848 | 0.00154 |
| 186 | 8.9 | 7 | 1194.8 | 0.13285 | 13.06 | 0.00145 |
| 187 | 9 | 7 | 1178.2 | 0.13100 | 12.316 | 0.00137 |
| 188 | 9.1 | 7 | 1161.7 | 0.12917 | 11.613 | 0.00129 |
| 189 | 9.2 | 7 | 1145.5 | 0.12736 | 10.95 | 0.00122 |
| 190 | 9.3 | 7 | 1129.5 | 0.12559 | 10.325 | 0.00115 |
| 191 | 9.4 | 7 | 1113.6 | 0.12382 | 9.7365 | 0.00108 |
| 192 | 9.5 | 7 | 1097.9 | 0.12207 | 9.1828 | 0.00102 |
| 193 | 9.6 | 7 | 1082.3 | 0.12034 | 8.6623 | 0.00096 |
| 194 | 9.7 | 7 | 1066.9 | 0.11862 | 8.1737 | 0.00091 |
| 195 | 9.8 | 7 | 1051.6 | 0.11692 | 7.7154 | 0.00086 |
| 196 | 9.9 | 7 | 1036.5 | 0.11524 | 7.286 | 0.00081 |
| 197 | 10 | 7 | 1021.5 | 0.11358 | 6.8844 | 0.00077 |
| 198 | 10.1 | 7 | 1006.6 | 0.11192 | 6.5091 | 0.00072 |
| 199 | 10.2 | 7 | 991.81 | 0.11028 | 6.1589 | 0.00068 |
| 200 | 10.3 | 7 | 977.14 | 0.10864 | 5.8327 | 0.00065 |
| 201 | 10.4 | 7 | 962.58 | 0.10703 | 5.5293 | 0.00061 |
| 202 | 10.5 | 7 | 948.11 | 0.10542 | 5.2475 | 0.00058 |
| 203 | 10.6 | 7 | 933.74 | 0.10382 | 4.9863 | 0.00055 |
| 204 | 10.7 | 7 | 919.45 | 0.10223 | 4.7446 | 0.00053 |
| 205 | 10.8 | 7 | 905.24 | 0.10065 | 4.5214 | 0.00050 |
| 206 | 10.9 | 7 | 891.1 | 0.09908 | 4.3156 | 0.00048 |
| 207 | 11 | 7 | 877.04 | 0.09751 | 4.1264 | 0.00046 |
| 208 | 11.1 | 7 | 863.04 | 0.09596 | 3.9526 | 0.00044 |
| 209 | 11.2 | 7 | 849.1 | 0.09441 | 3.7935 | 0.00042 |
| 210 | 11.3 | 7 | 835.21 | 0.09286 | 3.6479 | 0.00041 |
| 211 | 11.4 | 7 | 821.37 | 0.09133 | 3.515 | 0.00039 |
| 212 | 11.5 | 7 | 807.57 | 0.08979 | 3.3938 | 0.00038 |
| 213 | 11.6 | 7 | 793.81 | 0.08826 | 3.2834 | 0.00037 |
| 214 | 11.7 | 7 | 780.08 | 0.08673 | 3.1828 | 0.00035 |
| 215 | 11.8 | 7 | 766.38 | 0.08521 | 3.091 | 0.00034 |
| 216 | 11.9 | 7 | 752.7 | 0.08369 | 3.007 | 0.00033 |
| 217 | 12 | 7 | 739.03 | 0.08217 | 2.9298 | 0.00033 |
| 218 | 12.1 | 7 | 725.38 | 0.08065 | 2.8582 | 0.00032 |
| 219 | 12.2 | 7 | 711.72 | 0.07913 | 2.7911 | 0.00031 |
| 220 | 12.3 | 7 | 698.07 | 0.07762 | 2.7273 | 0.00030 |
| 221 | 12.4 | 7 | 684.4 | 0.07610 | 2.6654 | 0.00030 |
| 222 | 12.5 | 7 | 670.72 | 0.07457 | 2.6041 | 0.00029 |
| 223 | 12.6 | 7 | 657.02 | 0.07305 | 2.5416 | 0.00028 |
| 224 | 12.7 | 7 | 643.28 | 0.07152 | 2.4764 | 0.00028 |
| 225 | 12.8 | 7 | 629.51 | 0.06999 | 2.4065 | 0.00027 |
| 226 | 12.9 | 7 | 615.7 | 0.06846 | 2.3298 | 0.00026 |
| 227 | 13 | 7 | 601.83 | 0.06692 | 2.244 | 0.00025 |
| 228 | 13.1 | 7 | 587.9 | 0.06537 | 2.1465 | 0.00024 |

| 229 | 13.2 | 7 | 573.89 | 0.06381 | 2.0344 | 0.00023 |
|-----|------|---|--------|---------|--------|---------|
| 230 | 13.3 | 7 | 559.81 | 0.06224 | 1.9042 | 0.00021 |
| 231 | 13.4 | 7 | 545.65 | 0.06067 | 1.7524 | 0.00019 |
| 232 | 13.5 | 7 | 531.38 | 0.05908 | 1.5745 | 0.00018 |
| 233 | 13.6 | 7 | 517.01 | 0.05748 | 1.3657 | 0.00015 |
| 234 | 13.7 | 7 | 502.52 | 0.05587 | 1.1206 | 0.00012 |
| 235 | 13.8 | 7 | 487.9 | 0.05425 | 0.83288 | 0.00009 |
| 236 | 13.9 | 7 | 473.14 | 0.05261 | 0.49533 | 0.00006 |
| 237 | 14 | 7 | 458.24 | 0.05095 | 9.98E-02 | 0.00001 |
| 238 | 14.1 | 7 | 443.18 | 0.04928 | -0.36308 | -0.00004 |
| 239 | 14.2 | 7 | 427.95 | 0.04758 | -0.90396 | -0.00010 |
| 240 | 14.3 | 7 | 412.55 | 0.04587 | -1.5351 | -0.00017 |
| 241 | 14.4 | 7 | 396.97 | 0.04414 | -2.2703 | -0.00025 |
| 242 | 14.5 | 7 | 381.2 | 0.04238 | -3.1257 | -0.00035 |
| 243 | 14.6 | 7 | 365.24 | 0.04061 | -4.1195 | -0.00046 |
| 244 | 14.7 | 7 | 349.09 | 0.03881 | -5.2724 | -0.00059 |
| 245 | 14.8 | 7 | 332.74 | 0.03700 | -6.6085 | -0.00073 |
| 246 | 14.9 | 7 | 316.22 | 0.03516 | -8.1547 | -0.00091 |
| 247 | 15 | 7 | 299.53 | 0.03330 | -9.9423 | -0.00111 |
| 248 | 15.1 | 7 | 282.68 | 0.03143 | -12.007 | -0.00134 |
| 249 | 15.2 | 7 | 265.71 | 0.02954 | -14.388 | -0.00160 |
| 250 | 15.3 | 7 | 248.65 | 0.02765 | -17.132 | -0.00190 |
| 251 | 15.4 | 7 | 231.54 | 0.02574 | -20.292 | -0.00226 |
| 252 | 15.5 | 7 | 214.46 | 0.02385 | -23.925 | -0.00266 |
| 253 | 15.6 | 7 | 197.48 | 0.02196 | -28.099 | -0.00312 |
| 254 | 15.7 | 7 | 180.69 | 0.02009 | -32.889 | -0.00366 |
| 255 | 15.8 | 7 | 164.22 | 0.01826 | -38.376 | -0.00427 |
| 256 | 15.9 | 7 | 148.21 | 0.01648 | -44.654 | -0.00496 |
| 257 | 16 | 7 | 132.83 | 0.01477 | -51.822 | -0.00576 |
| 258 | 16.1 | 7 | 118.26 | 0.01315 | -59.986 | -0.00667 |
| 259 | 16.2 | 7 | 104.74 | 0.01165 | -69.258 | -0.00770 |
| 260 | 16.3 | 7 | 92.507 | 0.01029 | -79.748 | -0.00887 |
| 261 | 16.4 | 7 | 81.814 | 0.00910 | -91.562 | -0.01018 |
| 262 | 16.5 | 7 | 72.924 | 0.00811 | -104.79 | -0.01165 |
| 263 | 16.6 | 7 | 66.088 | 0.00735 | -119.48 | -0.01328 |
| 264 | 16.7 | 7 | 61.521 | 0.00684 | -135.67 | -0.01508 |
| 265 | 16.8 | 7 | 59.378 | 0.00660 | -153.28 | -0.01704 |
| 266 | 16.9 | 7 | 59.73 | 0.00664 | -172.2 | -0.01915 |
| 267 | 17 | 7 | 62.531 | 0.00695 | -192.08 | -0.02136 |
| 268 | 17.1 | 7 | 67.613 | 0.00752 | -212.69 | -0.02365 |
| 269 | 17.2 | 7 | 74.66 | 0.00830 | -232.57 | -0.02586 |
| 270 | 17.3 | 7 | 83.384 | 0.00927 | -253.65 | -0.02820 |
| 271 | 17.4 | 7 | 93.026 | 0.01034 | -262.25 | -0.02916 |
| 272 | 17.5 | 7 | 107.27 | 0.01193 | -301.27 | -0.03350 |
| 273 | 17.6 | 7 | 101.44 | 0.01128 | -161.31 | -0.01794 |
| 274 | 17.7 | 7 | 535.67 | 0.05956 | -661.29 | -0.07353 |
| 275 | 17.8 | 7 | 1230.1 | 0.13677 | 3251.6 | 0.36153 |
| 276 | 17.9 | 7 | 1160 | 0.12898 | 1198.2 | 0.13322 |

| 277 | 18 | 7 | 716.32 | 0.07965 | 720.02 | 0.08006 |
|-----|------|---|---------|----------|---------|----------|
| 278 | 18.1 | 7 | 518.61 | 0.05766 | 407.99 | 0.04536 |
| 279 | 18.2 | 7 | 399.38 | 0.04441 | 220.32 | 0.02450 |
| 280 | 18.3 | 7 | 311.31 | 0.03461 | 93.214 | 0.01036 |
| 281 | 18.4 | 7 | 242.79 | 0.02699 | 7.4312 | 0.00083 |
| 282 | 18.5 | 7 | 187.11 | 0.02080 | -49.978 | -0.00556 |
| 283 | 18.6 | 7 | 140.97 | 0.01567 | -86.707 | -0.00964 |
| 284 | 18.7 | 7 | 102.35 | 0.01138 | -108.28 | -0.01204 |
| 285 | 18.8 | 7 | 69.963 | 0.00778 | -118.79 | -0.01321 |
| 286 | 18.9 | 7 | 42.907 | 0.00477 | -121.36 | -0.01349 |
| 287 | 19 | 7 | 20.485 | 0.00228 | -118.43 | -0.01317 |
| 288 | 19.1 | 7 | 2.1226 | 0.00024 | -111.87 | -0.01244 |
| 289 | 19.2 | 7 | -12.682 | -0.00141 | -103.13 | -0.01147 |
| 290 | 19.3 | 7 | -24.382 | -0.00271 | -93.261 | -0.01037 |
| 291 | 19.4 | 7 | -33.395 | -0.00371 | -83.037 | -0.00923 |
| 292 | 19.5 | 7 | -40.104 | -0.00446 | -72.992 | -0.00812 |
| 293 | 19.6 | 7 | -44.857 | -0.00499 | -63.477 | -0.00706 |
| 294 | 19.7 | 7 | -47.972 | -0.00533 | -54.704 | -0.00608 |
| 295 | 19.8 | 7 | -49.731 | -0.00553 | -46.78 | -0.00520 |
| 296 | 19.9 | 7 | -50.387 | -0.00560 | -39.738 | -0.00442 |
| 297 | 20 | 7 | -50.159 | -0.00558 | -33.561 | -0.00373 |
| 298 | 20.1 | 7 | -49.238 | -0.00547 | -28.198 | -0.00314 |
| 299 | 20.2 | 7 | -47.788 | -0.00531 | -23.58 | -0.00262 |
| 300 | 20.3 | 7 | -45.949 | -0.00511 | -19.632 | -0.00218 |
| 301 | 20.4 | 7 | -43.842 | -0.00487 | -16.277 | -0.00181 |
| 302 | 20.5 | 7 | -41.566 | -0.00462 | -13.443 | -0.00149 |
| 303 | 20.6 | 7 | -39.21 | -0.00436 | -11.07 | -0.00123 |
| 304 | 20.7 | 7 | -36.845 | -0.00410 | -9.1089 | -0.00101 |
| 305 | 20.8 | 7 | -34.537 | -0.00384 | -7.5264 | -0.00084 |
| 306 | 20.9 | 7 | -32.339 | -0.00360 | -6.3059 | -0.00070 |
| 307 | 21 | 7 | -30.303 | -0.00337 | -5.4499 | -0.00061 |
| 308 | 21.1 | 7 | -28.475 | -0.00317 | -4.9819 | -0.00055 |
| 309 | 21.2 | 7 | -26.903 | -0.00299 | -4.9496 | -0.00055 |
| 310 | 21.3 | 7 | -25.641 | -0.00285 | -5.4309 | -0.00060 |
| 311 | 21.4 | 7 | -24.755 | -0.00275 | -6.5476 | -0.00073 |
| 312 | 21.5 | 7 | -24.336 | -0.00271 | -8.483 | -0.00094 |
| 313 | 21.6 | 7 | -24.533 | -0.00273 | -11.578 | -0.00129 |
| 314 | 21.7 | 7 | -25.639 | -0.00285 | -16.32 | -0.00181 |
| 315 | 21.8 | 7 | -28.315 | -0.00315 | -24.563 | -0.00273 |
| 316 | 21.9 | 7 | -37.134 | -0.00413 | -36.99 | -0.00411 |
| 317 | 22 | 7 | -11.255 | -0.00125 | -93.064 | -0.01035 |

# References

AASHTO 1992: *AASHTO Standard Bridge Design Specifications*, 15th Edition, American Association of State Highway and Transportation Officials, Washington, D.C., 1992.

AASHTO 1996: *AASHTO Standard Bridge Design Specifications*, 16th Edition, American Association of State Highway and Transportation Officials, Washington, D.C., 1996.

AASHTO 2002: *AASHTO Standard Bridge Design Specifications*, 17th Edition, American Association of State Highway and Transportation Officials, Washington, D.C., 2002.

AASHTO 1998: *AASHTO LRFD Bridge Design Specifications*, Customary U.S. Units, 2nd Edition, American Association of State Highway and Transportation Officials, Washington, D.C., 1998.

ACI 318-02: *Building Code Requirements for Structural Concrete* (ACI 318-02) and *Commentary* (ACI 318R-02), American Concrete Institute, Farmington Hills, Michigan, 2002.

AISC 2002: *LRFD Manual of Steel Construction*, 3rd Edition, American Institute of Steel Construction, U.S.A., 2001.

ENV 1994-1-1:1992: *Eurocode 4, Design of Composite Steel and Concrete Structures, Part 1-1: General Rules and Rules for Buildings*, Brussels, Belgium, October 1992.

Klingner 2003: Klingner, R. E., "ACI 318-02 Appendix D: Basics for the Designer," *Proceedings*, University of Kansas Structural Engineering Conference, Lawrence, Kansas, March 2, 2003.

Meinheit and Anderson 2002: Meinheit, D. F. and Anderson, N. S., "Design Criteria for Headed Stud Groups in Shear: Part 1 - Steel Capacity and Back Edge Effects," *PCI Journal*, vol. 45, no. 5, September 2000, pp. 46-75.

Ollgaard *et al.* 1971: Ollgaard, J. G., Slutter, R. G. and Fisher, J. W., "Shear Strength of Stud Connectors in Lightweight and Normal-Weight Concrete," *AISC Engineering Journal*, vol. 8, April 1971, pp. 55-64.

Schaap 2004:  Schaap, B., "Methods to Develop Composite Action in Non-Composite Bridge Floor Systems: Part I," MS Thesis, Department of Civil Engineering, The University of Texas at Austin, May 2004.


**The following references were used for general background but not specifically cited in this thesis:**


3M 2003:  "3M Scotch-Weld$^{TM}$ Epoxy Adhesive DP-460 NS," *Technical Data*, 3M Engineered Adhesives Division, July 2003.

Beck, Engelhardt and Glaser 2003:  Beck, H., Engelhardt, M. D. and Glaser, N. J., "Static Pullout of Powder Actuated Fasteners in Steel: State-of-the-Art Review," *AISC Engineering Journal*, vol. 40, no. 2, 2003.

Borowicz 2002:  Borowicz, D. T., "Rapid Strengthening of Concrete Beams with Powder-Actuated Fastening Systems and Fiber Reinforced Polymer (FRP) Composite Materials," MS Thesis, Department of Civil Engineering, University of Wisconsin - Madison, May 2002.

ChemCo 2004:  "ChemCo Systems, Tech Links, Plate Bonding," http://www.chemcosytems.com/tech_platebond.html, January 2004.

Easterling and Murray 2000:  Easterling, W. S. and Murray, T. M., "Performance and Strength of Welded Shear Studs," *Proceedings* of the Conference: Composite Construction in Steel and Concrete IV, May 28-June 2, 2000, Banff, Alberta., Canada, pp. 458-469.

Engelhardt, Zates and Beck 1998:  Engelhardt, M. D., Kates, Z. and Beck, H., "Experiments on the Effects of Power Actuated Fasteners on the Strength of Open Web Steel Joists," *AISC Engineering Journal*, vol. 37, no. 4**,** 2000.

ENR 1963:  "Epoxy Bonds Composite Beams," *Engineering News-Record*, Editorial, 10 October 1963.

Fontana, Beck and Bartschi 2001:  Fontana, M., Beck, H. and Bartschi, R., "Experimental Investigations on the Behaviour of Strip Shear Connectors with Powder Actuated Fasteners," *Proceedings*, International Symposium on Connections between Steel and Concrete, R. Eligehausen, Ed., University of Stuttgart, Stuttgart, Germany, September 10-12, 2001.

Gattesco and Giuriani 1996:  Gattesco, N. and Giuriani, E., "Experimental Study on Shear Connectors Subjected to Cyclic Loading," *Journal of Construction Steel Research*, Vol. 38, No. 1, pp. 1-21, 1996.

Hanson 2003:  "Drive Rivets," Facsimile, Hanson Rivet & Supply Co., June, 2003.

Hanswille, Beck and Neubauer 2001:  Hanswille, G., Beck, H. and Neubauer, T., "Design Concept of Nailed Shear Connections in Composite Tube Columns," *Proceedings*, International Symposium on Connections between Steel and Concrete, R. Eligehausen, Ed., University of Stuttgart, Stuttgart, Germany, September 10-12, 2001.

Hicks and McConnel 1996:  Hicks, S. J. and McConnel, R. E., "The Shear Resistance of Headed Studs Used With Profile Steel Sheeting," *Proceedings of the 1996 Engineering Foundation Conference on Composite Construction in Steel and Concrete III*, June 9-14, 1996, Irsee, Germany, pp. 325-338.

Hilti 2002: Hilti Product Technical Guide, "Hilti Anchoring Systems, HIT HY 150/HIT-ICE Injection Adhesive Anchor," 2002.

Kuenzlen and Sippel 2001:  Kuenzlen, J. H. R. and Sippel, T. M., "Behaviour and Design of Fastenings with Concrete Screws," *Proceedings*, International Symposium on Connections between Steel and Concrete, R. Eligehausen, Ed., University of Stuttgart, Stuttgart, Germany, September 10-12, 2001.

Powers 00142 2000:  "Powers Fasteners A&E Design Manual Addendum," Cat. No. 00142, Powers Fasteners, Inc., 2000.

Powers 00200 2000:  "Powers Fasteners Wedge-Bolt[TM] Brochure," Cat. No. 00200, Powers Fasteners, Inc., 2000.

Powers Online 2003:  "Powers Fasteners Online Product Catalog, Mechanical, Wedge-Bolt[TM]," http://www.powers.com/44-47.pdf, 2003.

Roads and Bridges 1994: "Strengthening of Concrete Highway Structures Using Externally Bonded Plates," *Design Manual for Roads and Bridges*, Vol. 3, Sec. 3, Part 1, February 1994.

Schaich 2001: Schaich, J., "Development and Application of Saw-Tooth Connections for Composite Structures," *Proceedings*, International Symposium on Connections between Steel and Concrete, R. Eligehausen, Ed., University of Stuttgart, Stuttgart, Germany, September 10-12, 2001.

Schmid 2001: Schmid, V., "Geometry, Behaviour and Design of High Capacity Saw-Tooth Connections," *Proceedings*, International Symposium on Connections between Steel and Concrete, R. Eligehausen, Ed., University of Stuttgart, Stuttgart, Germany, September 10-12, 2001.

Thurlimann 1959: Thurlimann, B., "Fatigue and Static Strength of Stud Shear Connectors," *ACI Journal*, American Concrete Institute, Farmington Hills, Michigan, vol. 30, no. 12, 1959, pp. 1287-1302.

Yan 1965: Yan, H. T., *Composite Construction in Steel and Concrete*, Orient Longmans Limited, Calcutta, India, 1965, pp. 100-102.

# VITA

Brent Ericson Hungerford was born December 27, 1979 in Des Moines, Iowa to parents Dan and Linda Hungerford. He attended Valley High School in West Des Moines, Iowa where he graduated in May 1998. Brent obtained his B.S.C.E. from Purdue University in West Lafayette, Indiana in May 2002, enrolled at The University of Texas in Fall 2002 as a Graduate Research Assistant, and completed his M.S.E. in May 2004.

Permanent Address:  4200 Francrest Circle

West Des Moines, Iowa 50266

This thesis was typed by the author.